

# NAVAL POSTGRADUATE SCHOOL MONTEREY, CALIFORNIA



## THESIS

**LASER ANEMOMETRY AND PRESSURE MEASUREMENTS  
IN THE ENDWALL REGION OF AN ANNULAR TURBINE  
CASCADE UTILIZING A PRESSURIZED AERODYNAMIC  
WINDOW**

by  
Michael H. Guerrero  
September 1996

Thesis Advisor:

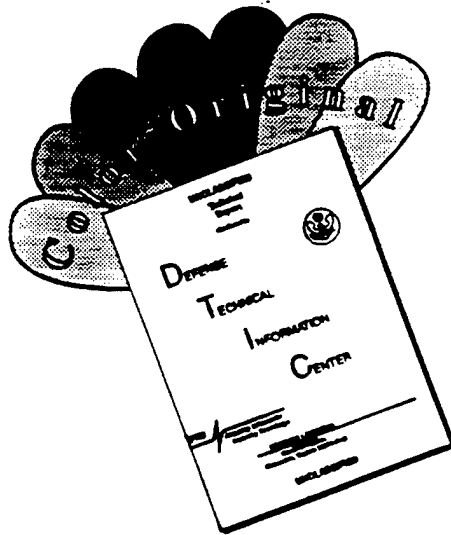
Garth V. Hobson

Approved for public release; distribution is unlimited

19970129 073

DTIC QUALITY INSPECTED 4

# DISCLAIMER NOTICE



THIS DOCUMENT IS BEST QUALITY AVAILABLE. THE COPY FURNISHED TO DTIC CONTAINED A SIGNIFICANT NUMBER OF COLOR PAGES WHICH DO NOT REPRODUCE LEGIBLY ON BLACK AND WHITE MICROFICHE.

| REPORT DOCUMENTATION PAGE   |  |  | Form Approved<br>OMB No. 0704-0188 |  |
|---|--|--|------------------------------------|--|
| Public reporting burden for this collection of information is estimated to average 1 hour per response, including the time for reviewing instruction, searching existing data sources, gathering and maintaining the data needed, and completing and reviewing the collection of information. Send comments regarding this burden estimate or any other aspect of this collection of information, including suggestions for reducing this burden, to Washington headquarters Services, Directorate for Information Operations and Reports, 1215 Jefferson Davis Highway, Suite 1204, Arlington, VA 22202-4302, and to the Office of Management and Budget, Paperwork Reduction Project (0704-0188) Washington DC 20503.   |  |  |                                    |  |
| 1.AGENCY USE ONLY (Leave blank)   | 2.REPORT DATE<br>September 1996                          | 3.REPORT TYPE AND DATES COVERED<br>Master's Thesis     |                                    |  |
| 4.TITLE AND SUBTITLE<br>LASER ANEMOMETRY AND PRESSURE MEASUREMENTS IN THE ENDWALL REGION OF AN ANNULAR TURBINE CASCADE UTILIZING A PRESSURIZED AERODYNAMIC WINDOW   |  | 5.FUNDING NUMBERS                                      |                                    |  |
| 6.AUTHOR(S)<br>Guerrera, Michael H.   |  |  |                                    |  |
| 7.PERFORMING ORGANIZATION NAME(S) AND ADDRESS(ES)<br>Naval Postgraduate School<br>Monterey CA 93943-5000  |  | 8.PERFORMING ORGANIZATION REPORT NUMBER                |                                    |  |
| 9.SPONSORING/MONITORING AGENCY NAME(S) AND ADDRESS(ES)<br>Naval Air Warfare Center Aircraft Division, AIR-4.4.3.1(Attn: D. Parish)<br>Propulsion and Power Engineering, Building 106, Patuxent River, MD 20670-5304   |  | 10.SPONSORING/MONITORING AGENCY REPORT NUMBER          |                                    |  |
| 11.SUPPLEMENTARY NOTES The views expressed in this thesis are those of the author and do not reflect the official policy or position of the Department of Defense or the U.S. Government.   |  |  |                                    |  |
| 12a.DISTRIBUTION/AVAILABILITY STATEMENT<br>Approved for public release; distribution is unlimited.  |  | 12b. DISTRIBUTION CODE                                 |                                    |  |
| 13.ABSTRACT(maximum 200 words)<br>The purpose of this research was to compare previous laser-anemometry measurements obtained through an unpressurized laser window with the results from a pressurized laser window and to validate this innovative measuring technique in the endwall region of a confined annulus. Two-dimensional velocity, flow angle, and turbulence intensity measurements were obtained with a fiber-optics laser-Doppler velocimeter. The measurements were performed through a 1.09 mm opening in the endwall region of an annular turbine cascade at depths ranging from 0.01 mm to 0.89 mm with varying pressure applied to the chamber of the modified window. Cobra probe measurements were performed to validate the flow angles obtained by the laser anemometer. The cascade was modified to measure the inlet profile, which was performed with a three-hole probe. |  |  |                                    |  |
| 14. SUBJECT TERMS Annular Turbine Cascade, Surface Pressure Measurement, Laser-Doppler Velocimetry, Cobra Probe   |  | 15.NUMBER OF PAGES<br>108                              |                                    |  |
|   |  | 16.PRICE CODE  |                                    |  |
| 17. SECURITY CLASSIFICATION OF REPORT<br>Unclassified   | 18. SECURITY CLASSIFICATION OF THIS PAGE<br>Unclassified | 19.SECURITY CLASSIFICATION OF ABSTRACT<br>Unclassified | 20.LIMITATION OF ABSTRACT<br>UL    |  |

NSN 7540-01-280-5500  
Form 298 (Rev. 2-89)

Std. 239-18

Standard

Prescribed by ANSI

298-102



Approved for public release; distribution is unlimited.

**LASER ANEMOMETRY AND PRESSURE MEASUREMENTS IN THE ENDWALL  
REGION OF AN ANNULAR TURBINE CASCADE UTILIZING A PRESSURIZED  
AERODYNAMIC WINDOW**

Michael H. Guerrero  
Lieutenant, United States Navy  
B.S., United States Naval Academy, 1986

Submitted in partial fulfillment of the  
requirements for the degree of

**MASTER OF SCIENCE IN AERONAUTICAL ENGINEERING**

from the

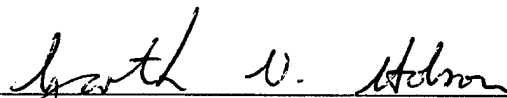
**NAVAL POSTGRADUATE SCHOOL**

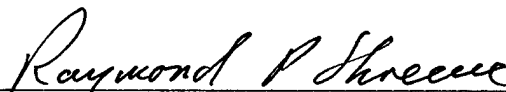
**September 1996**

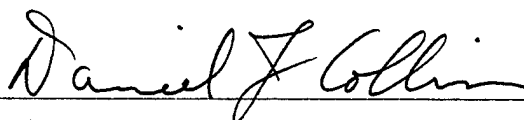
Author:

  
Michael H. Guerrero

Approved by:

  
Garth V. Hobson, Thesis Advisor

  
Raymond P. Shreeve, Second Reader

  
Daniel J. Collins, Chairman  
Department of Aeronautics and Astronautics



## ABSTRACT

The purpose of this research was to compare previous laser-anemometry measurements obtained through an unpressurized laser window with the results from a pressurized laser window and to validate this innovative measuring technique in the endwall region of a confined annulus. Two-dimensional velocity, flow angle, and turbulence intensity measurements were obtained with a fiber-optics laser-Doppler velocimeter. The measurements were performed through a 1.09 mm opening in the endwall region of an annular turbine cascade at depths ranging from 0.01 mm to 0.89 mm with varying pressure applied to the chamber of the modified window. Cobra probe measurements were performed to validate the flow angles obtained by the laser anemometer. The cascade was modified to measure the inlet profile, which was performed with a three-hole probe.





## TABLE OF CONTENTS

|  |    |
|--|----|
| I. INTRODUCTION.....   | 1  |
| II. EXPERIMENTAL APPARATUS.....  | 3  |
| A. TEST FACILITY AND ANNULAR TURBINE CASCADE .....   | 3  |
| B. PRESSURE DATA ACQUISITION.....  | 5  |
| C. LASER-DOPPLER VELOCIMETER.....  | 6  |
| D. PRESSURIZED LASER WINDOW.....   | 7  |
| E. COBRA PROBE .....   | 9  |
| III. EXPERIMENTAL PROCEDURE.....   | 11 |
| A. MIDSPAN SURFACE PRESSURE MEASUREMENTS.....  | 11 |
| B. LASER MEASUREMENTS .....  | 11 |
| C. COBRA PROBE CALIBRATION AND MEASUREMENTS.....   | 14 |
| IV. RESULTS AND DISCUSSION.....  | 17 |
| A. BLADE MIDSPAN SURFACE PRESSURE MEASUREMENTS .....   | 17 |
| B. LASER-DOPPLER VELOCIMETRY MEASUREMENTS .....  | 19 |
| 1. Comparison of a 1-D Procedure with 2-Component Measurements.....                                  | 19 |
| 2. Laser Blank Measurements at a Pressure Ratio of 0.9620 .....                                      | 23 |
| 3. Radial Measurements with Pressurized Window at Various Chamber Pressures.....                     | 28 |
| 4. Radial Survey Comparison between Pressurized Laser Window and Laser Blank.....                    | 32 |
| 5. Effect of Various Chamber Pressures Compared to Laser Blank.....                                  | 35 |
| 6. Circumferential Surveys with Pressurized Window at 76.2 mm (3 in) water Chamber<br>Pressure ..... | 38 |
| 7. Final Comparison with Laser Blank, Pressurized LDV Window, and Cobra Probe ....                   | 41 |
| V. CONCLUSIONS AND RECOMMENDATIONS .....   | 47 |
| APPENDIX A. PRESSURE DATA ACQUISITION.....   | 49 |
| APPENDIX B. BLADE MIDSPAN SURFACE PRESSURE DATA.....   | 51 |

|   |    |
|---|----|
| APPENDIX C. LDV DATA.....                             | 63 |
| APPENDIX D. 3 HOLE COBRA PROBE DATA.....              | 75 |
| APPENDIX E. PRESSURIZED WINDOW DRAWINGS.....          | 77 |
| APPENDIX F. FREEJET .....                             | 81 |
| APPENDIX G. PRESSURIZED WINDOW AT PRAT OF 0.9054..... | 85 |
| LIST OF REFERENCES.....                               | 89 |
| INITIAL DISTRIBUTION LIST .....                       | 91 |

## LIST OF FIGURES

|  |    |
|--|----|
| Figure 1. Annular turbine cascade (ATC).....   | 3  |
| Figure 2. Side view of ATC, Scanivalve, and six-jet atomizer.....                        | 4  |
| Figure 3. Hewlett Packard pressure data acquisition schematic.....                       | 5  |
| Figure 4. LDV bread board (with laser, color separator, and color link).....             | 7  |
| Figure 5a. Laser blank and pressurized LDV window .....                                  | 8  |
| Figure 5b. Cross-section of pressurized LDV window .....                                 | 8  |
| Figure 6. Cobra probe pressure data acquisition schematic .....                          | 9  |
| Figure 7. LINTECH traverse table .....   | 12 |
| Figure 8. LDV system schematic .....   | 13 |
| Figure 9. LDV alignment schematic .....  | 13 |
| Figure 10. Measurement test matrix.....  | 14 |
| Figure 11. Three-hole cobra probe calibration apparatus.....                             | 15 |
| Figure 12. $P/P_0$ vs. $x/c$ for 0.9620 pressure ratio.....                              | 17 |
| Figure 13. $P/P_0$ vs. $x/c$ for 0.9826 through 0.9575 pressure ratios .....             | 18 |
| Figure 14. $P/P_0$ vs. $x/c$ for 0.9527 through 0.9313 pressure ratios .....             | 18 |
| Figure 15a. A radial survey through the laser blank at a $Prat$ of 0.9054.....           | 20 |
| Figure 15b. A radial survey through the laser blank at a $Prat$ of 0.9054.....           | 20 |
| Figure 16a. A radial survey through the laser blank at a $Prat$ of 0.9054.....           | 22 |
| Figure 16b. A radial survey through the laser blank at a $Prat$ of 0.9054.....           | 22 |
| Figure 17. A radial survey through the laser blank at a $Prat$ of 0.9054.....            | 23 |
| Figure 18. A radial survey through the laser blank at a $Prat$ of 0.9620.....            | 24 |
| Figure 19. A radial survey through the laser blank at a $Prat$ of 0.9620.....            | 24 |
| Figure 20. A radial survey through the laser blank at a $Prat$ of 0.9620.....            | 25 |
| Figure 21a. A circumferential survey through the laser blank at a $Prat$ of 0.9620 ..... | 26 |
| Figure 21b. A circumferential survey through the laser blank at a $Prat$ of 0.9620.....  | 26 |

|  |    |
|--|----|
| Figure 22a. A circumferential survey through the laser blank at a Prat of 0.9620 .....                                 | 27 |
| Figure 22b. A circumferential survey through the laser blank at a Prat of 0.9620.....                                  | 27 |
| Figure 23. A circumferential survey through the laser blank at a Prat of 0.9620.....                                   | 28 |
| Figure 24a. A radial survey through the pressurized LDV window at a Prat of 0.9620.....                                | 30 |
| Figure 24b. A radial survey through the pressurized LDV window at a Prat of 0.9620.....                                | 30 |
| Figure 25a. A radial survey through the pressurized LDV window at a Prat of 0.9620.....                                | 31 |
| Figure 25b. A radial survey through the pressurized LDV window at a Prat of 0.9620.....                                | 31 |
| Figure 26. A radial survey through the pressurized LDV window at a Prat of 0.9620.....                                 | 32 |
| Figure 27a. Comparisons of radial surveys using the laser blank and pressurized LDV<br>window at a Prat of 0.9620..... | 33 |
| Figure 27b. Comparisons of radial surveys using the laser blank and pressurized LDV<br>window at a Prat of 0.9620..... | 33 |
| Figure 28a. Comparisons of radial surveys using the laser blank and pressurized LDV<br>window at a Prat of 0.9620..... | 34 |
| Figure 28b. Comparisons of radial surveys using the laser blank and pressurized LDV<br>window at a Prat of 0.9620..... | 34 |
| Figure 29. Comparisons of radial surveys using the laser blank and pressurized LDV window<br>at a Prat of 0.9620 ..... | 35 |
| Figure 30a. Pressurized LDV window and laser blank comparisons at Prat of 0.9620 .....                                 | 36 |
| Figure 30b. Pressurized LDV window and laser blank comparisons at Prat of 0.9620.....                                  | 36 |
| Figure 31a. Pressurized LDV window and laser blank comparisons at Prat of 0.9620 .....                                 | 37 |
| Figure 31b. Pressurized LDV window and laser blank comparisons at Prat of 0.9620.....                                  | 37 |
| Figure 32. Pressurized LDV window and laser blank comparisons at Prat of 0.9620.....                                   | 38 |
| Figure 33a. A circumferential survey through the pressurized LDV window at a Prat of<br>0.9620.....                    | 39 |
| Figure 33b. A circumferential survey through the pressurized LDV window at a Prat of<br>0.9620.....                    | 39 |

|  |    |
|--|----|
| Figure 34a. A circumferential survey through the pressurized LDV window at a Prati of 0.9620.....  | 40 |
| Figure 34b. A circumferential survey through the pressurized LDV window at a Prati of 0.9620.....  | 40 |
| Figure 35. A circumferential survey through the pressurized LDV window at a Prati of 0.9620.....   | 41 |
| Figure 36. Final total non-dimensional velocity comparison between laser blank, pressurized window, and 3-hole cobra probe at a Prati of 0.9620..... | 42 |
| Figure 37. Final flow angle comparison between laser blank, pressurized window, and 3-hole cobra probe at a Prati of 0.9620.....                     | 42 |
| Figure 38. ATC flow depiction - the 3-hole cobra probe .....   | 44 |
| Figure 39. ATC flow depiction - laser blank.....   | 44 |
| Figure 40. ATC flow depiction - pressurized window.....  | 45 |
| Figure D1. 3-Hole cobra probe calibration curve.....   | 75 |
| Figure E1. Side view of pressurized window .....   | 77 |
| Figure E2. Top view of pressurized window.....   | 78 |
| Figure E3. Front view of pressurized window.....   | 79 |
| Figure E4. Plexiglas window cover .....  | 80 |
| Figure F1. Freejet Survey .....  | 83 |
| Figure F2. Freejet Survey .....  | 83 |
| Figure F3a. Freejet Survey.....  | 84 |
| Figure F3b. Freejet Survey .....   | 84 |
| Figure G1a. A radial survey through the pressurized window at a Prati of 0.9054.....   | 86 |
| Figure G1b. A radial survey through the pressurized window at a Prati of 0.9054.....   | 86 |
| Figure G2a. A radial survey through the pressurized window at a Prati of 0.9054.....   | 87 |
| Figure G2b. A radial survey through the pressurized window at a Prati of 0.9054.....   | 87 |
| Figure G3. A radial survey through the pressurized window at a Prati of 0.9054.....  | 88 |



## LIST OF TABLES

|  |    |
|--|----|
| Table A1. Pressure data acquisition connections.....   | 49 |
| Table B1. Surface pressures at 0.9825 pressure ratio .....   | 51 |
| Table B2. Surface pressures at 0.9757 pressure ratio .....   | 52 |
| Table B3. Surface pressures at 0.9710 pressure ratio .....   | 53 |
| Table B4. Surface pressures at 0.9669 pressure ratio .....   | 54 |
| Table B5. Surface pressures at 0.9621 pressure ratio .....   | 55 |
| Table B6. Surface pressures at 0.9575 pressure ratio .....   | 56 |
| Table B7. Surface pressures at 0.9527 pressure ratio .....   | 57 |
| Table B8. Surface pressures at 0.9483 pressure ratio .....   | 58 |
| Table B9. Surface pressures at 0.9445 pressure ratio .....   | 59 |
| Table B10. Surface pressures at 0.9392 pressure ratio .....  | 60 |
| Table B11. Surface pressures at 0.9359 pressure ratio .....  | 61 |
| Table B12. Surface pressures at 0.9312 pressure ratio .....  | 62 |
| Table C1. 04/16/96 Laser blank radial survey at 0.9054 pressure ratio.....   | 63 |
| Table C2. 04/26/96 Laser blank radial survey at 0.9054 pressure ratio.....   | 64 |
| Table C3. 04/26/96 Laser blank circumferential survey at 0.9054 pressure ratio .....   | 68 |
| Table C4. 04/19/96 Laser blank radial survey at 0.9620 pressure ratio.....   | 69 |
| Table C5. 04/30/96 Laser blank and pressurized window comparison at 0.9620 pressure ratio.....                                   | 70 |
| Table C6. 05/14/96 Pressurized window radial survey at 0.9620 pressure ratio.....  | 71 |
| Table C7. 05/10/96 Pressurized window circumferential survey at 76.2 mm water chamber<br>pressure and 0.9620 pressure ratio..... | 74 |
| Table D1. 3-Hole cobra probe calibration data.....   | 75 |
| Table D2. A radial survey utilizing the 3-hole cobra probe at a Pr <sub>at</sub> of 0.9620.....                                  | 76 |
| Table F1. Freejet data.....  | 82 |
| Table G1. Pressurized window data at a Pr <sub>at</sub> of 0.9054.....   | 85 |





## ACKNOWLEDGMENTS

This work would not have been possible without the guidance and support of several dedicated individuals. I thank Professor Garth Hobson for his friendship, patience, and sincere passion for engineering. His ability to touch the lives of so many with his vast knowledge while motivating individual interests make him one of the finest instructors that I have ever had.

The combination of a friendly working environment and technical expertise make the Turbopropulsion Laboratory an outstanding place for research. My thanks to Professor Shreeve, Rick Still, Thad Best, and Don Harvey who assisted me numerous times during my project. ---"Don't Touch the Blue Knob!"

My greatest thanks go to my family. The continuous motivation instilled in me by my parents, Louis and Miyuki, and the sense of humor provided by my brother, Peter, will guide me for life. They have accomplished everything along with me and have made me a better person. Finally, my thanks to my best friend and wife, Eleanor. Her constant drive, continuous support, and smiling face will always be in my heart. Aloha to you all.



## I. INTRODUCTION

Modern propulsion systems have improved rapidly over the last few decades which in turn have required continual developments in measurement techniques in turbomachinery. Non-intrusive measurement techniques are essential for providing the fundamental insight of the secondary flows in the annular blade rows of the next generation turbines. The design and performance of turbomachinery begin with this understanding. Secondary flows, together with tip leakage flows, produce considerable flow distortions in the endwall region which results in the majority of the losses within a turbine [Ref. 1]. By understanding the flow mechanics in this region, current CFD programs can be validated, improving both current blade designs and turbine efficiencies.

Three previous investigations of the flow through the annular turbine cascade (ATC) have been conducted at the Naval Postgraduate School [Ref. 2-4]. Reference 4 included design and manufacturing information of the annular turbine cascade that was developed to determine the limitations of laser-Doppler velocity (LDV) measurements in a confined annulus. Reference 3 included additional laser and pressure probe access modifications and initial LDV measurements within the same ATC. Reference 2 included further ATC modifications for midspan blade surface pressure measurements and LDV measurements of the endwall flow. The present study was of the feasibility of an innovative pressurized laser window and then to determine its effect on current LDV near-wall flow measurements. Three-hole pressure probe measurements were also conducted to compare with the LDV measurements. Radial LDV surveys were performed through a small access hole in the outer casing through the pressurized window to compare with previous results that used an open aerodynamic window (laser blank). Circumferential surveys were obtained at different radial locations close to the endwall. Blade midspan surface pressures were measured within one blade passage at various inlet total-to-downstream hub-static pressure ratios. Blade surface pressure and endwall flow measurements were compared with previous measurements.



## II. EXPERIMENTAL APPARATUS

### A. TEST FACILITY AND ANNULAR TURBINE CASCADE

The ATC was developed to provide small-scale testing of flow through a turbine stator. Airflow for the Annular Turbine Cascade experiment was provided by a VA-312 Allis-Chalmers 12-stage axial-flow compressor located at the Turbopropulsion Laboratory of the Naval Postgraduate School. The compressor was operated at 12,000 rpm at various discharge pressures and provided metered air to a plenum chamber. Air from the plenum was routed to a 232 mm (9.170 in) diameter bellmouth and test section through honeycomb flow straighteners in a 254 mm (10 in) flanged steel pipe as shown in Figure 1.

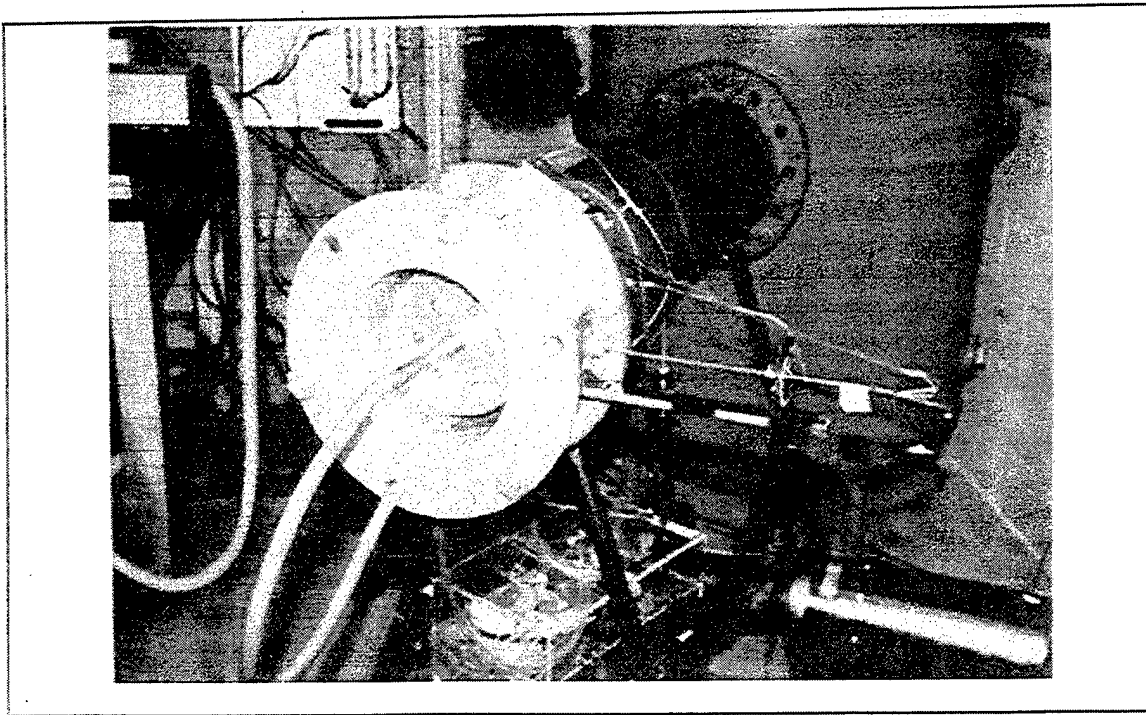


Figure 1. Annular turbine cascade (ATC)

Flow stagnation pressure was measured at two upstream locations. One combination probe provided pressure-setting information to a mercury manometer board and a digital readout of flow stagnation temperature, while the second probe was connected to a Scanivalve (Figure 2). Four (averaged) upstream static ports and four (averaged) inner hub downstream (one-half axial chord) static ports were also connected to the Scanivalve for automated pressure data acquisition.

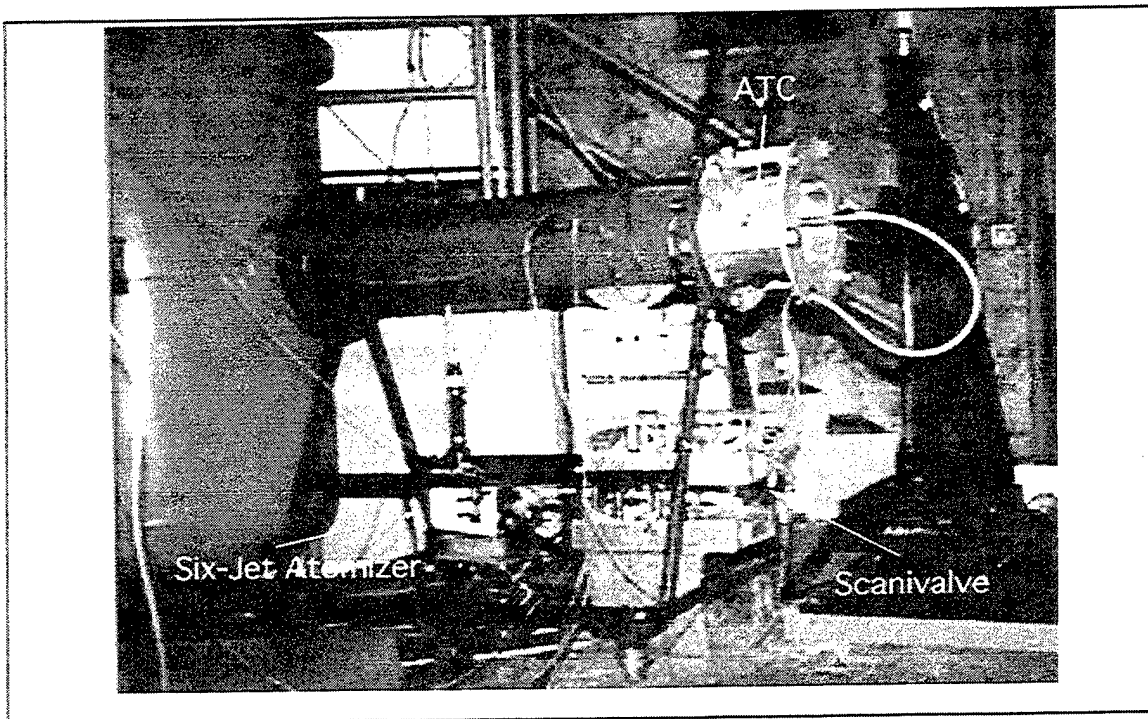


Figure 2. Side view of ATC, Scanivalve, and six-jet atomizer

Atomized glycerin particles constituted the LDV seed material which were introduced through a 8 mm (0.31 in) diameter copper tube approximately more than 100 tube diameters upstream of the test section. Seed atomization was performed using a commercial TSI, Inc., Six-Jet Atomizer connected to the laboratory compressed air supply as shown in Figure 2.

Each blade was designed with a combination of simple circular arcs and line segments and included a leading edge radius of 2 mm (0.095 in), trailing edge radius of 0.31 mm

(0.012 in), and axial chord of 25 mm (0.975 in). The annular stator row was manufactured from 2218-T61 aluminum and consisted of 31 blades with a midspan spacing of 22 mm (0.857 in), resulting in a blade solidity of 1.14. The inner hub radius was 99 mm (3.895 in) and the outer case radius was 116 mm (4.585 in) with the same profile at all radii [Ref. 2]. Reference 4 included the original set of ATC manufacturing drawings. Reference 3 included a description of the wake positioning system. Reference 2 included the location of the blade surface static pressure ports.

## B. PRESSURE DATA ACQUISITION

The data acquisition system, for the blade surface pressure measurements, is shown schematically in Figure 3. All data acquisition was remotely controlled by a Hewlett-Packard 9000 computer system. Reference 2 contains the program utilized to conduct all pressure data acquisition.

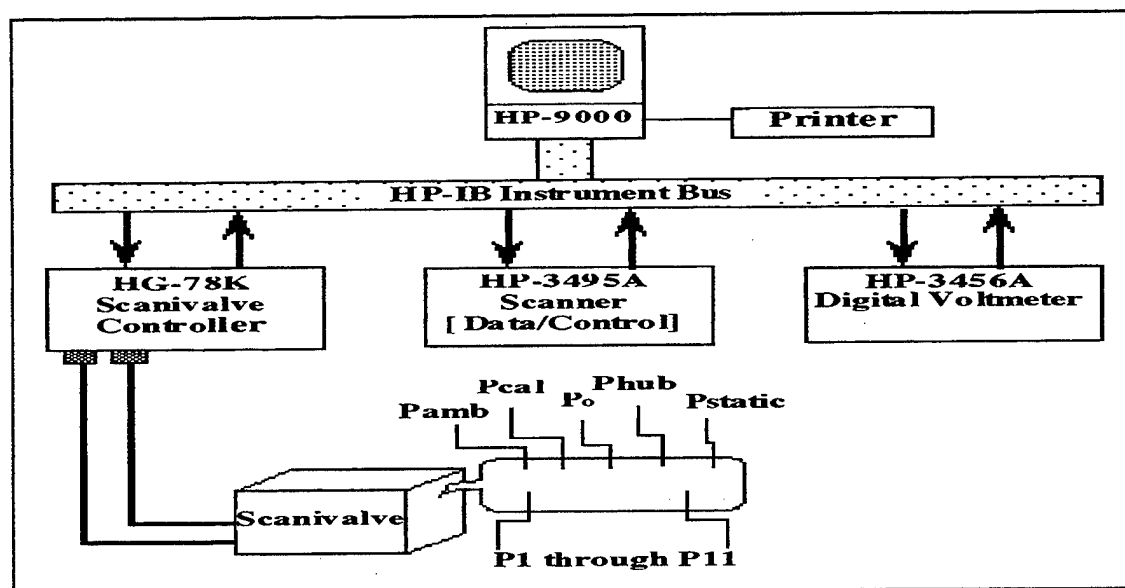


Figure 3. Hewlett Packard pressure data acquisition schematic

A Scanivalve was connected to a Model HG-78K Scanivalve controller, which in turn was connected to a Hewlett-Packard, Model 3456A Digital Voltmeter and Model 3495A Scanner

via a HP-IB instrument bus. Scanivalve calibration was performed to within an accuracy of  $\pm 0.1$  inches mercury. Table A1 in Appendix A relates each Scanivalve port to its respective pressure measurement.

### C. LASER-DOPPLER VELOCIMETER

The LDV system consisted of a LEXEL Model 95 four-Watt argon-ion laser connected to a TSI, Inc., Model 9201 ColorBurst multicolor beam separator (Figure 4). The beam separator divided the incoming light into shifted and unshifted beams, with the shifted beam receiving a 40 MHz frequency shift from a Bragg cell. The two beams were further split into three polarized pairs: green (514.5 nm), blue (488 nm), and violet (476.5 nm). The complete system was shown schematically in Figure 8.

Individual couplers on the ColorBurst directed each beam to the laser probe via a fiber-optic cable. Each fiber-optic probe contained receiving optics which directed the return signal to a TSI, Inc., Model 9230 ColorLink multicolor receiver (Figure 4). The ColorLink provided photomultiplier and frequency-shifting functions. All conditioned ColorLink signals were sent to a TSI, Inc., Model 1990C signal processor where valid Doppler signals were counted with reference to characteristics selected by the user. Utilizing only the green beam due to its greater strength, the MI-990 interface monitored the random criteria (1-component measurement) and then transferred the valid counter information to computer memory.

The laser apparatus included the laser probe and traverse mechanism. The fiber-optic probe was mounted to a LINTECH, Model 41583 traverse table (Figure 7). An Applied Motion Products System 1618 traverse controller was used to control the traverse table movement both manually and by computer. All ColorLink, MI-990 functions, and LDV data processing were accomplished remotely by computer using TSI's menu-driven software, FIND (FLOW INFORMATION DISPLAY) version 4.04.



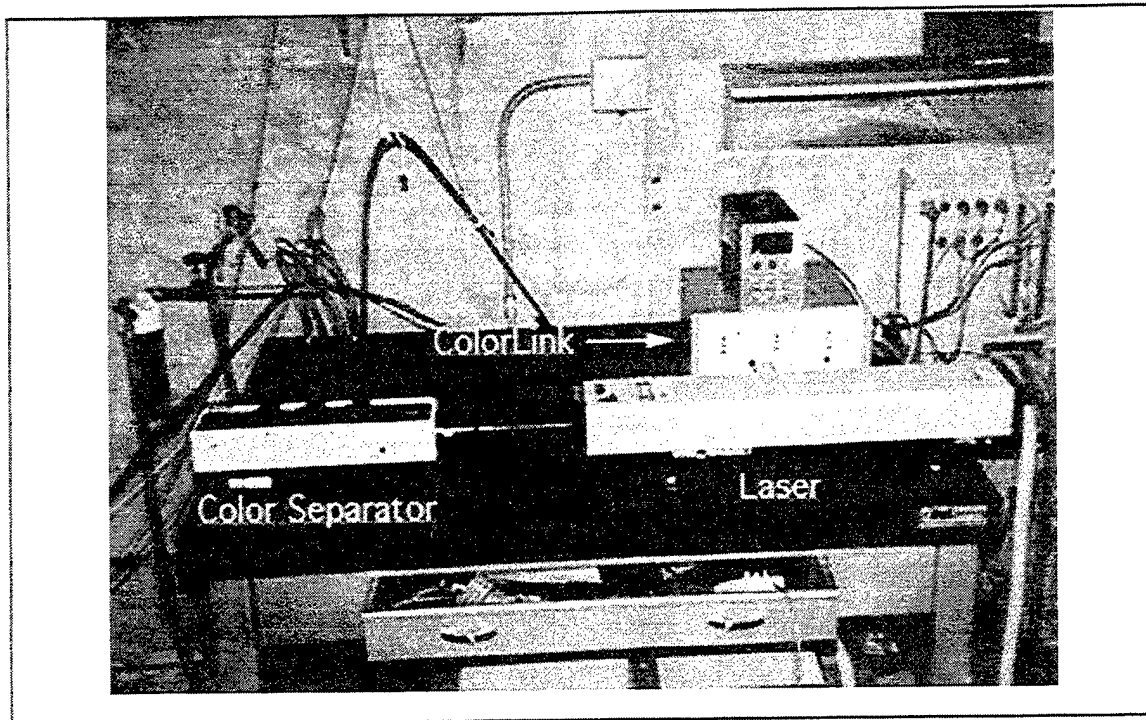


Figure 4. LDV bread board (with laser, color separator, and color link)

#### D. PRESSURIZED LASER WINDOW

A pressurized laser window was designed and manufactured in order to prevent the flow of air and seed material out of the 1.092 mm optical access hole. The new laser window entailed three modifications (Figure 5a). The first was to transform the previously flat laser blank into a chambered component. The second was to install internal plumbing into the chamber which included a .33 mm (.013 in) diameter static pressure port near the 1.092 mm (.043 in) diameter laser opening and two 1.27 mm (.05 in) diameter ports for pressurizing and sensing the chamber pressure. The third was to install a 6.35 mm (.25 in) acrylic window on a 1.58 mm (.0625 in) O-ring for sealing. The positioning of the new window and its components are depicted in Figure 5b. Appendix E shows the complete engineering drawings of the new pressurized LDV window.

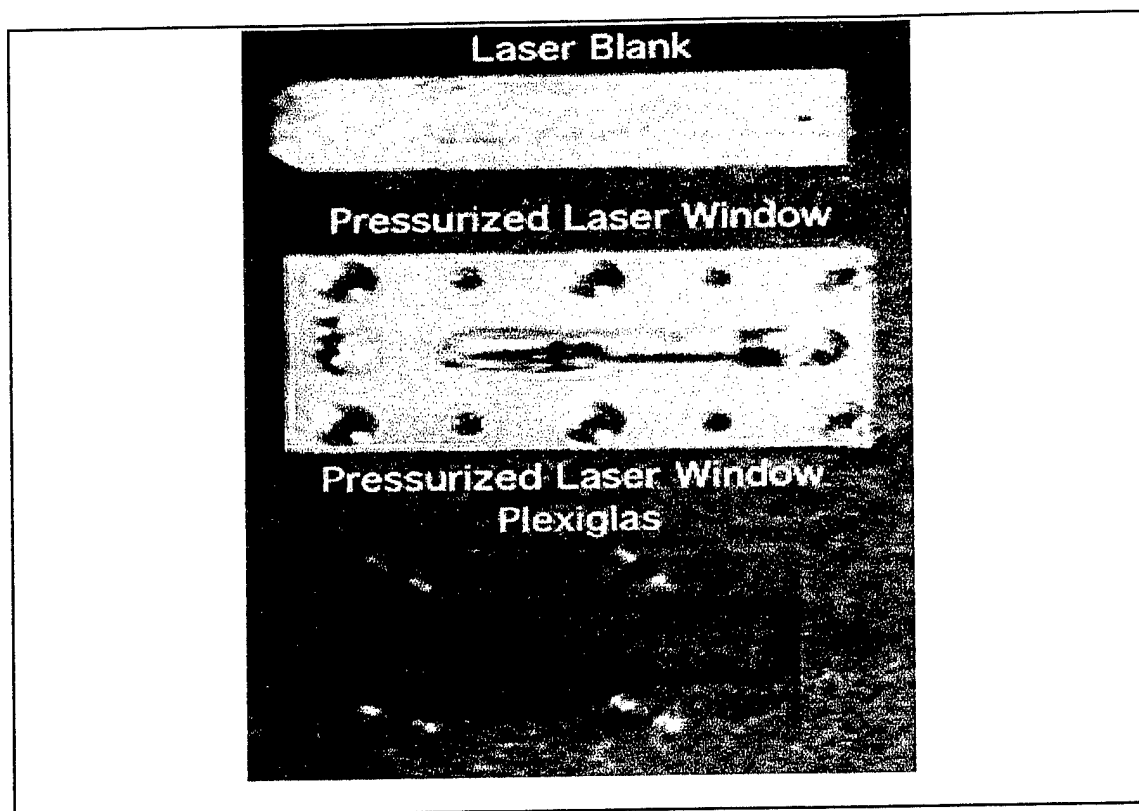


Figure 5a. Laser blank and pressurized LDV window

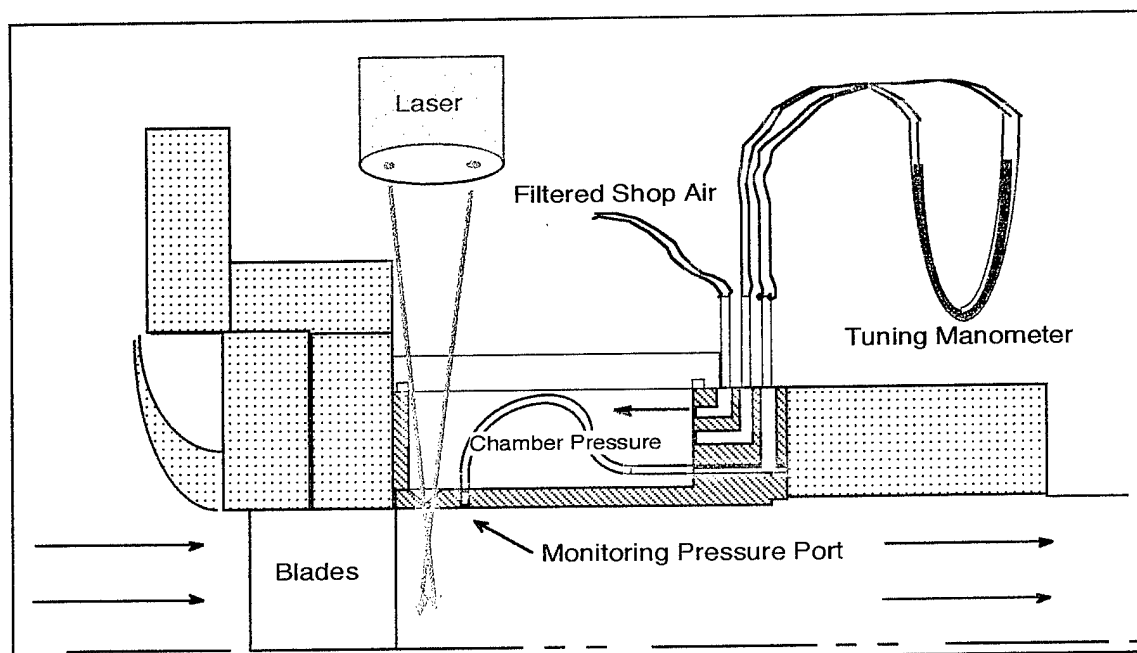


Figure 5b. Cross-section of pressurized LDV window

### E. COBRA PROBE

Scanivalve control and data recording were accomplished using National Instruments' software, LabView, operating on a 486 PC system whose schematic is shown in Figure 6. Total pressure, non-dimensional velocity and flow angle measurements were performed with a three-hole yaw probe [Ref. 3]. All pressure taps were connected to a Scanivalve with a 2.5 psi differential pressure transducer. Probe calibration was also accomplished using this acquisition system. Appendix D contains the probe calibration measurement data and third-order calibration curves.

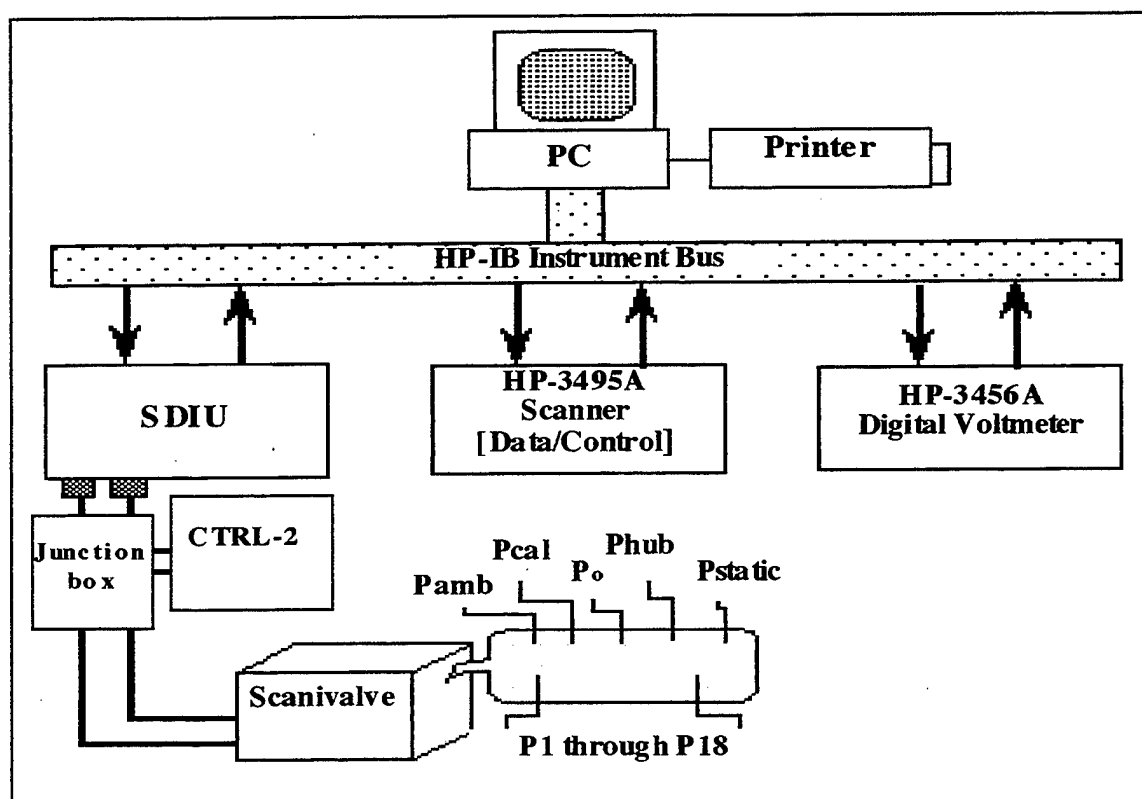


Figure 6. Cobra probe pressure data acquisition schematic



### III. EXPERIMENTAL PROCEDURE

#### A. MIDSPAN SURFACE PRESSURE MEASUREMENTS

Midspan surface pressure measurements were obtained with the Hewlett Packard (HP) data acquisition system. The pressure ratio ( $P_{rat}$ ) was defined as the downstream hub-static pressure ( $P_{hub}$ ) divided by the upstream stagnation pressure ( $P_0$ ). Each pressure ratio was achieved by metering the upstream stagnation pressure until a desired water column height was achieved. Twelve pressure ratios from 0.9826 to 0.9313 in steps of 0.0048 were considered and during each run all blade surface pressures,  $P_0$ , and  $P_{hub}$  were recorded. A midpoint  $P_{rat}$  of 0.9620 which was equivalent to 408.94 mm (16.1 in) of water was decided upon as the desired pressure ratio for the LDV surveys utilizing the pressurized laser window.

#### B. LASER MEASUREMENTS

LDV alignment for endwall flow measurements was accomplished as shown in Figure 9. The objective of the LDV alignment procedure was to center the probe volume into the 1.092 mm optical access hole and reset the traverse table coordinates to a relative home position. A one-component fiber-optic probe was attached to the traverse table (Figure 7) which was controlled both manually and by computer.

Using the laser blank as an alignment guide for the green laser beams, the traverse table was manually advanced radially until the beam separation was minimized on its surface, yet discernible with the naked eye (Figure 9, Point A). The traverse table was then manually positioned to the midpoint of the optical hole which placed the LDV probe volume at a consistent starting point. The traverse table was then homed relative to this new position. Once the horizontal measurements were completed, the LDV probe was then manually rotated and the alignment process was repeated for the vertical measurements. This alignment technique was repeatable and ensured that the probe volume was consistently positioned at the

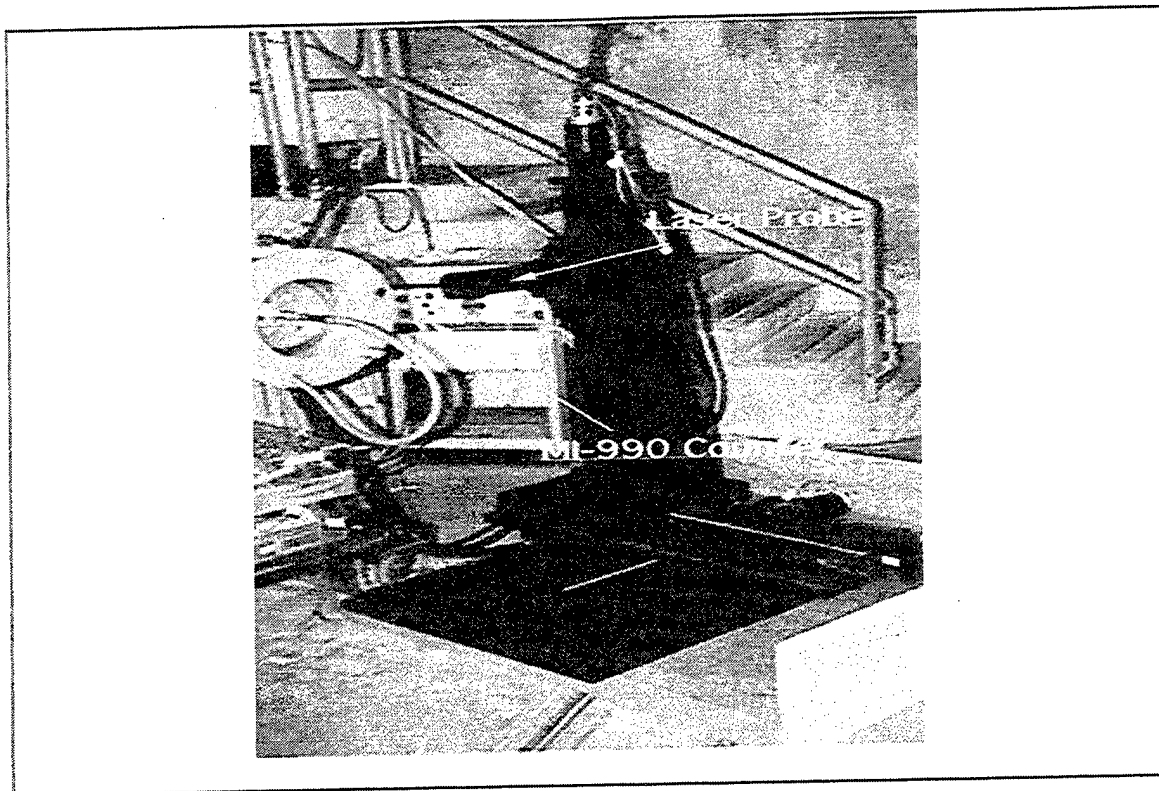


Figure 7. LINTECH traverse table

center of the optical access hole. Hole alignment and laser power (2.0 Watts) were periodically verified as these could drift due to temperature changes within the testing cell. Reference 3 described complete dimensions of the laser blank.

Radial traversing of the LDV positioned the measurement volume at various depths within the ATC and measurements were performed through the new pressurized window's optical access hole in the outer casing. These results were compared with previous measurements utilizing the laser blank. The circumferential LDV surveys were executed in a similar manner. The probe volume was first positioned by the traverse table to a fixed radial depth within the ATC. The stator ring was then circumferentially positioned from -8 to +8 degrees of its initial setting. These circumferential surveys were obtained at different radial locations close to the endwall. With both of these surveys completed, the measurement test matrix near the end wall was defined (Figure 10).

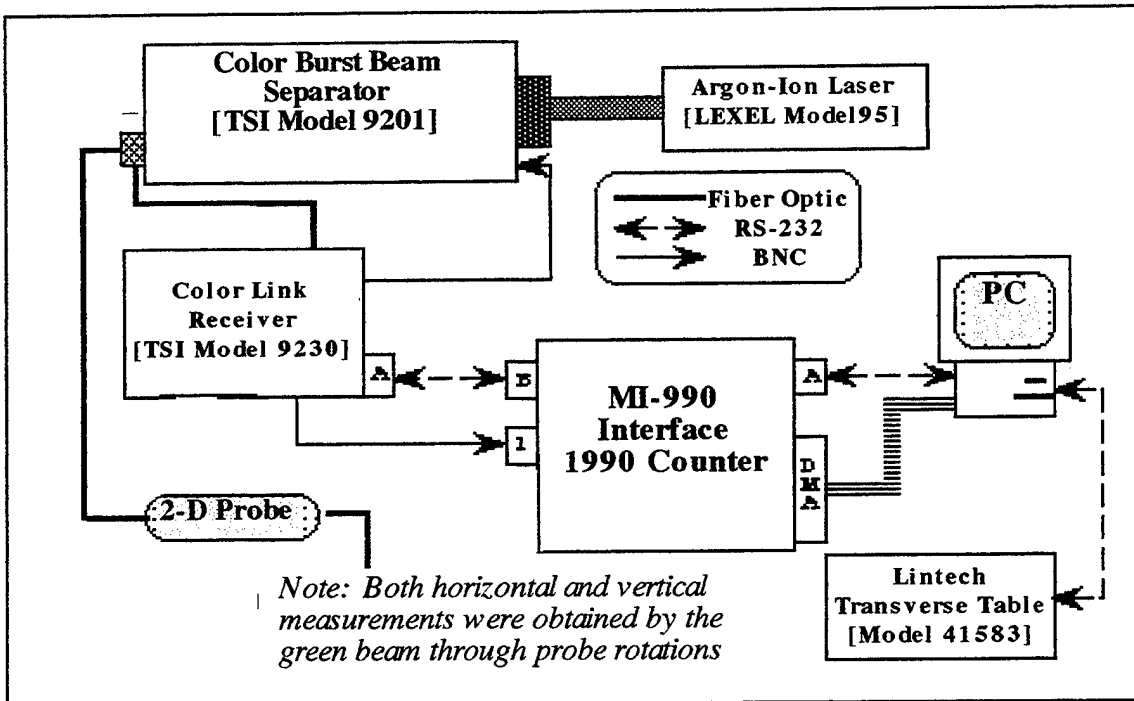


Figure 8. LDV system schematic

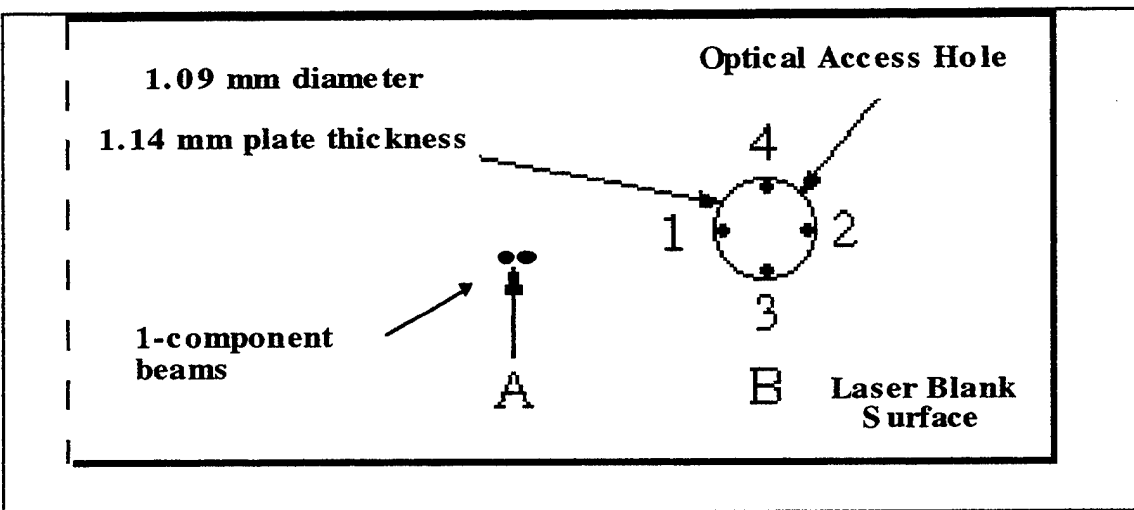


Figure 9. LDV alignment schematic

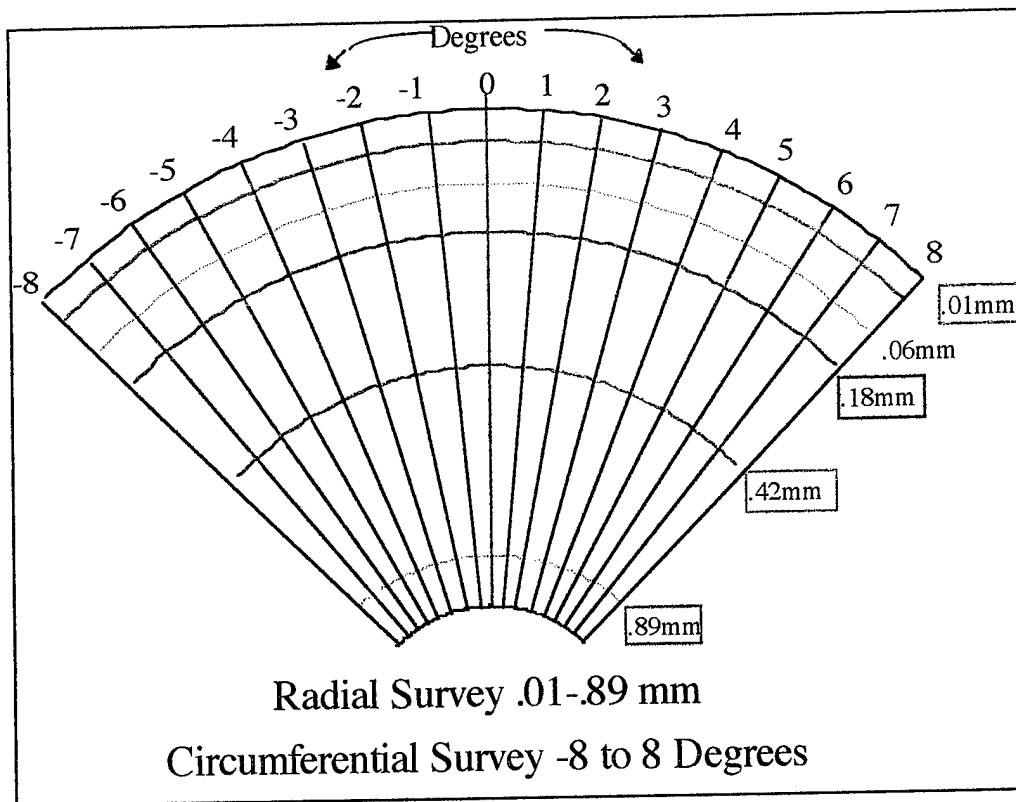


Figure 10. Measurement test matrix

### C. COBRA PROBE CALIBRATION AND MEASUREMENTS

The calibration of the three-hole cobra probe was accomplished using the free-jet apparatus connected to the air supply previously used for the ATC (Figure 11). The LabView software program controlled the calibration procedure and the resultant data was transferred to a spreadsheet for further processing.



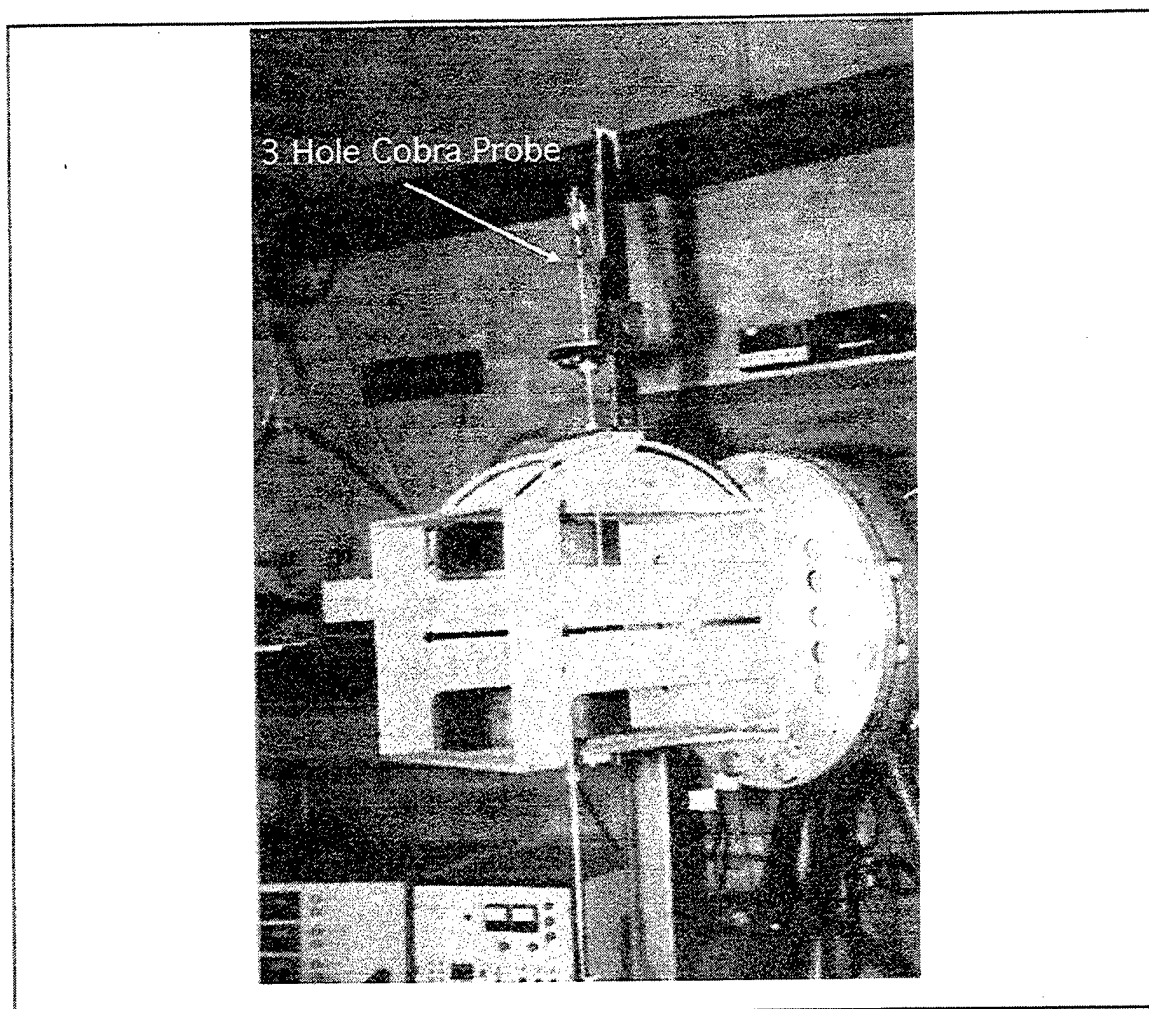


Figure 11. Three-hole cobra probe calibration apparatus

The probe was manually aligned in yaw using a water manometer at 406 mm (16.1 in) water of air pressure. Once the manometer equalized, the probe was checked at both pressure ratio extremes of the planned calibration. The probe was then calibrated at 101 mm (4 in) of water and in increments of approximately 101 mm (4 in) to 716 mm (28.2 in) of water. Reference 3 contains a description of the calibration variables and formulas. Third-order polynomials were fit through the calibration data and these are given in Appendix D.

Radial surveys of 0.42, 0.89, and 1.78 mm (0.016, 0.035, and 0.070 in) at a pressure ratio of 0.9620 were conducted to compare with previous LDV data from both the laser blank

and pressurized window. The probe measured total pressure and flow angle. Utilizing formulas from Reference 3, the values for velocity were calculated and non-dimensionalized. The total non-dimensional velocity ( $X$ ) was defined as the measured velocity divided by the 'total' velocity. The total velocity was the square root of twice the total temperature multiplied by the specific heat at constant pressure. The same data acquisition system was used for both the surveys and the probe calibration. Flow angles were read from a vernier scale attached to the probe with an accuracy of plus or minus 0.2 degrees and recorded manually into the front panel of the LabView software program.

## IV. RESULTS AND DISCUSSION

### A. BLADE MIDSPAN SURFACE PRESSURE MEASUREMENTS

Experimental blade-surface pressure measurements were conducted over a range of pressure ratios which covered the pressure ratio at which LDV data were to be collected through the new laser window. Each blade static port reading was non-dimensionalized by the upstream stagnation pressure ( $P_0$ ). Appendix B contains the pressure data for the 12 pressure ratios tested.

From the twelve pressure ratios measured, the middle pressure ratio of 0.9620 was selected to test the new pressurized window. Figure 12 shows the pressure profile around the blades for the above pressure ratio. Figures 13 and 14 show the remaining pressure ratios measured which show increased loading with decreased pressure ratio.

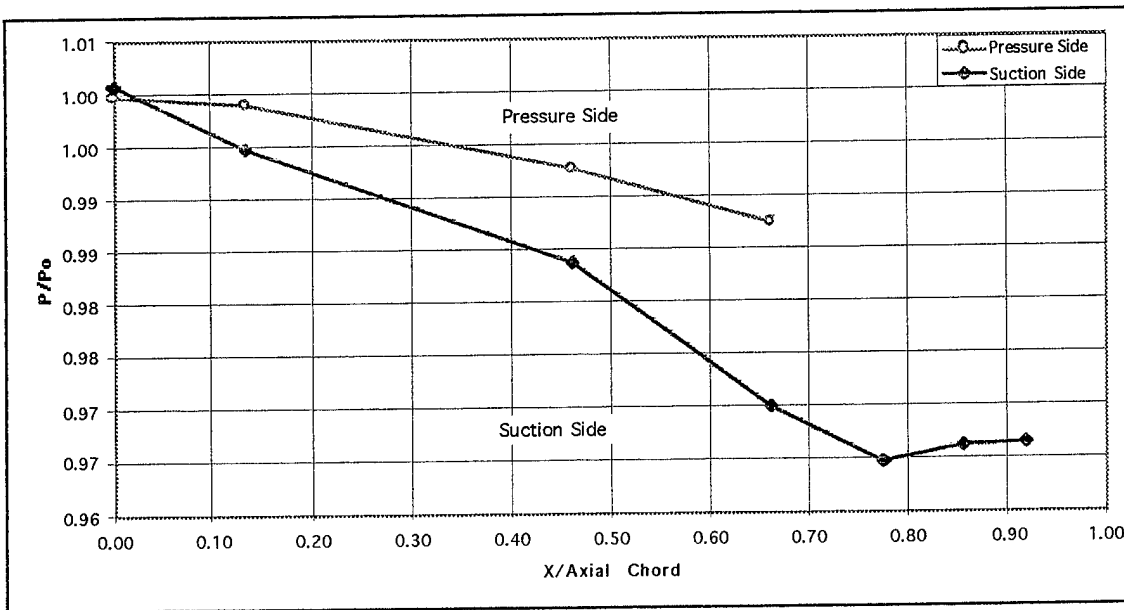


Figure 12.  $P/P_0$  vs.  $x/c$  for 0.9620 pressure ratio

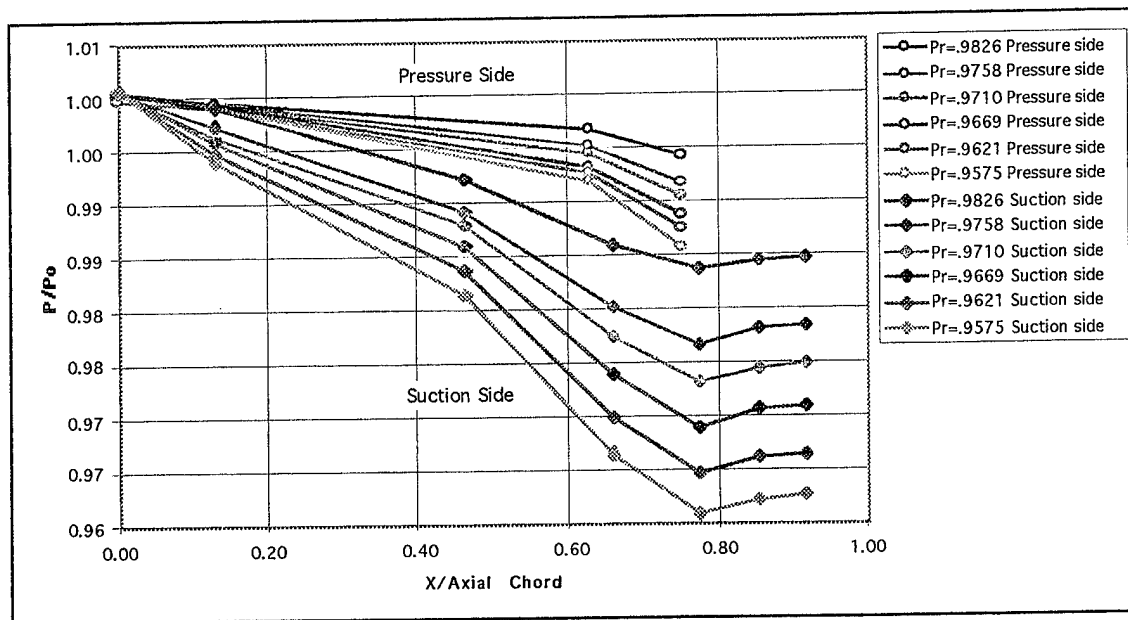


Figure 13.  $P/P_0$  vs.  $x/c$  for 0.9826 through 0.9575 pressure ratios

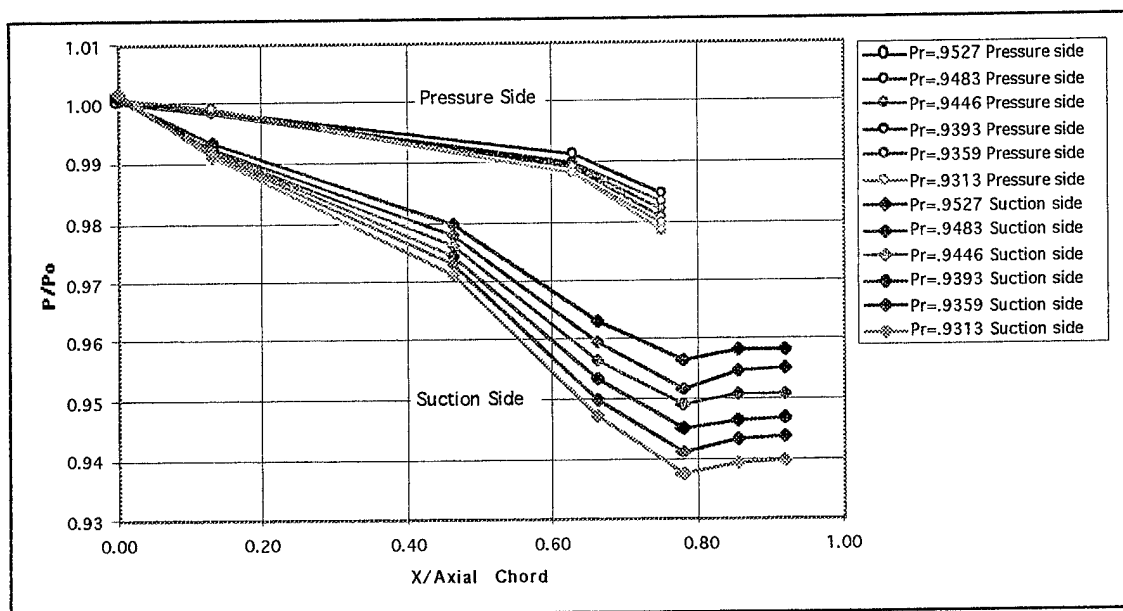


Figure 14.  $P/P_0$  vs.  $x/c$  for 0.9527 through 0.9313 pressure ratios

## **B. LASER-DOPPLER VELOCIMETRY MEASUREMENTS**

### **1. Comparison of a 1-D Procedure with 2-Component Measurements**

The previous LDV experiments on the ATC were carried out using a two-component laser probe (both blue and green beams); however, due to the significant weakness in the signal strength of the blue beam and subsequent low data rates, this was abandoned. The current LDV measurements were conducted utilizing only the green beam for both horizontal (axial) and vertical (tangential) measurements of the flow field. Manual repositioning of the laser probe (Figure 7) allowed measurements in both directions. Initial LDV data were acquired at a pressure ratio of 0.9054 to allow comparisons with previous data taken in Reference 2.

LDV measurements were made first to determine the repeatability of the one-dimensional technique. The values of velocity, turbulence intensity, and flow angle were recorded and compared. Each velocity reading was non-dimensionalized by the total velocity based on the upstream stagnation temperature ( $T_0$ ) to correct for varying conditions. Experimental repeatability was achieved by conducting runs on different days at both a zero degree and a pinned circumferential wake position.

The initial LDV radial measurement at the 0.9054 pressure ratio provided satisfactory seeding conditions and low ATC vibrations. Data rates ranged from approximately 100 samples per second at the 1.78 mm depth to 50 samples per second at the 0.01 mm depth.

Figures 15a and 15b contain the non-dimensionalized horizontal and vertical components of velocities that correlated over the different days of the experiment. Both the horizontal and vertical components seem to increase as the depth of the probe volume was increased. This is typical of an endwall boundary layer survey with the flow magnitude increasing to freestream conditions. The boundary layer was also distorted due to secondary flows, wake, and corner vortices that possibly formed within the blade passage.

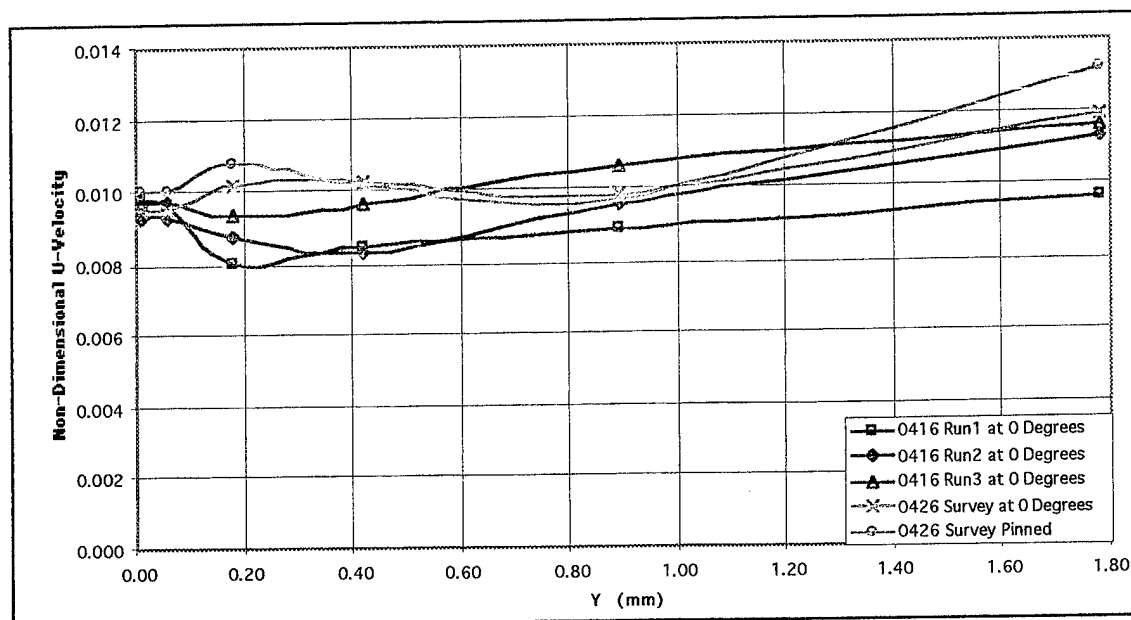


Figure 15a. A radial survey through the laser blank at a Prandtl of 0.9054

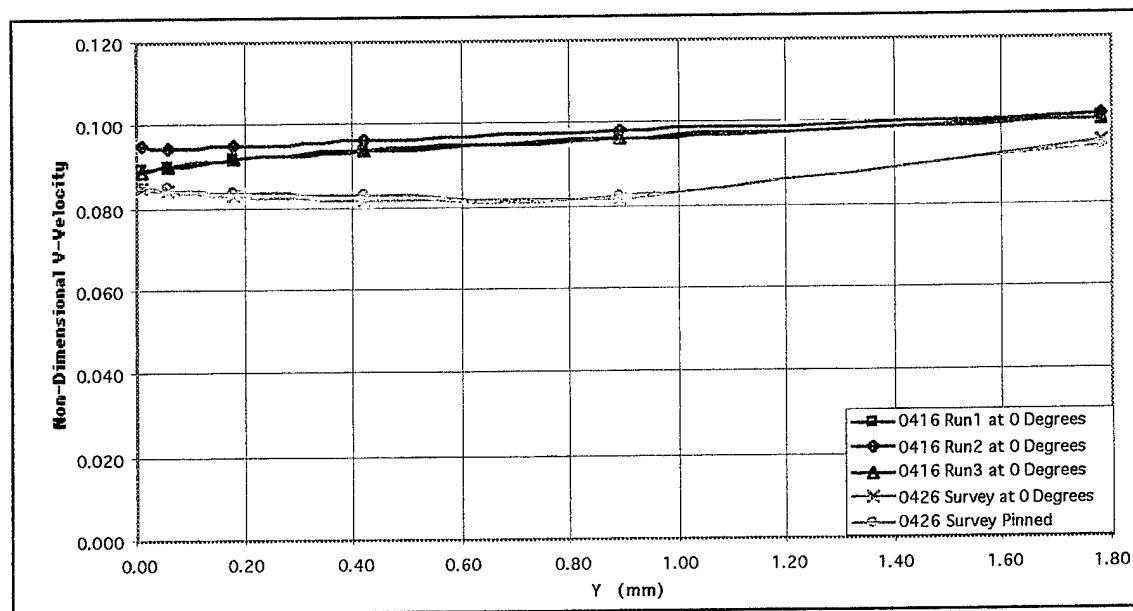


Figure 15b. A radial survey through the laser blank at a Prandtl of 0.9054

Figure 16a and 16b contain the horizontal and vertical turbulence intensities which also correlated well over the two days. The horizontal turbulence intensity was approximately 9% and was slightly less than the vertical turbulence intensity of about 10%. The horizontal turbulence intensity also remained relatively constant over the range of the radial survey where the vertical turbulence intensity was higher near the optical access hole and decreased as the survey point moved inwards. This indicated that the larger vertical velocity component was more susceptible to the complex and highly turbulent boundary layer and access hole interactions than the smaller horizontal component of the flow.

Figure 17 contains the mean angle from the two days and previous angles from Reference 2. The present data correlated well and indicated a flow angle of approximately 83.5 degrees. The previous flow angles were less, at about 75 degrees. The current flow angles started at a higher value near the endwall and then decreased as the survey point moved inwards. The previous angles [Ref. 2] started at lower flow values and increased as the survey point moved inwards. This former trend seemed to be inconsistent with the high turbulence intensity (lower velocities) currently found near the optical access hole and lower turbulence intensity (higher velocities) away from it. Initial velocity components would be expected to be low due to this highly turbulent location near the endwall. The measured velocity should then increase as the turbulence intensity decreased as the survey progressed. Endwall flow angle was defined as the arc tangent of the vertical (tangential) velocity divided by the horizontal (axial) velocity components. Since a greater change occurred in the horizontal than in the vertical velocity during the radial survey, the angles should first increase, but then decrease as the survey progressed. This is seen to be the case in the data given in Figure 17.

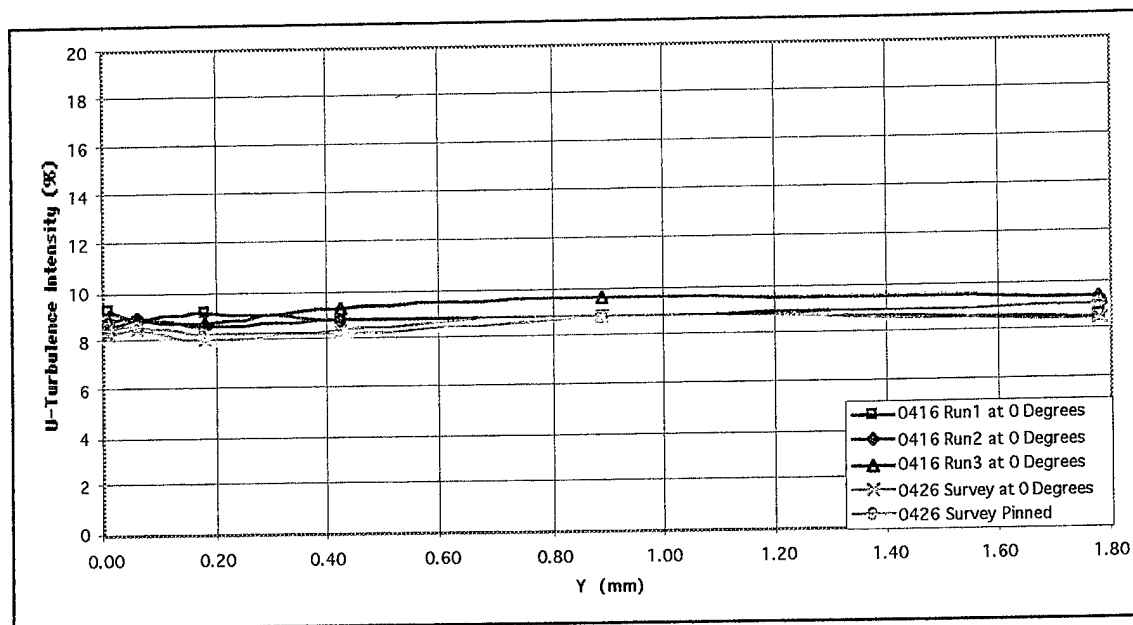


Figure 16a. A radial survey through the laser blank at a Prati of 0.9054

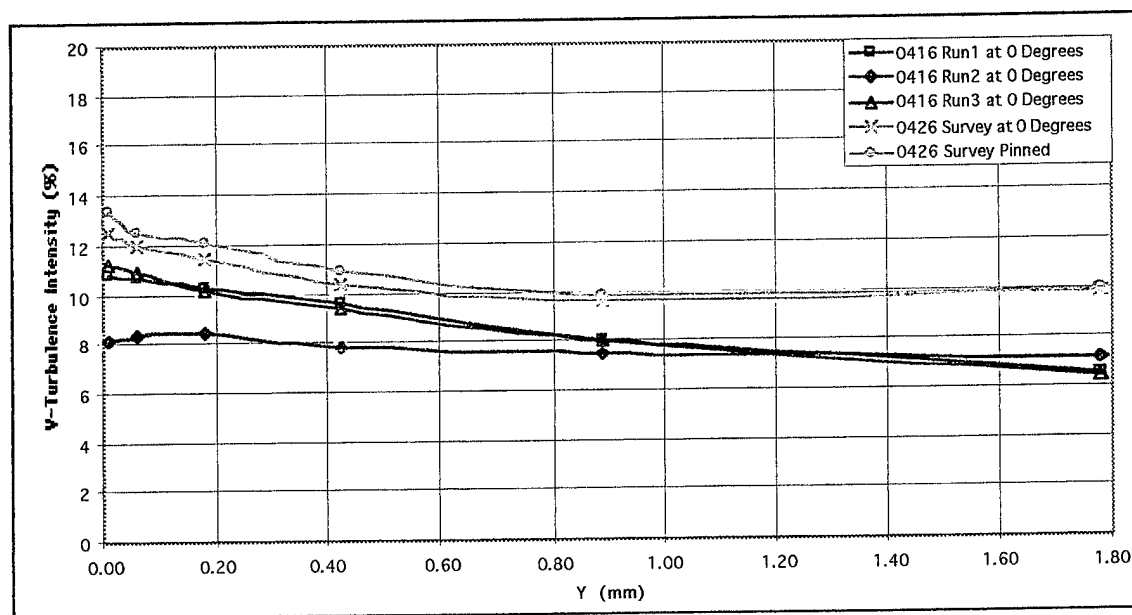


Figure 16b. A radial survey through the laser blank at a Prati of 0.9054



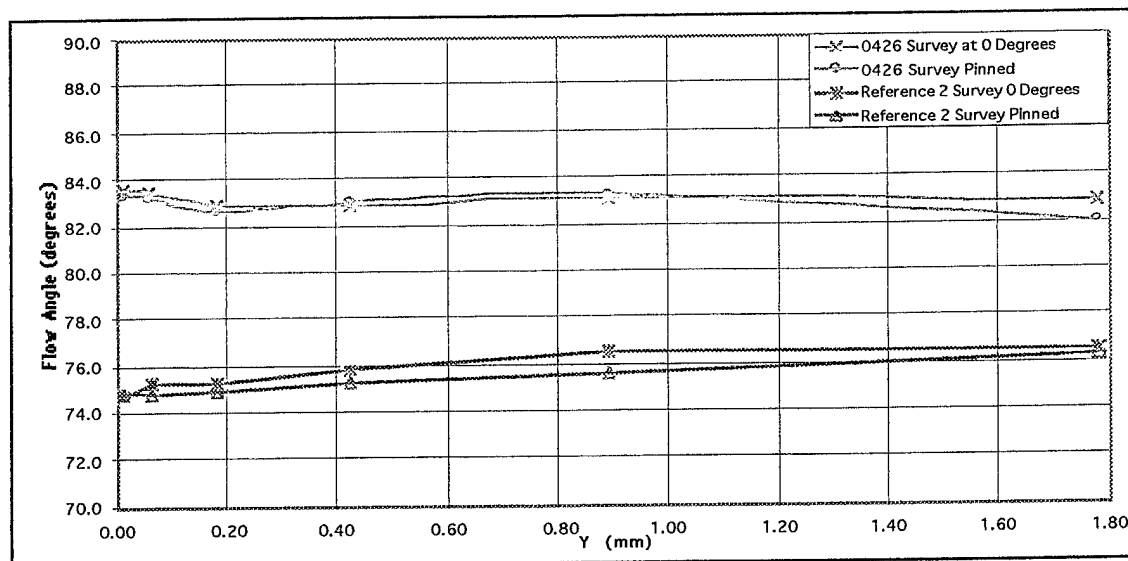


Figure 17. A radial survey through the laser blank at a Prandtl of 0.9054

## 2. Laser Blank Measurements at a Pressure Ratio of 0.9620

The laser blank was used and surveys were conducted at a pressure ratio of 0.9620, both radially and circumferentially, to provide data to compare with for later measurements with the pressurized laser window. The execution of these surveys was similar to the previous surveys at a pressure ratio of 0.9054.

Figures 18, 19, and 20 show the non-dimensional velocity, turbulence intensity, and flow angle respectively at 3 circumferential wake positions (0, 7, -8 degrees). Figure 18 shows similar velocity trends to those in Figures 15a and 15b; however, the turbulence intensities shown in Figure 19 were much higher, reaching values as high as 14%. Vertical turbulence intensity followed a similar trend to that in Figure 16b, starting high and then decreasing. Flow angles at this pressure ratio were 3 degrees higher than those in Figure 20. The LDV measurement at the 0.9620 pressure ratio provided much better seeding and improved data rates over those for the 0.9054 pressure ratio. Data rates ranged from approximately 175 samples per second at the 1.78 mm depth to 90 samples per second at the 0.01 mm depth.

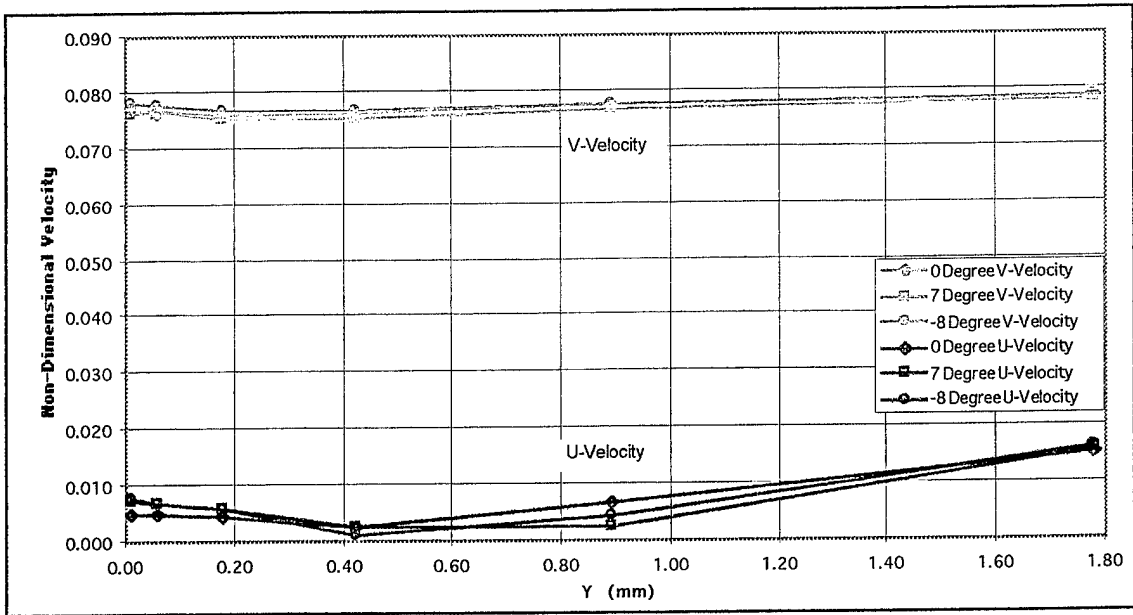


Figure 18. A radial survey through the laser blank at a Prandtl number of 0.9620

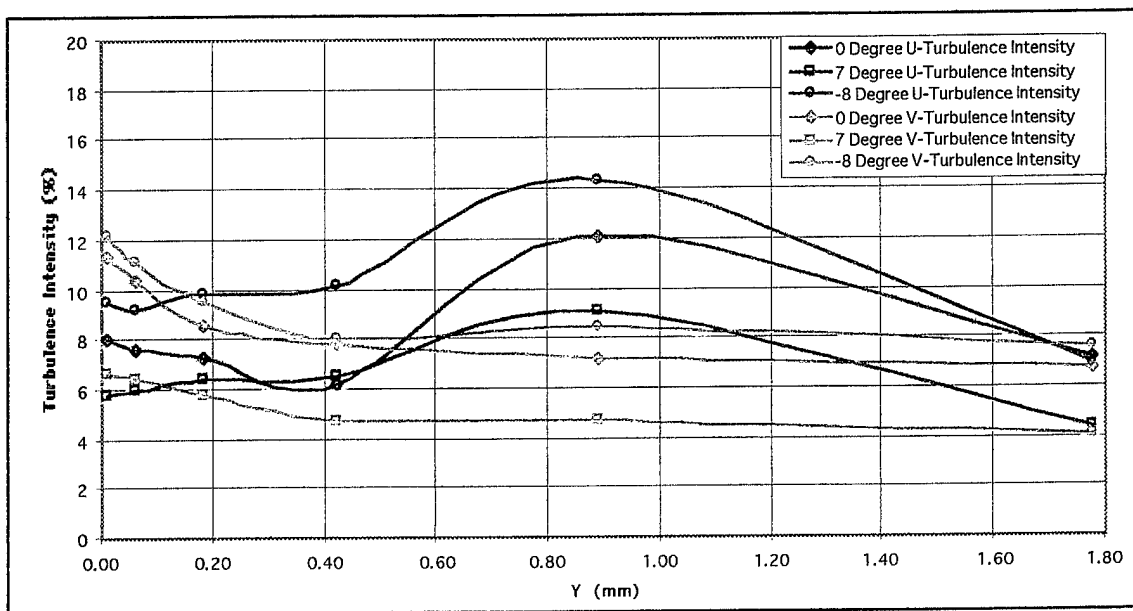


Figure 19. A radial survey through the laser blank at a Prandtl number of 0.9620

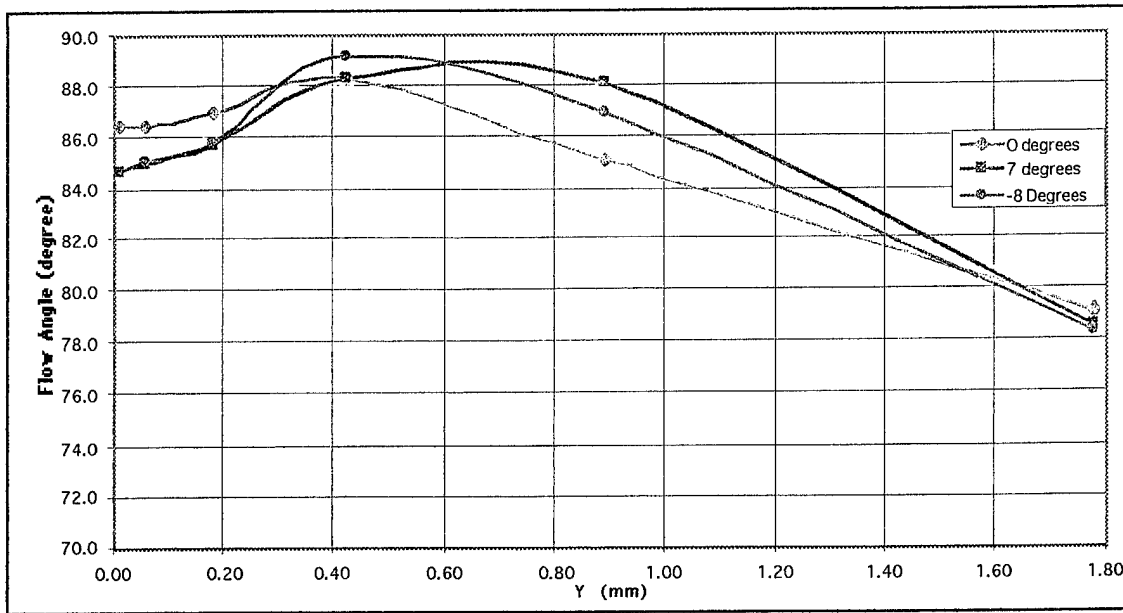


Figure 20. A radial survey through the laser blank at a  $Prat$  of 0.9620

A circumferential survey was conducted after the initial radial surveys to complete the test matrix (Figure 10) near the endwall. Figures 21 through 23 graphically depict velocity, turbulence intensity, and flow angle for circumferential wake positions of -8 to +8 degrees. Figures 21a and 21b once again show the lower velocity near the endwall which increased as the survey progressed. Horizontal turbulence intensity was consistent throughout the survey at about 6.5%. The vertical turbulence had a high of about 13% to a low of about 6% which, in showing a decrease in turbulence as the survey location moved further from the wall, was consistent to the previous surveys.

Figure 23 shows the flow angle to be varying only between 80 and 82 degrees, so the flow angle was relatively insensitive to circumferential variations of the ATC.

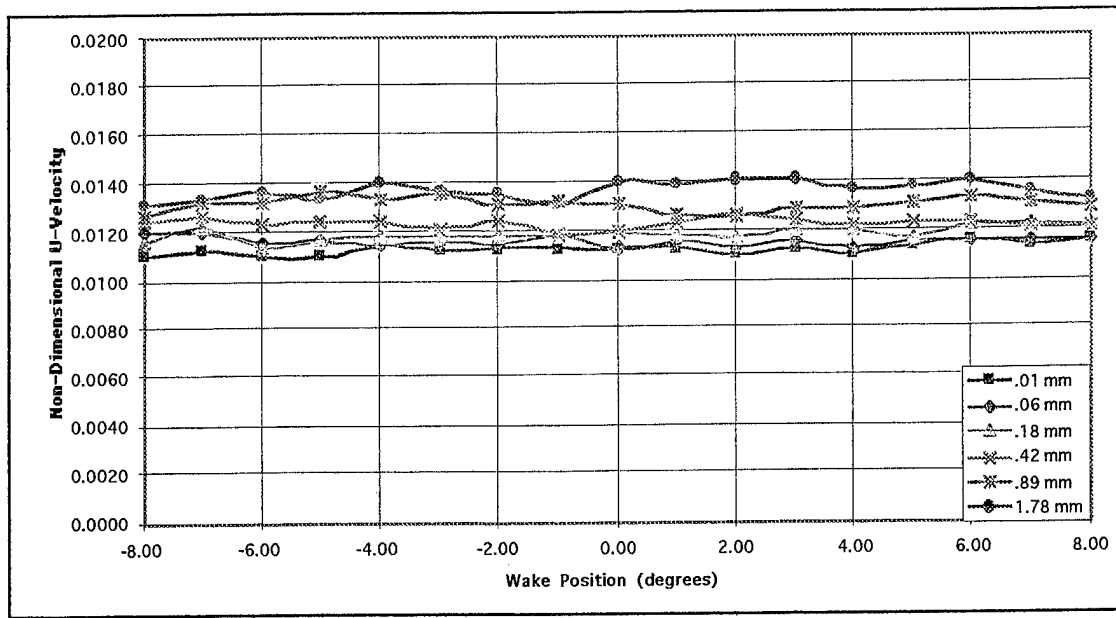


Figure 21a. A circumferential survey through the laser blank at a Prat of 0.9620

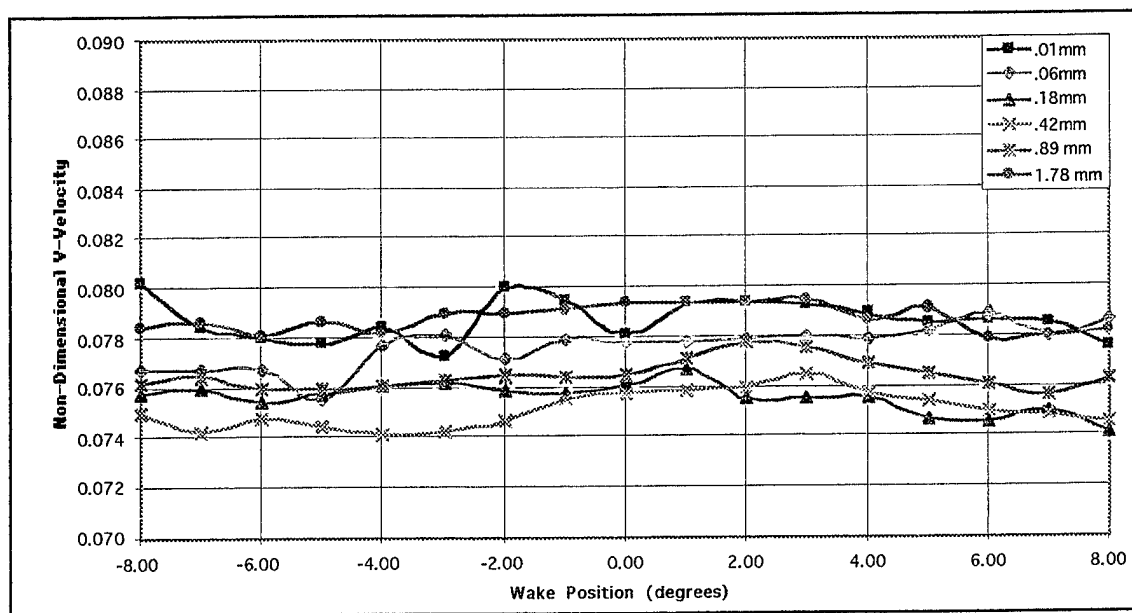


Figure 21b. A circumferential survey through the laser blank at a Prat of 0.9620

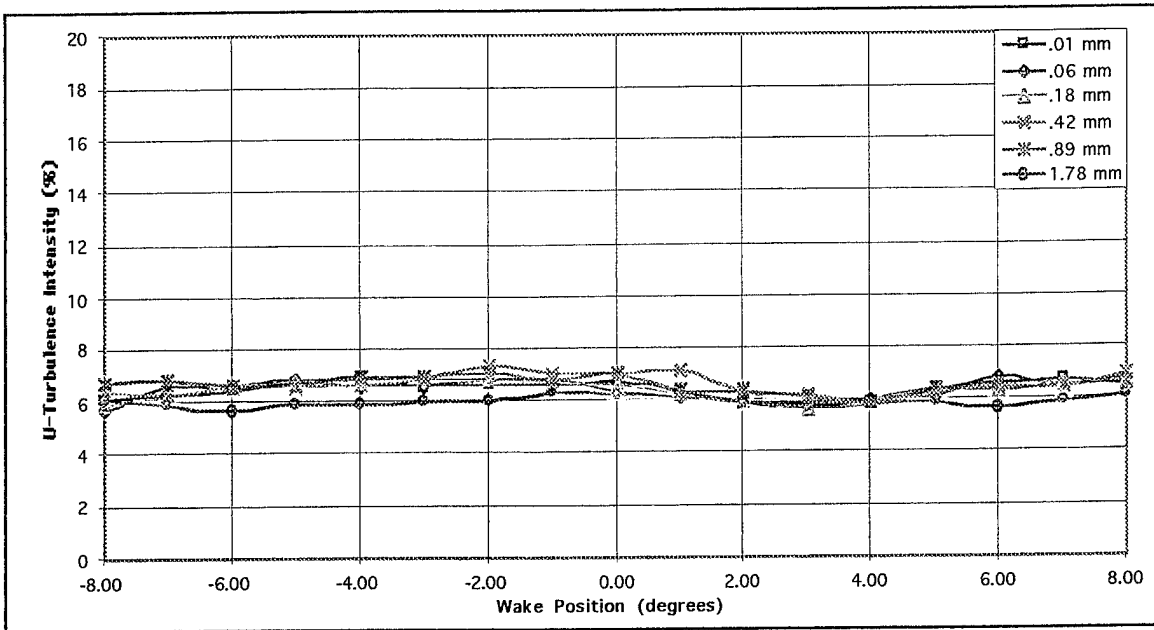


Figure 22a. A circumferential survey through the laser blank at a Prat of 0.9620

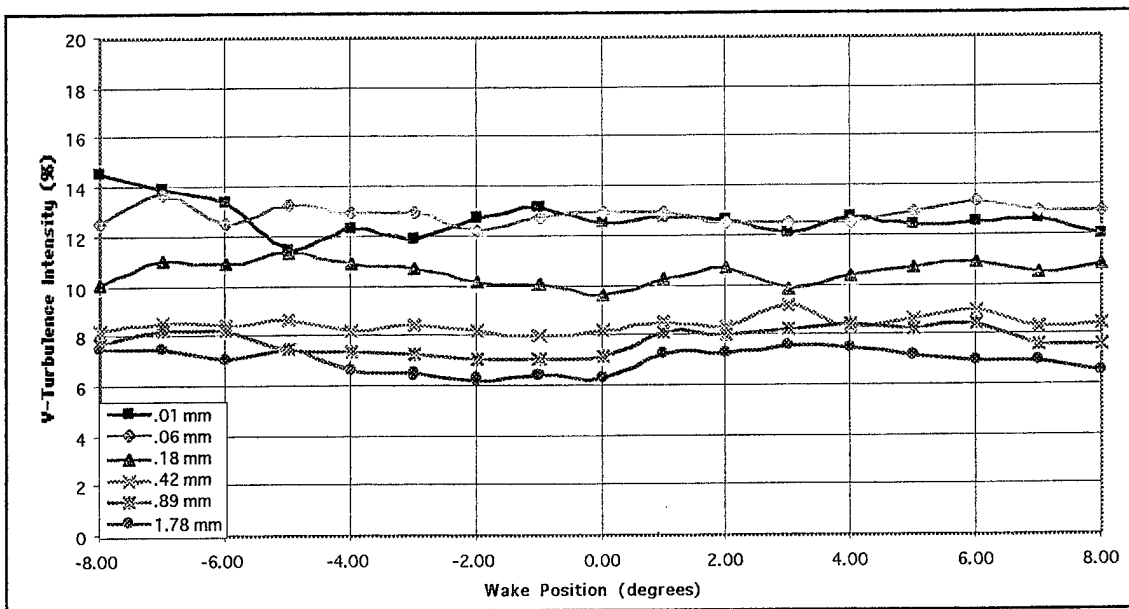


Figure 22b. A circumferential survey through the laser blank at a Prat of 0.9620

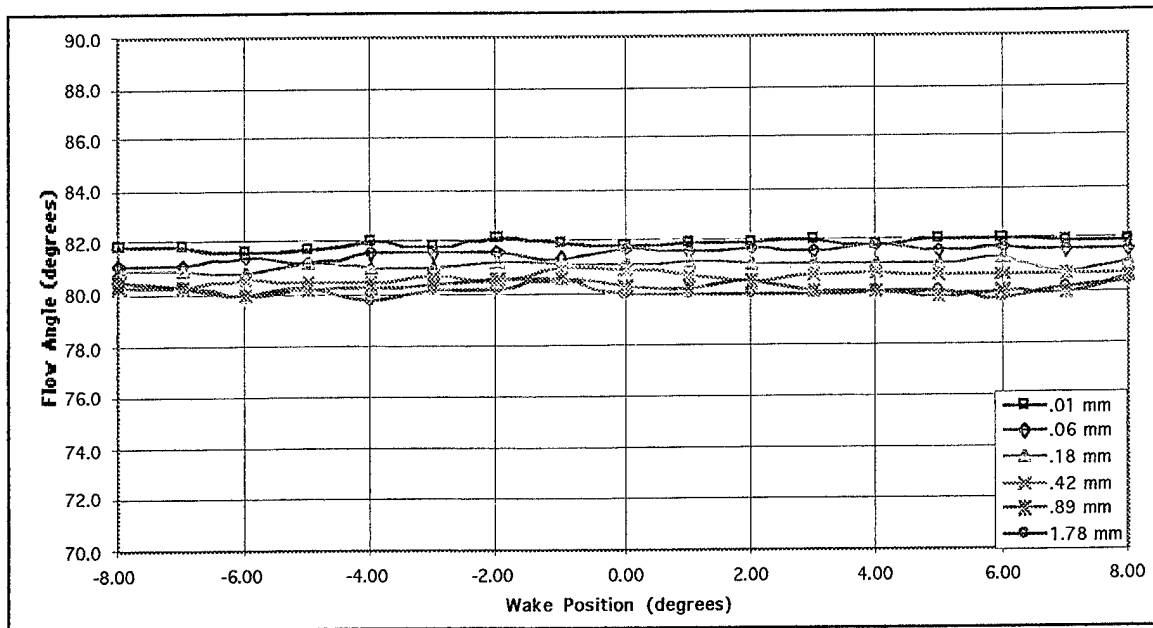


Figure 23. A circumferential survey through the laser blank at a Pr of 0.9620

### 3. Radial Measurements with Pressurized Window at Various Chamber Pressures

During both the radial and circumferential surveys with the laser blank, seeding material quickly accumulated inside the lower portion of the optical access hole and interfered with LDV data acquisition. The laser blank did not provide any pressure equalization across the optical access hole which allowed the flow to escape from it. The atomizer then had to be switched off to remove and clean the laser blank. Because of this problem, a window was designed which created a pressurized chamber between the optical access hole and the LDV. This resulted in a laser window that did not allow the air flow to escape from the ATC and never needed to be cleaned during the experiment. The window could also be pressurized to force air back into the flow to determine the effects of such a procedure.

A radial survey was conducted through the pressurized window at 3 chamber pressures to further investigate the effects of this optical device on LDV measurements. The

radial survey was decreased from the previous maximum depth of 1.78 mm to .89 mm due to the lack of accessibility at the 1.78 mm radial position.

Figures 24-26 show the influence of the increasing chamber pressure on the flow within the ATC. In both the horizontal and vertical velocities, the increase in chamber pressure led to a decrease in the measured velocity. This was especially evident in Figure 24b for the vertical (tangential) velocity which had a 3% decrease in magnitude due to the increased chamber pressure.

Figure 25a and 25b show the turbulence intensity remaining constant at about 6% for both velocities, implying that the pressurized window did not contribute significantly to increasing the turbulence of the flow near the endwall at this pressure ratio.

Figure 26 shows the flow angle results. The angle of the flow near the endwall tended to decrease initially as chamber pressure was increased, but followed the former trends of increasing near the end wall, and then decreasing. At 0 mm of pressure, the initial flow angle was about 79.8 degrees. At 152.4 mm, the angle was 79.5 degrees. With the exception of the one measurement at 79.8 degrees at 0 mm of pressure, all measurements of flow angle were constant (79.5) to within a tenth of a degree.

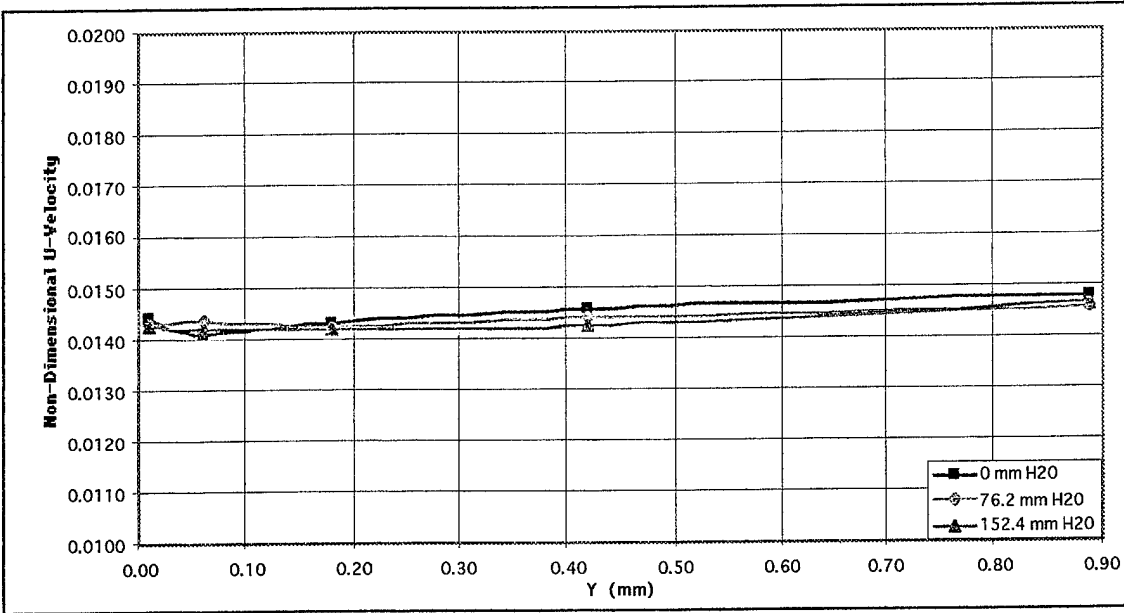


Figure 24a. A radial survey through the pressurized LDV window at a  $Pr_{at}$  of 0.9620

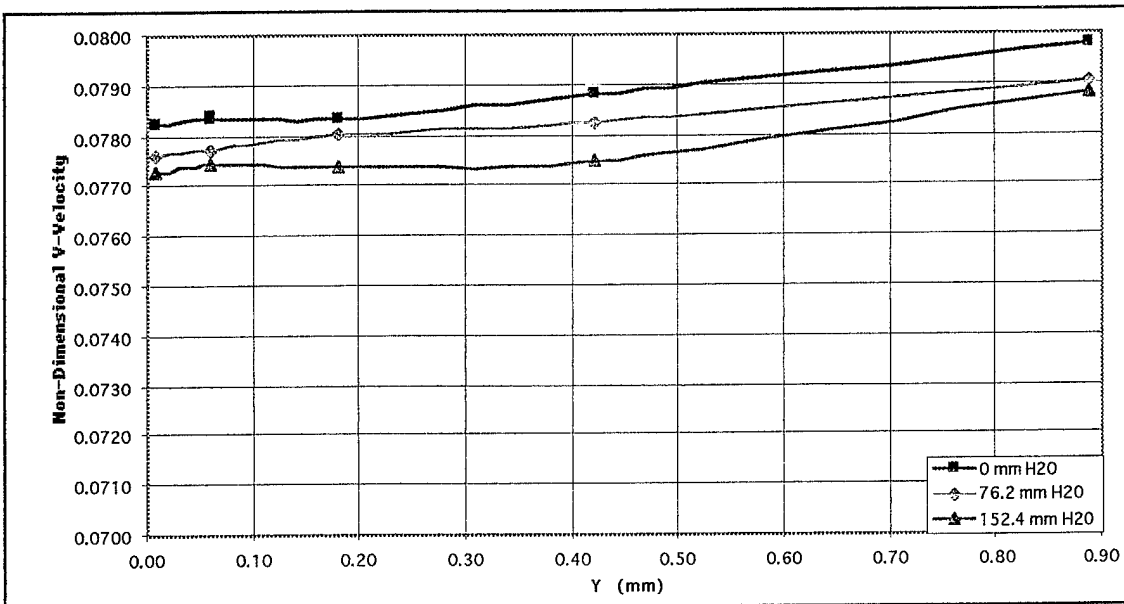


Figure 24b. A radial survey through the pressurized LDV window at a  $Pr_{at}$  of 0.9620



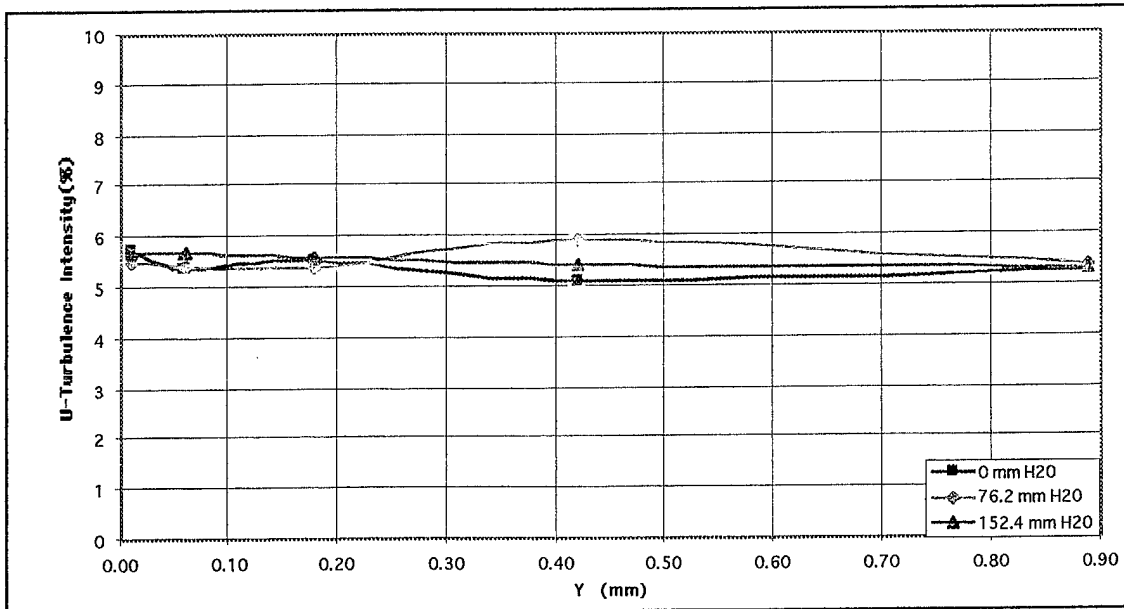


Figure 25a. A radial survey through the pressurized LDV window at a  $Prat$  of 0.9620

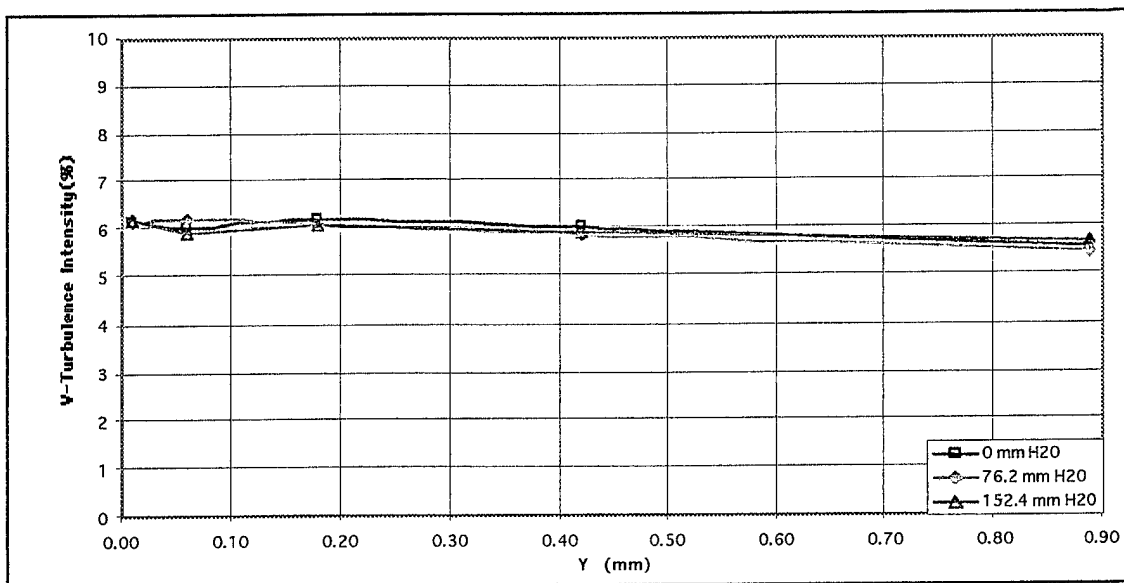


Figure 25b. A radial survey through the pressurized LDV window at a  $Prat$  of 0.9620

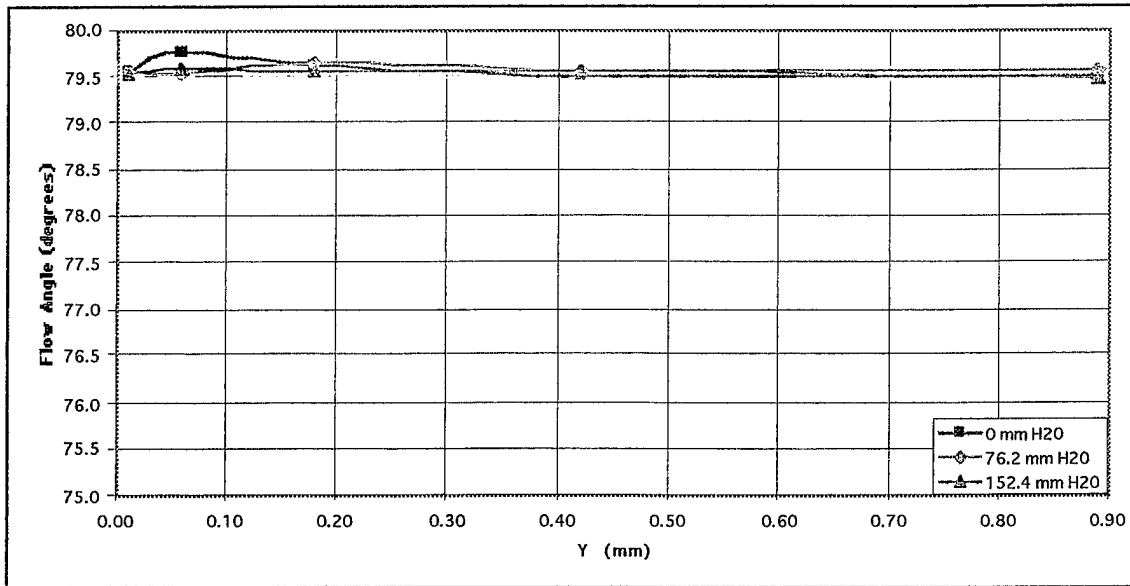


Figure 26. A radial survey through the pressurized LDV window at a  $Prat$  of 0.9620

#### 4. Radial Survey Comparison between Pressurized Laser Window and Laser Blank

Radial surveys of flow velocity, turbulence intensity, and flow angle obtained using the new pressurized LDV window and the laser blank are compared in Figures 27-29.

Figures 27a and 27b show the pressurized window velocities were greater than the laser blank velocities at all chamber pressures. Figures 28a and 28b show turbulence intensities were about 6%, lower than with the laser blanks. This suggests that the pressurized window had little effect on the flow during the survey as compared to the laser blank. Figure 29 shows the flow angle with the laser blank to be about 87 degrees whereas with the pressurized window it was at 79.5 degrees. This 7.5 degree difference in flow angle was the result of the differences in the component velocities seen in Figures 27a and 27b.

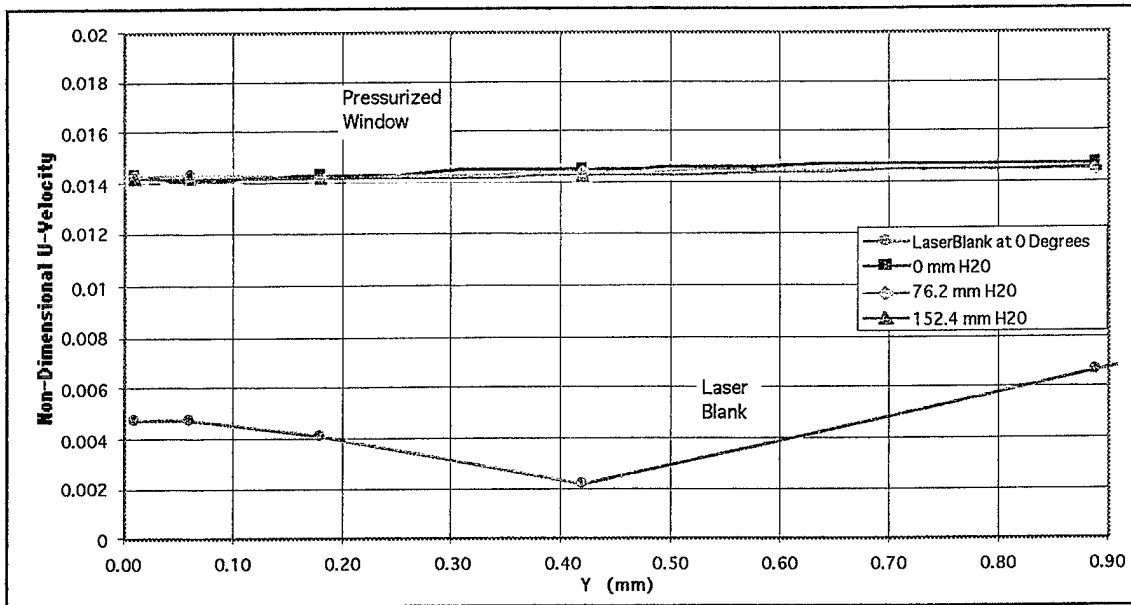


Figure 27a. Comparisons of radial surveys using the laser blank and pressurized LDV window at a Prandtl of 0.9620

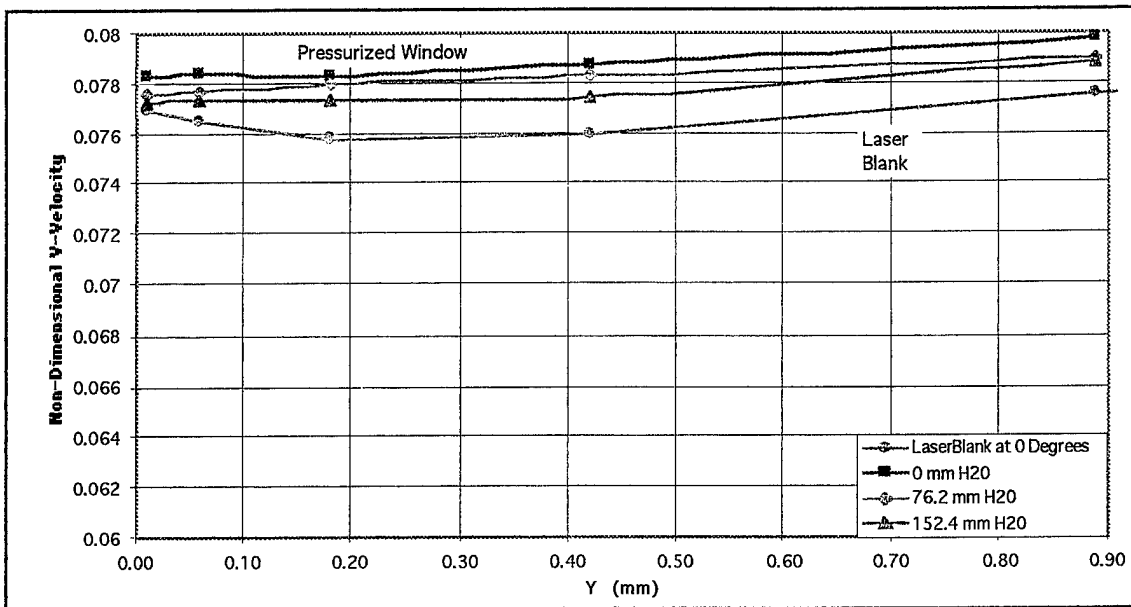


Figure 27b. Comparisons of radial surveys using the laser blank and pressurized LDV window at a Prandtl of 0.9620

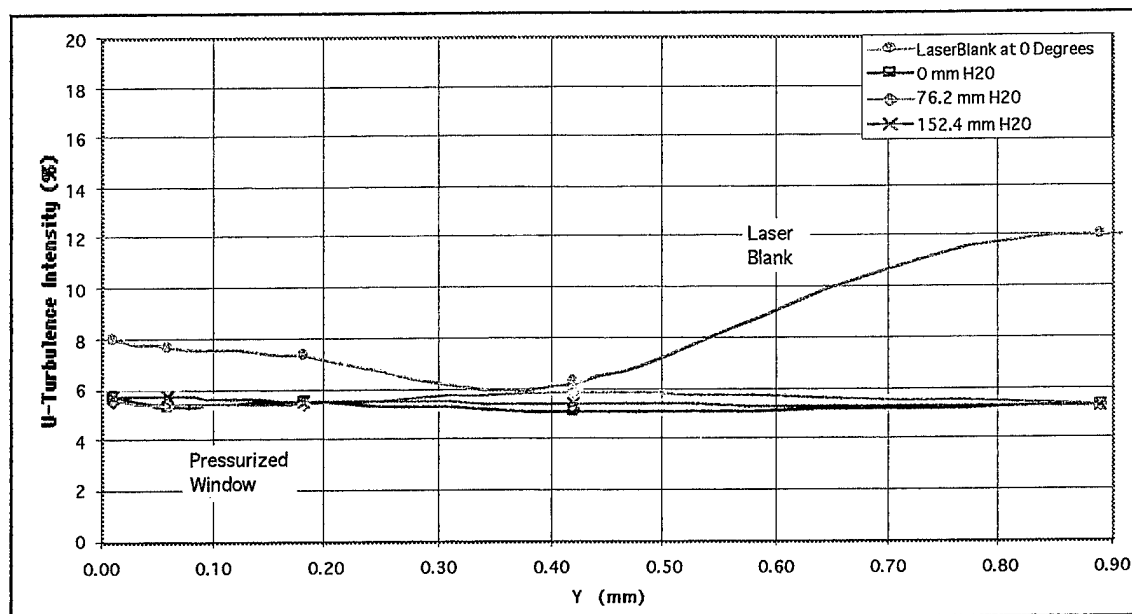


Figure 28a. Comparisons of radial surveys using the laser blank and pressurized LDV window at a Pr<sub>at</sub> of 0.9620

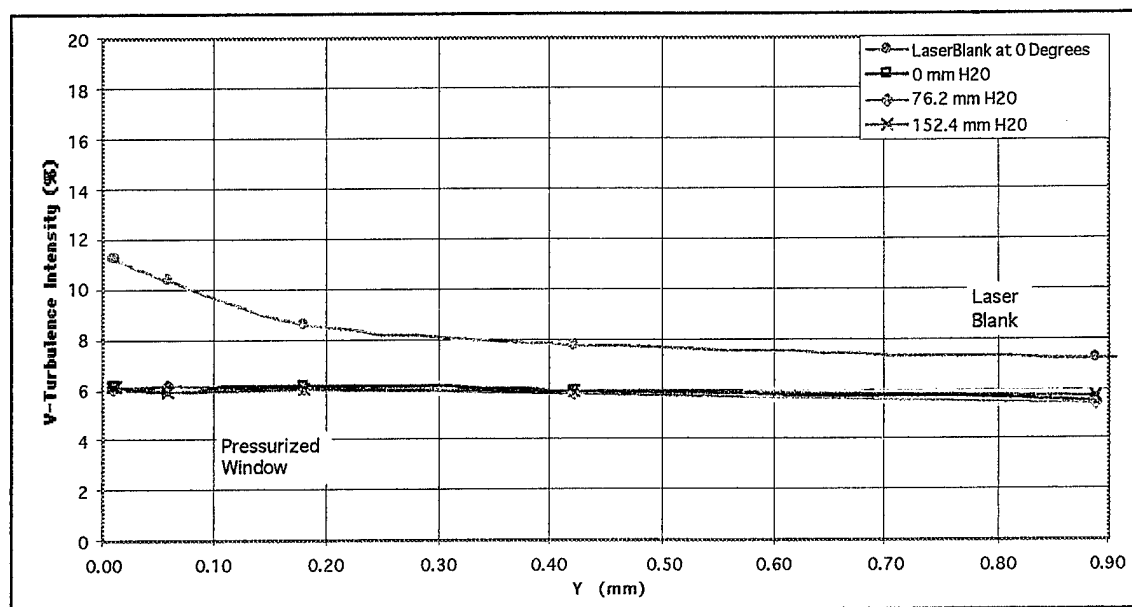


Figure 28b. Comparisons of radial surveys using the laser blank and pressurized LDV window at a Pr<sub>at</sub> of 0.9620

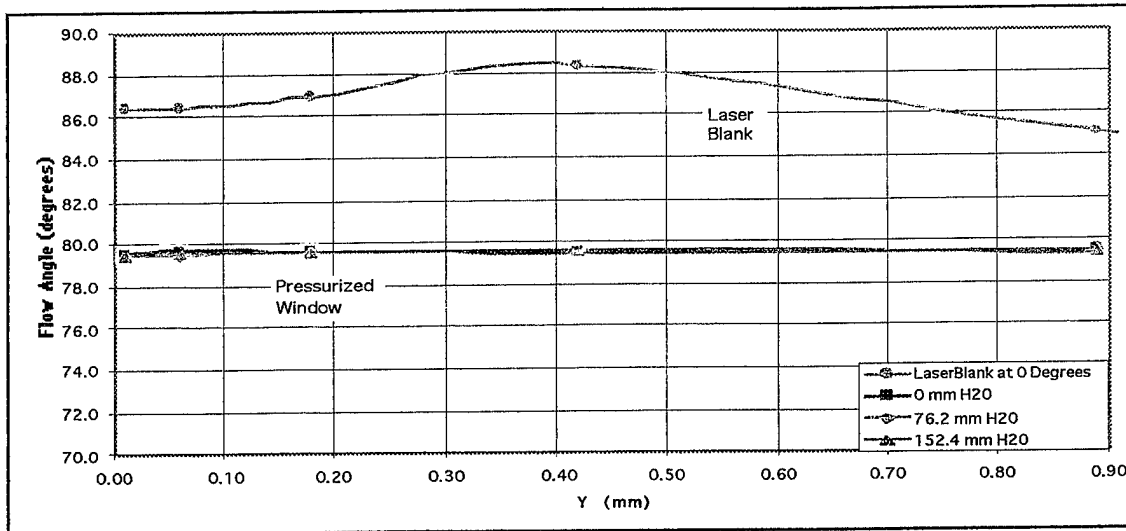


Figure 29. Comparisons of radial surveys using the laser blank and pressurized LDV window at a Prat of 0.9620

## 5. Effect of Various Chamber Pressures Compared to Laser Blank

Figures 30-32 show a comparison between results obtained with the new pressurized window under various chamber pressures and the laser blank, with the LDV fixed at a point within the flow. Chamber pressures of 0, 76.2, and 152.4 millimeters of water (0, 3, and 6 inches of water) were applied to the new window to determine their effect on flow measurements.

Figure 30a and 30b show the pressurized window velocity data to be significantly above the velocities obtained with the laser blank. This could be due to the flow escaping out of the optical access hole of the laser blank causing a lower-than-actual velocity to be detected by the LDV. Both the horizontal and vertical velocities also showed a slight increase when the pressure was increased within the chamber.

Figures 31a and 31b show reduced turbulence intensities in both the horizontal and vertical directions when utilizing the new LDV window, as previously shown. This reduction in turbulence intensity could be due to the containment of the flow within the new window, reducing the turbulence caused by the flow previously escaping from the optical access hole.

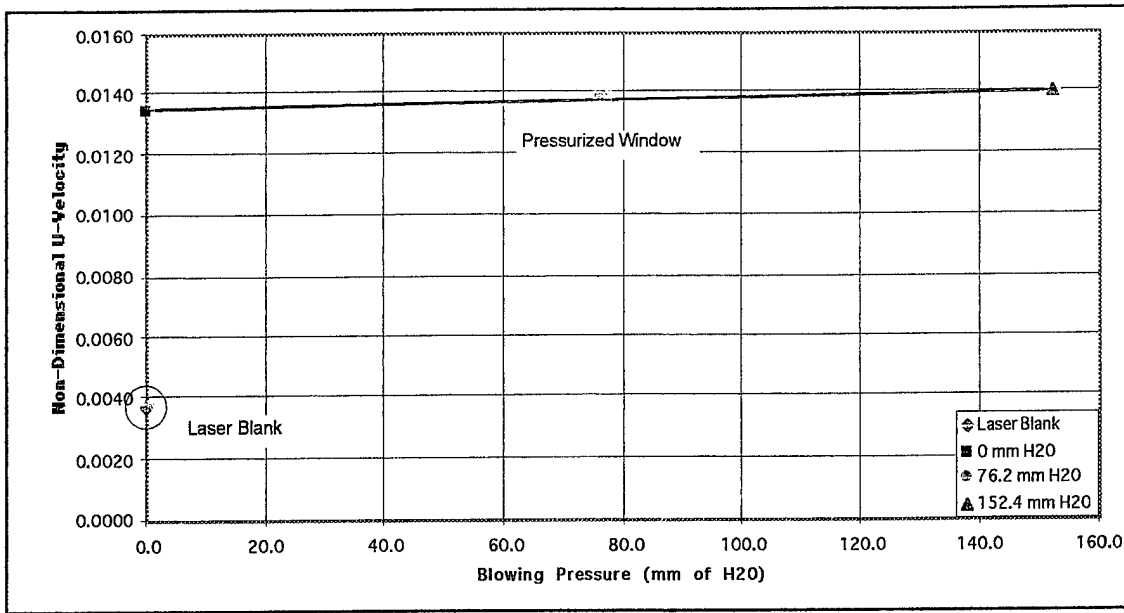


Figure 30a. Pressurized LDV window and laser blank comparisons at  $Pr_{at}$  of 0.9620

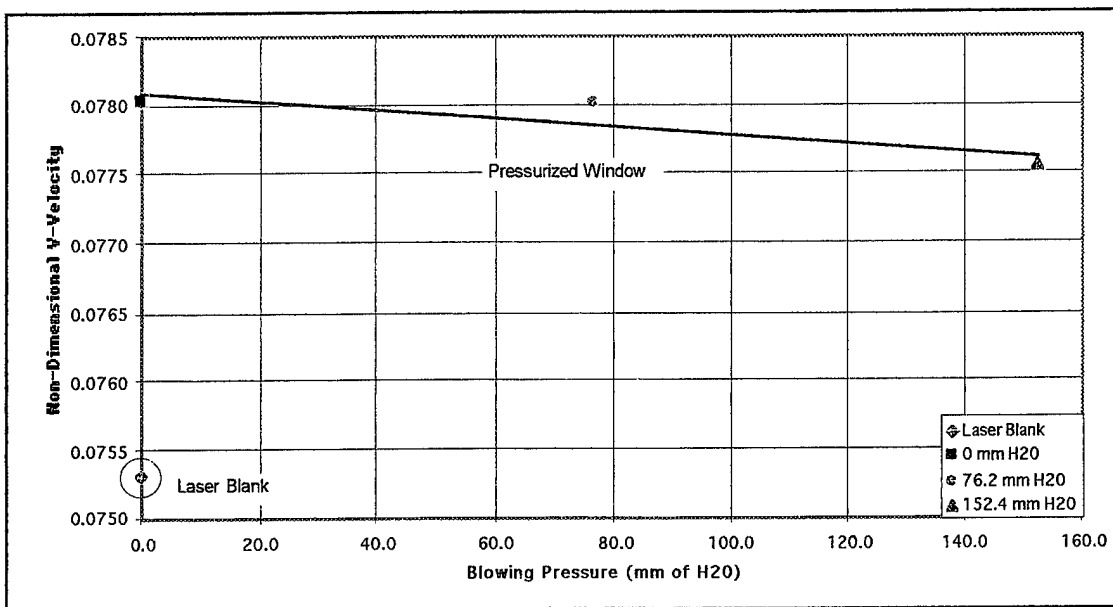


Figure 30b. Pressurized LDV window and laser blank comparisons at  $Pr_{at}$  of 0.9620

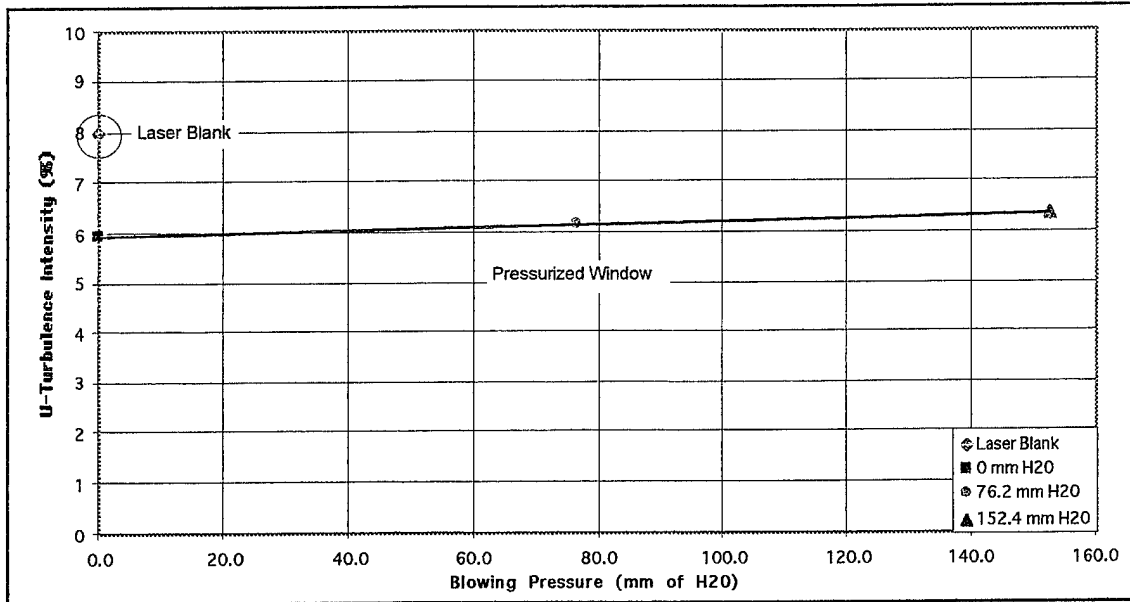


Figure 31a. Pressurized LDV window and laser blank comparisons at  $Prat$  of 0.9620

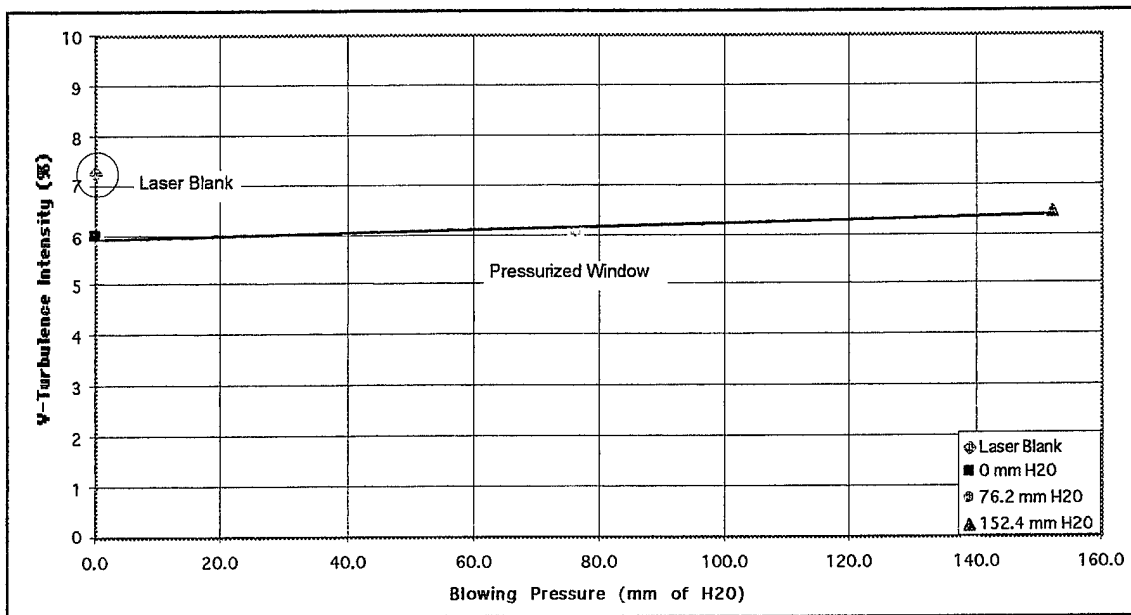


Figure 31b. Pressurized LDV window and laser blank comparisons at  $Prat$  of 0.9620

Figure 32 shows a difference in flow angle of about 6 degrees between the laser blank and the pressurized window, with the pressurized window having the lower angle.

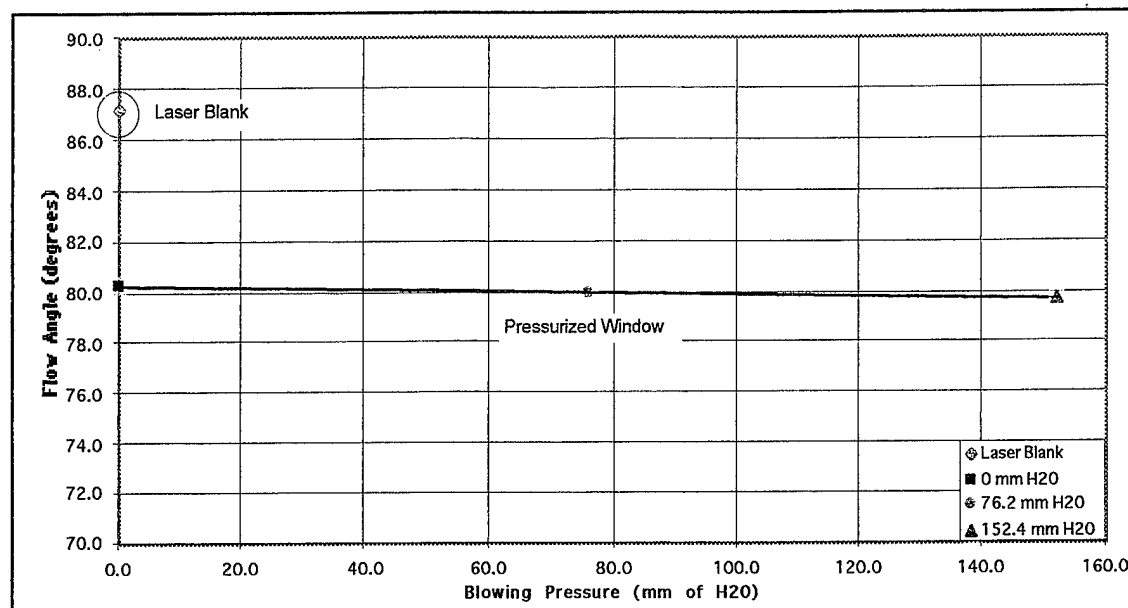


Figure 32. Pressurized LDV window and laser blank comparisons at  $Prat$  of 0.9620

## 6. Circumferential Surveys with Pressurized Window at 76.2 mm (3 in) water Chamber Pressure

Circumferential surveys from -8 to +8 degrees wake position were conducted with the new pressurized LDV window at a constant mid-range chamber pressure of 76.2 mm (3 in) water to further determine the effects of this window on this survey. Figures 33-35 show these results.

Figures 33a and 33b show the velocity profiles over the circumferential range. Similar trends to those in the radial survey also occurred here. The circumferential velocity profiles of the new window were also higher than those obtained with the laser blank (Figures 27a and 27b).

Figures 34a and 34b show the turbulence intensity with the pressurized window again to be lower than the turbulence intensity with the laser blank.



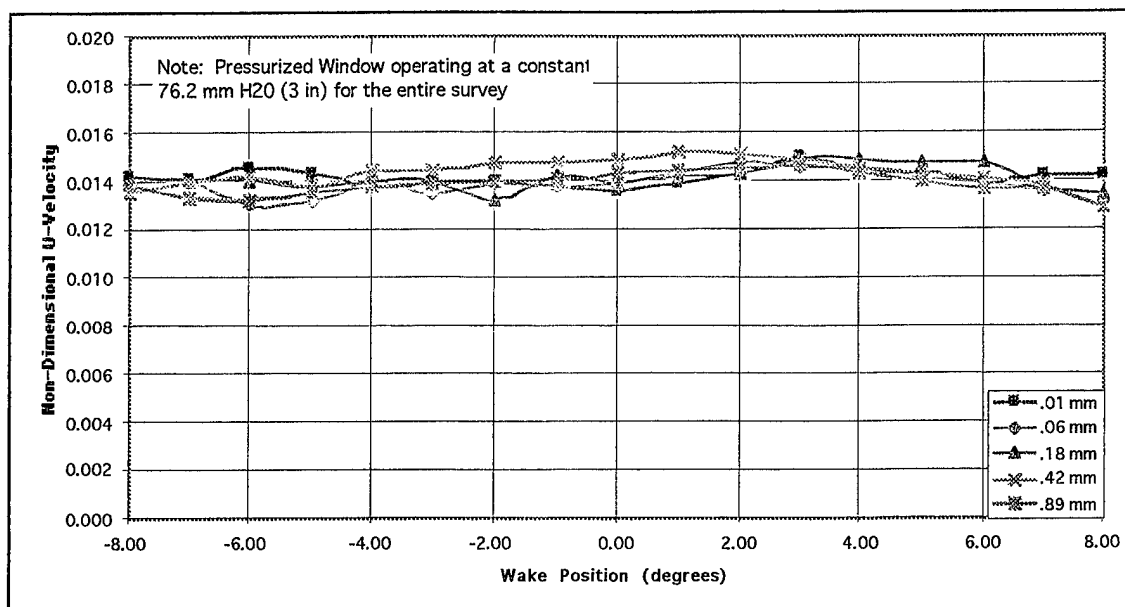


Figure 33a. A circumferential survey through the pressurized LDV window at a Prat of 0.9620

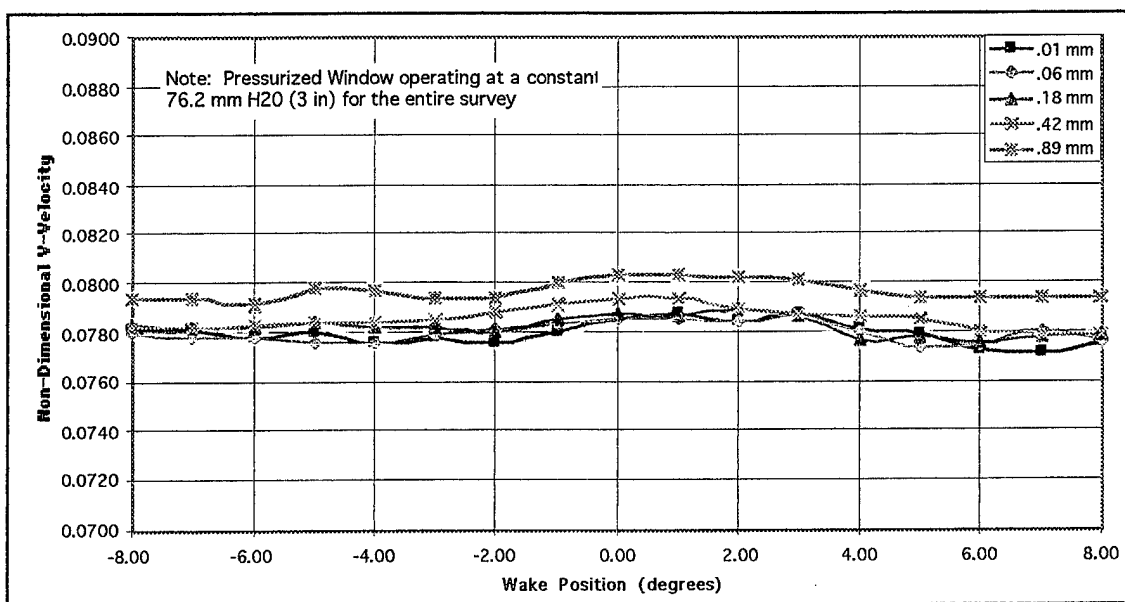


Figure 33b. A circumferential survey through the pressurized LDV window at a Prat of 0.9620

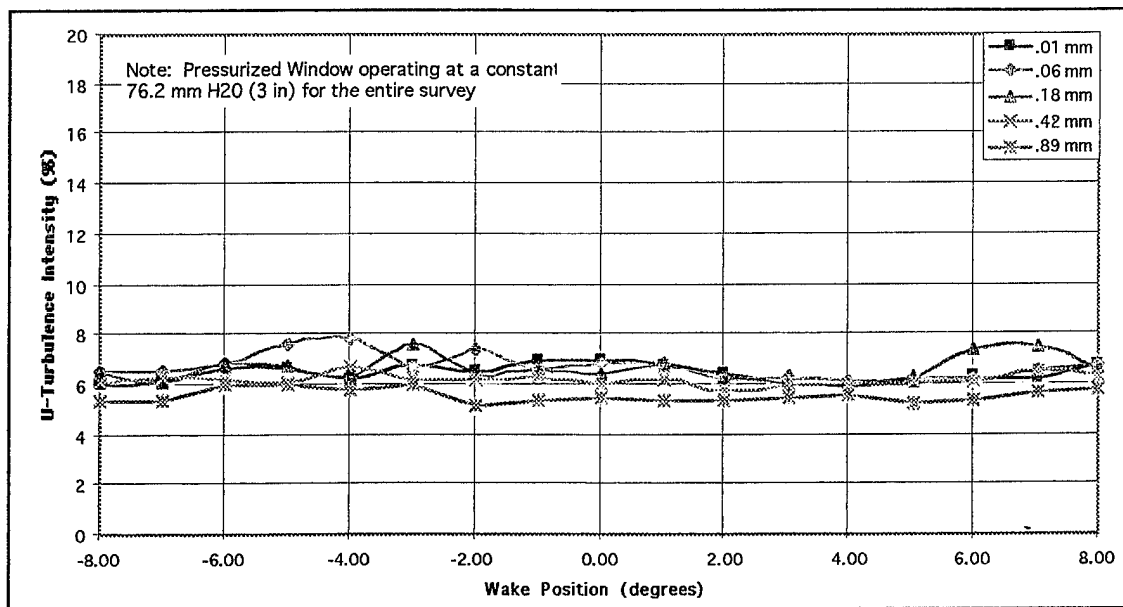


Figure 34a. A circumferential survey through the pressurized LDV window at a Pr of 0.9620

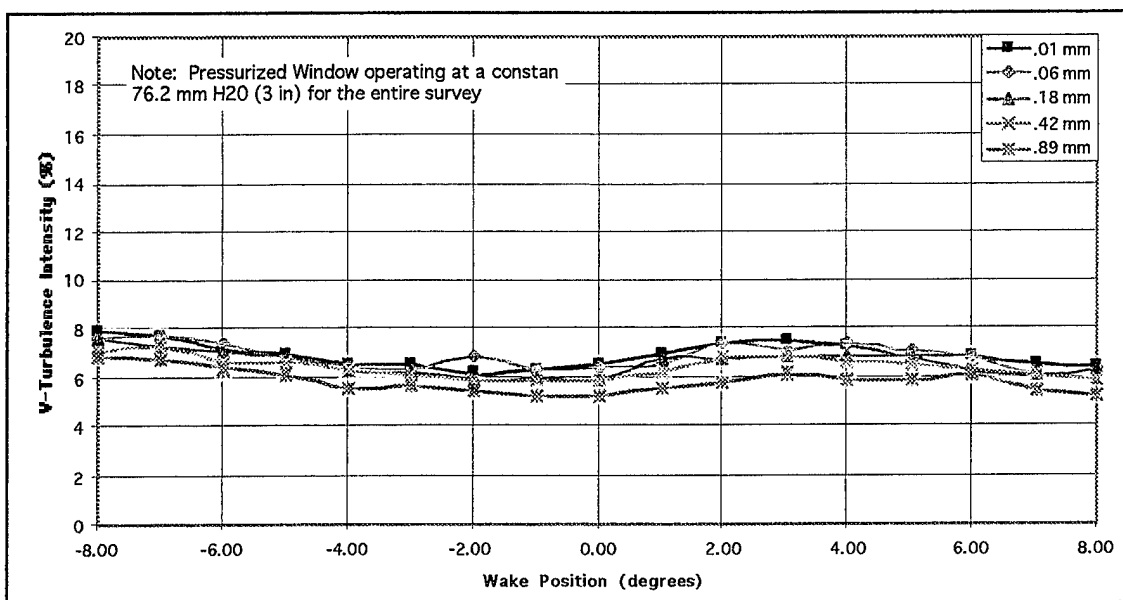


Figure 34b. A circumferential survey through the pressurized LDV window at a Pr of 0.9620

Figure 35 also shows flow angles lower than with the laser blank, which is consistent with the flow angles measured in the previous radial surveys. The results from the circumferential survey were fully consistent with those from the previous radial surveys indicating good repeatability of the one dimensional measuring technique with the new LDV window.

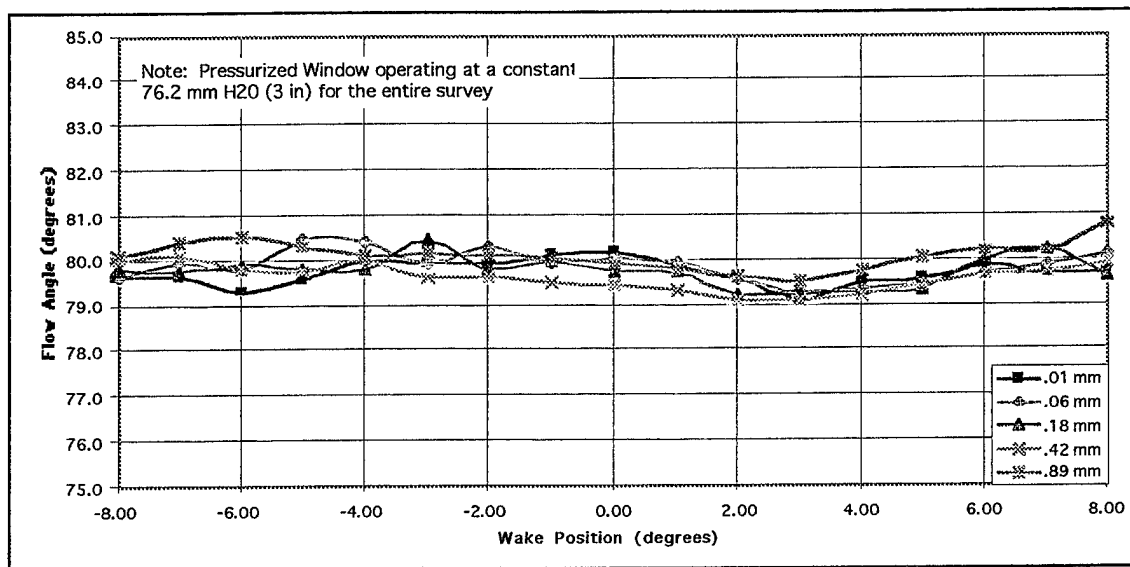


Figure 35. A circumferential survey through the pressurized LDV window at a  $Prat$  of 0.9620

## 7. Final Comparison with Laser Blank, Pressurized LDV Window, and Cobra Probe

Three-hole cobra probe surveys were performed to verify the aforementioned LDV data, with the probe at the same location as the LDV windows (Figure 1). Cobra-probe data were taken at a pressure ratio of 0.9620. Utilizing the equations in Reference 3 and the third-order calibration curve from Figure D1 of Appendix D, the values for (X), total non-dimensional velocity, were calculated from the measurements. Flow angle was read from the vernier scale on the probe holder and recorded in the front panel of the LabView program.

Figures 36 and 37 are the final comparisons of total non-dimensional velocity and flow angle between these three measuring methods. Figure 36 shows the probe velocity increasing as the probe was radially traversed into the ATC.

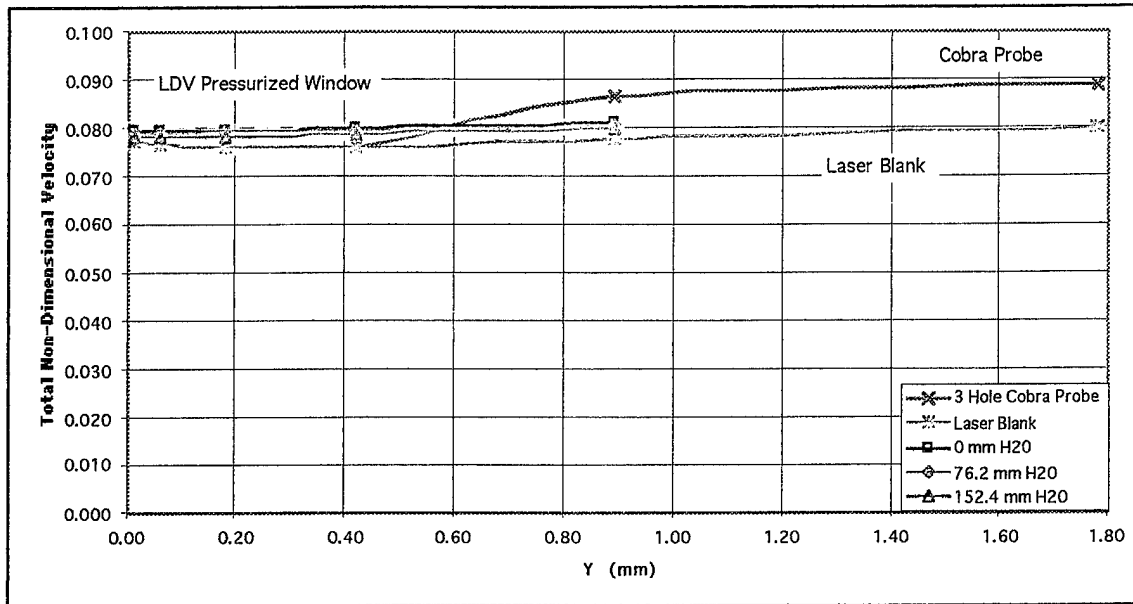


Figure 36. Final total non-dimensional velocity comparison between laser blank, pressurized window, and 3-hole cobra probe at a  $Prat$  of 0.9620

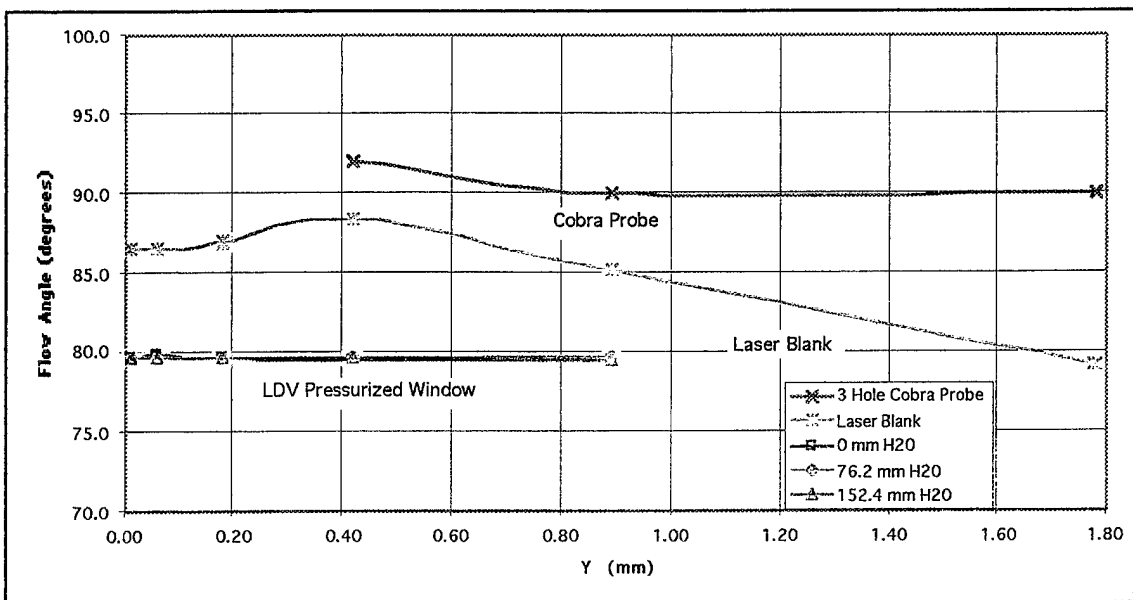


Figure 37. Final flow angle comparison between laser blank, pressurized window, and 3-hole cobra probe at a  $Prat$  of 0.9620

Figure 38 is a pictorial illustration of the possible interaction of the probe within the ATC. Figure 38a shows the probe approximately at the 1.78 mm radial position. At this position, the probe stem sealed the hole and the flow did not leak. The internal flow was relatively undisturbed. Figure 38b shows the probe head at the endwall. In this position, the probe no longer sealed the hole and the flow could leak out of the ATC. The LDV windows were in behavior, with the laser blank giving lower velocities due to the flow leakage and the pressurized window giving higher velocities due to no leakage (Figures 39 and 40).

Figure 36 shows the total non-dimensional velocity which was the vectorial sum of the U and V velocities. The cobra probe initially measured a velocity similar to the LDV measurement with the laser blank, since the flow was leaking out at this time. As the probe stem plugged the hole and stopped the leakage, the velocity rose to slightly above the LDV measurement obtained with the pressurized window. This suggested that as the flow leaked out of the optical access hole, the measurements indicated lower velocities due to the flow slowing down within the ATC in order to exit the opening. The higher value of velocity recorded by the cobra probe when set as shown in Figure 38a could be due to wall-proximity effects.

Figure 37 shows the flow angles obtained from the three measurement methods. The probe gave the largest angles which could be due to its intrusion and large size as compared to the non-intrusive and small LDV probe volume. The laser blank gave higher angles near the endwall which decreased to about 79 degrees as the survey progressed. The pressurized window was the most consistent of the two methods, even with varying chamber pressures. It gave approximately 79.5 degrees throughout its radial survey. The flow angles given by the two LDV methods seem to agree well at the final point within the ATC farthest away from the endwall. Both methods measured 79.5 degrees at the 1.78 mm position.

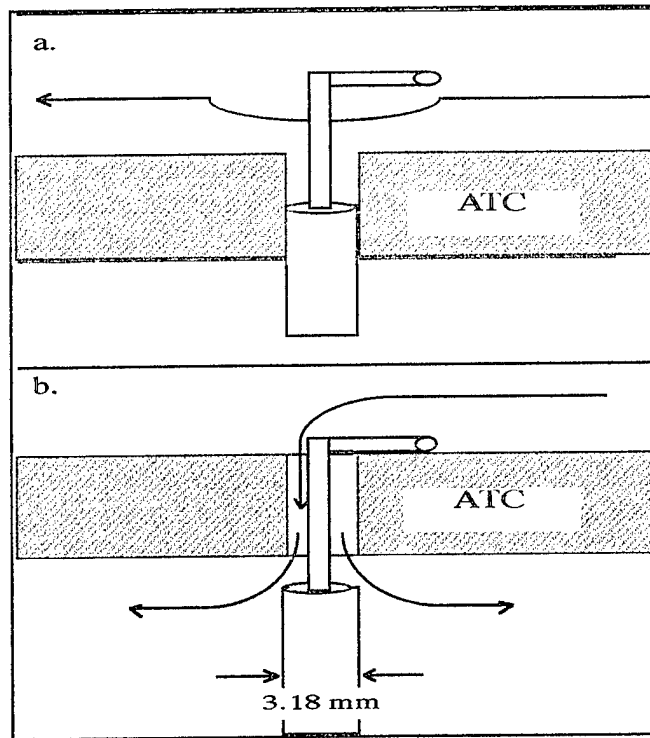


Figure 38. ATC flow depiction - the 3-hole cobra probe

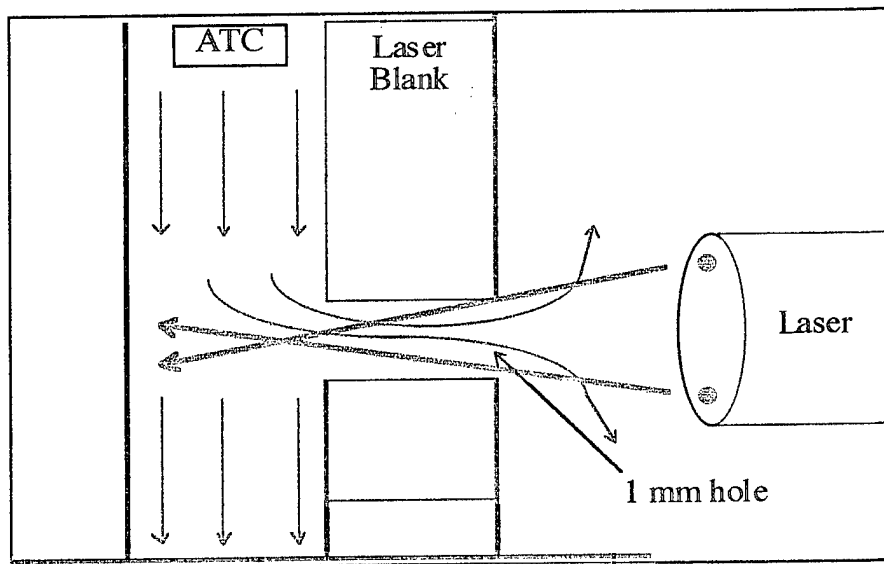


Figure 39. ATC flow depiction - laser blank

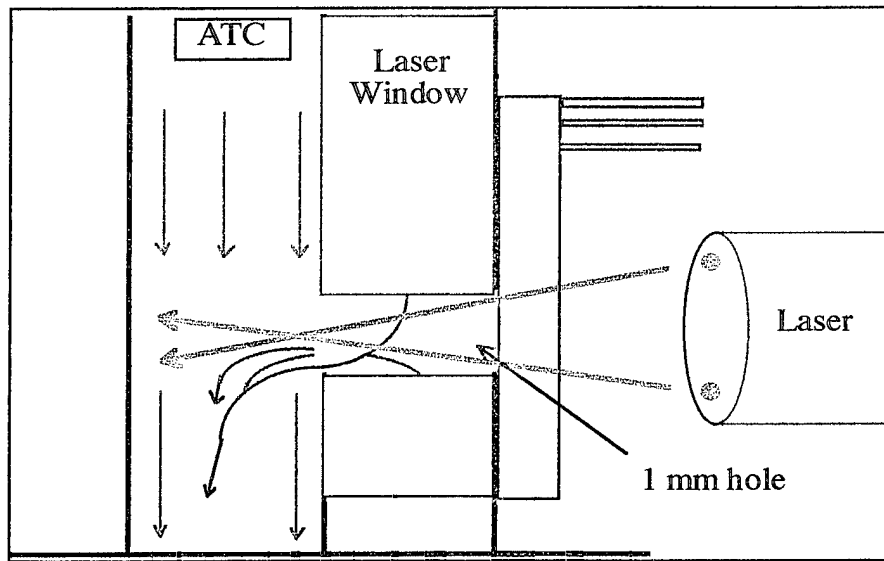


Figure 40. ATC flow depiction - pressurized window





## V. CONCLUSIONS AND RECOMMENDATIONS

An experimental investigation with an innovative pressurized LDV window was conducted on the flow through an annular turbine cascade to determine the effects of such a window on laser measurements. A pressure ratio ( $P_{rat}$ ) of .09620, defined as the downstream hub-static pressure ( $P_{hub}$ ) divided by the upstream stagnation pressure ( $P_0$ ), was chosen to test the new window. Three chamber pressures of 0, 76.2 and 152.4 mm (0, 3, and 6 in) of water were applied to the pressurized window resulting in LDV measurements that were compared with those obtained with a laser blank and velocity distributions obtained with a three-hole cobra probe.

An equalized pressure condition of 0 mm of water was considered preferable when measuring. In this condition the pressurized window eliminated any influence that the optical access hole may have had and the internal flow was not then affected by any pressurized air from the window. When the chamber was pressurized, the effect on the ATC flow of the increasing the pressure was found to be surprisingly small up to 152.4 mm (6 in) of water chamber pressure. The ATC flow seemed to be relatively insensitive to this procedure, which could be used to purge the window of any seed build up during the experiment.

LDV alignment and radial survey procedures were devised and repeated. The probe volume passed cleanly through the optical access hole and radial surveys were conducted to provide complete coverage for data recording. Introduction of a second fiber-optic probe for three component measurements would decrease the effective probe volume and increase radial position accuracy.

Initial measurements with the 1-dimensional probe showed good repeatability, but did not compare well with previous 2-component measurements. The previous measurements used a different data acquisition system than the one available for the present experiment, which may have contributed to the discrepancy. However, the 1-D procedure did prove to be both repeatable and accurate, despite the large amount of movement of the laser probe head.

Successful two-dimensional measurements of velocity, flow angle, and turbulence intensity through a 1.092 mm diameter optical access hole were demonstrated using both the 1-dimensional procedure and the new pressurized window. All LDV data were acquired one-half axial chord downstream of the turbine stator over five radial positions and 17 separate circumferential displacements. The range of experimental flow velocities was decreased from that used in Reference 2 due to the unavailability of the former processor and the limitations of the current signal processor.

The coarse circumferential (wake) positioning mechanism needed modification to allow more precise adjustment. Experimental circumferential positioning uncertainties may have contributed to some of the differences in the compared data.

Successful cobra probe measurements were conducted to help verify the measurements taken using the pressurized window. The result of a comparison of all three flow measurement devices was that, when the flow was contained (pressurized window), the measurements indicated higher velocities, lower turbulence intensities, and lower flow angles. If the flow was not contained (laser blank), the measurements indicated lower velocities, higher turbulence intensities, and higher flow angles. As the flow turned to exit the optical access hole, the flow angle increased.

The pressurized window provided accurate and repeatable LDV measurements with fewer disturbances to the flow than the previous laser blank. Future efforts to improve on this initial design would be to modify the shape to accommodate the laser probe volume deeper into the turbine. Increased flow velocities could also be attempted with subsequent increased chamber pressures to determine the benefits of this window on LDV measurements at higher flow speeds.

## APPENDIX A. PRESSURE DATA ACQUISITION

The following table relates each Scanivalve port to its respective pressure measurement.

| Scanivalve Port Number | Pressure Measured                            |
|------------------------|--|
| 1                      | Ambient Pressure                             |
| 2                      | Calibration Pressure (set at 20 inches hg)   |
| 3                      | Not Used                                     |
| 4                      | Upstream Total Pressure ( $P_0$ )            |
| 5                      | Downstream Hub Static Pressure ( $P_{hub}$ ) |
| 6                      | Upstream Static Pressure ( $P_{static}$ )    |
| 7                      | Not Used                                     |
| 8                      | Not Used                                     |
| 9                      | Blade Static Port #1 (at leading edge)       |
| 10                     | Blade Static Port #2 (suction side)          |
| 11                     | Blade Static Port #3 (suction side)          |
| 12                     | Blade Static Port #4 (suction side)          |
| 13                     | Blade Static Port #5 (suction side)          |
| 14                     | Blade Static Port #6 (suction side)          |
| 15                     | Blade Static Port #7 (suction side)          |
| 16                     | Blade Static Port #8 (at leading edge)       |
| 17                     | Blade Static Port #9 (pressure side)         |
| 18                     | Blade Static Port #10 (pressure side)        |
| 19                     | Blade Static Port #11 (pressure side)        |

Table A1. Pressure data acquisition connections



## APPENDIX B. BLADE MIDSPAN SURFACE PRESSURE DATA

| Prat of .9825     | Date: 04/05/96                           | Baro=30.06 in Hg      | Temp=78 F |
|-------------------|--|-----------------------|-----------|
| Scanivalve Port # | Scanivalve Port Value                    | Static Pressure (psi) | P/Po      |
| 1                 | P ambient                                | 14.7690               |           |
| 2                 | P calibration                            | 15.7554               |           |
| 4                 | Po (Ref. Upstream Stagnation)            | 15.0334               | 1.0000    |
| 5                 | P hub exit (Static @ 0.5c<br>downstream) | 14.7897               |           |
| 6                 | P up static (Ref. Upstream Static)       | 15.0398               |           |
| 9                 | P Static Port 1 (@ leading edge)         | 15.0399               | 1.0004    |
| 10                | P Static Port 2                          | 15.0207               | 0.9992    |
| 11                | P Static Port 3                          | 14.9188               | 0.9924    |
| 12                | P Static Port 4                          | 14.821                | 0.9859    |
| 13                | P Static Port 5                          | 14.788                | 0.9837    |
| 14                | P Static Port 6                          | 14.8013               | 0.9846    |
| 15                | P Static Port 7                          | 14.8046               | 0.9848    |
| 16                | P Static Port 8 (@ leading edge)         | 15.0384               | 1.0003    |
| 17                | P Static Port 9                          | 15.0281               | 0.9996    |
| 18                | P Static Port 10                         | 14.9838               | 0.9967    |
| 19                | P Static Port 11                         | 14.9462               | 0.9942    |

Table B1. Surface pressures at 0.9825 pressure ratio

| Prat of .9757     | Date: 04/05/96                           | Baro=30.06 in Hg      | Tstag=83 F |
|-------------------|--|-----------------------|------------|
| Scanivalve Port # | Scanivalve Port Value                    | Static Pressure (psi) | P/Po       |
| 1                 | P ambient                                | 14.7641               |            |
| 2                 | P calibration                            | 15.7586               |            |
| 4                 | Po (Ref. Upstream Stagnation)            | 15.1364               | 1.0000     |
| 5                 | P hub exit (Static @ 0.5c<br>downstream) | 14.7923               |            |
| 6                 | P up static (Ref. Upstream Static)       | 15.1430               |            |
| 9                 | P Static Port 1 (@ leading edge)         | 15.1430               | 1.0004     |
| 10                | P Static Port 2                          | 15.0970               | 0.9974     |
| 11                | P Static Port 3                          | 14.9739               | 0.9893     |
| 12                | P Static Port 4                          | 14.8382               | 0.9803     |
| 13                | P Static Port 5                          | 14.7836               | 0.9767     |
| 14                | P Static Port 6                          | 14.8068               | 0.9782     |
| 15                | P Static Port 7                          | 14.811                | 0.9785     |
| 16                | P Static Port 8 (@ leading edge)         | 15.1439               | 1.0005     |
| 17                | P Static Port 9                          | 15.1278               | 0.9994     |
| 18                | P Static Port 10                         | 15.0646               | 0.9953     |
| 19                | P Static Port 11                         | 15.0121               | 0.9918     |

Table B2. Surface pressures at 0.9757 pressure ratio

| Prat of .9710     | Date: 04/05/96                        | Baro=30.06 in Hg      | Tstag=84 F |
|-------------------|---------------------------------------|-----------------------|------------|
| Scanivalve Port # | Scanivalve Port Value                 | Static Pressure (psi) | P/Po       |
| 1                 | P ambient                             | 14.7641               |            |
| 2                 | P calibration                         | 15.7587               |            |
| 4                 | Po (Ref. Upstream Stagnation)         | 15.2046               | 1.0000     |
| 5                 | P hub exit (Static @ 0.5c downstream) | 14.7981               |            |
| 6                 | P up static (Ref. Upstream Static)    | 15.2119               |            |
| 9                 | P Static Port 1 (@ leading edge)      | 15.2141               | 1.0006     |
| 10                | P Static Port 2                       | 15.1462               | 0.9962     |
| 11                | P Static Port 3                       | 15.0207               | 0.9879     |
| 12                | P Static Port 4                       | 14.8607               | 0.9774     |
| 13                | P Static Port 5                       | 14.7972               | 0.9732     |
| 14                | P Static Port 6                       | 14.8174               | 0.9745     |
| 15                | P Static Port 7                       | 14.8243               | 0.9750     |
| 16                | P Static Port 8 (@ leading edge)      | 15.2113               | 1.0004     |
| 17                | P Static Port 9                       | 15.1929               | 0.9992     |
| 18                | P Static Port 10                      | 15.1203               | 0.9945     |
| 19                | P Static Port 11                      | 15.0582               | 0.9904     |

Table B3. Surface pressures at 0.9710 pressure ratio

| Prat of .9669     | Date: 04/05/96                           | Baro=30.06 in Hg      | Tstag=84 F |
|-------------------|--|-----------------------|------------|
| Scanivalve Port # | Scanivalve Port Value                    | Static Pressure (psi) | P/Po       |
| 1                 | P ambient                                | 14.7641               |            |
| 2                 | P calibration                            | 15.7586               |            |
| 4                 | Po (Ref. Upstream Stagnation)            | 15.2744               | 1.0000     |
| 5                 | P hub exit (Static @ 0.5c<br>downstream) | 14.8050               |            |
| 6                 | P up static (Ref. Upstream Static)       | 15.2841               |            |
| 9                 | P Static Port 1 (@ leading edge)         | 15.2865               | 1.0008     |
| 10                | P Static Port 2                          | 15.2107               | 0.9958     |
| 11                | P Static Port 3                          | 15.0609               | 0.9860     |
| 12                | P Static Port 4                          | 14.8758               | 0.9739     |
| 13                | P Static Port 5                          | 14.8012               | 0.9690     |
| 14                | P Static Port 6                          | 14.8283               | 0.9708     |
| 15                | P Static Port 7                          | 14.8306               | 0.9709     |
| 16                | P Static Port 8 (@ leading edge)         | 15.2846               | 1.0007     |
| 17                | P Static Port 9                          | 15.2625               | 0.9992     |
| 18                | P Static Port 10                         | 15.1727               | 0.9933     |
| 19                | P Static Port 11                         | 15.1026               | 0.9888     |

Table B4. Surface pressures at 0.9669 pressure ratio



| Prat of .9621     | Date: 04/05/96                        | Baro=30.06 in Hg      | Tstag=85 F |
|-------------------|---------------------------------------|-----------------------|------------|
| Scanivalve Port # | Scanivalve Port Value                 | Static Pressure (psi) | P/Po       |
| 1                 | P ambient                             | 14.7641               |            |
| 2                 | P calibration                         | 15.7583               |            |
| 4                 | Po (Ref. Upstream Stagnation)         | 15.3525               | 1.0000     |
| 5                 | P hub exit (Static @ 0.5c downstream) | 14.8108               |            |
| 6                 | P up static (Ref. Upstream Static)    | 15.3636               |            |
| 9                 | P Static Port 1 (@ leading edge)      | 15.3639               | 1.0007     |
| 10                | P Static Port 2                       | 15.2706               | 0.9947     |
| 11                | P Static Port 3                       | 15.1029               | 0.9837     |
| 12                | P Static Port 4                       | 14.8922               | 0.9700     |
| 13                | P Static Port 5                       | 14.8123               | 0.9648     |
| 14                | P Static Port 6                       | 14.8349               | 0.9663     |
| 15                | P Static Port 7                       | 14.8383               | 0.9665     |
| 16                | P Static Port 8 (@ leading edge)      | 15.3492               | 0.9998     |
| 17                | P Static Port 9                       | 15.3361               | 0.9989     |
| 18                | P Static Port 10                      | 15.24                 | 0.9927     |
| 19                | P Static Port 11                      | 15.1585               | 0.9874     |

Table B5. Surface pressures at 0.9621 pressure ratio

| Prat of .9575     | Date: 04/05/96                           | Baro=30.06 in Hg      | Tstag=86 F |
|-------------------|--|-----------------------|------------|
| Scanivalve Port # | Scanivalve Port Value                    | Static Pressure (psi) | P/Po       |
| 1                 | P ambient                                | 14.7641               |            |
| 2                 | P calibration                            | 15.7555               |            |
| 4                 | Po (Ref. Upstream Stagnation)            | 15.4209               | 1.0000     |
| 5                 | P hub exit (Static @ 0.5c<br>downstream) | 14.4318               |            |
| 6                 | P up static (Ref. Upstream Static)       | 15.4318               |            |
| 9                 | P Static Port 1 (@ leading edge)         | 15.4335               | 1.0008     |
| 10                | P Static Port 2                          | 15.3285               | 0.9940     |
| 11                | P Static Port 3                          | 15.1364               | 0.9816     |
| 12                | P Static Port 4                          | 14.906                | 0.9666     |
| 13                | P Static Port 5                          | 14.8175               | 0.9609     |
| 14                | P Static Port 6                          | 14.8389               | 0.9623     |
| 15                | P Static Port 7                          | 14.8454               | 0.9627     |
| 16                | P Static Port 8 (@ leading edge)         | 15.4295               | 1.0006     |
| 17                | P Static Port 9                          | 15.4039               | 0.9989     |
| 18                | P Static Port 10                         | 15.2961               | 0.9919     |
| 19                | P Static Port 11                         | 15.2016               | 0.9858     |

Table B6. Surface pressures at 0.9575 pressure ratio

| Prat of .9527     | Date: 04/05/96                        | Baro=30.06 in Hg      | Tstag=87 F |
|-------------------|---------------------------------------|-----------------------|------------|
| Scanivalve Port # | Scanivalve Port Value                 | Static Pressure (psi) | P/Po       |
| 1                 | P ambient                             | 14.7641               |            |
| 2                 | P calibration                         | 15.7545               |            |
| 4                 | Po (Ref. Upstream Stagnation)         | 15.4937               | 1.0000     |
| 5                 | P hub exit (Static @ 0.5c downstream) | 14.8297               |            |
| 6                 | P up static (Ref. Upstream Static)    | 15.5083               |            |
| 9                 | P Static Port 1 (@ leading edge)      | 15.5087               | 1.0010     |
| 10                | P Static Port 2                       | 15.3948               | 0.9936     |
| 11                | P Static Port 3                       | 15.1786               | 0.9797     |
| 12                | P Static Port 4                       | 14.9241               | 0.9632     |
| 13                | P Static Port 5                       | 14.8256               | 0.9569     |
| 14                | P Static Port 6                       | 14.8482               | 0.9583     |
| 15                | P Static Port 7                       | 14.8526               | 0.9586     |
| 16                | P Static Port 8 (@ leading edge)      | 15.4951               | 1.0001     |
| 17                | P Static Port 9                       | 15.477                | 0.9989     |
| 18                | P Static Port 10                      | 15.3583               | 0.9913     |
| 19                | P Static Port 11                      | 15.2577               | 0.9848     |

Table B7. Surface pressures at 0.9527 pressure ratio

| Prat of .9483     | Date: 04/05/96                        | Baro=30.06 in Hg      | Tstag=88 F |
|-------------------|---------------------------------------|-----------------------|------------|
| Scanivalve Port # | Scanivalve Port Value                 | Static Pressure (psi) | P/Po       |
| 1                 | P ambient                             | 14.7641               |            |
| 2                 | P calibration                         | 15.7528               |            |
| 4                 | Po (Ref. Upstream Stagnation)         | 15.5657               | 1.0000     |
| 5                 | P hub exit (Static @ 0.5c downstream) | 14.8287               |            |
| 6                 | P up static (Ref. Upstream Static)    | 15.5851               |            |
| 9                 | P Static Port 1 (@ leading edge)      | 15.5843               | 1.0012     |
| 10                | P Static Port 2                       | 15.4564               | 0.9930     |
| 11                | P Static Port 3                       | 15.2216               | 0.9779     |
| 12                | P Static Port 4                       | 14.9405               | 0.9598     |
| 13                | P Static Port 5                       | 14.8176               | 0.9519     |
| 14                | P Static Port 6                       | 14.8631               | 0.9549     |
| 15                | P Static Port 7                       | 14.8673               | 0.9551     |
| 16                | P Static Port 8 (@ leading edge)      | 15.5804               | 1.0009     |
| 17                | P Static Port 9                       | 15.5473               | 0.9988     |
| 18                | P Static Port 10                      | 15.4147               | 0.9903     |
| 19                | P Static Port 11                      | 15.3053               | 0.9833     |

Table B8. Surface pressures at 0.9483 pressure ratio

| Prat of .9445     | Date: 04/05/96                        | Baro=30.06 in Hg      | Tstag=89 F |
|-------------------|---------------------------------------|-----------------------|------------|
| Scanivalve Port # | Scanivalve Port Value                 | Static Pressure (psi) | P/Po       |
| 1                 | P ambient                             | 14.7641               |            |
| 2                 | P calibration                         | 15.7510               |            |
| 4                 | Po (Ref. Upstream Stagnation)         | 15.6278               | 1.0000     |
| 5                 | P hub exit (Static @ 0.5c downstream) | 14.8335               |            |
| 6                 | P up static (Ref. Upstream Static)    | 15.6487               |            |
| 9                 | P Static Port 1 (@ leading edge)      | 15.6442               | 1.0010     |
| 10                | P Static Port 2                       | 15.5066               | 0.9922     |
| 11                | P Static Port 3                       | 15.2518               | 0.9759     |
| 12                | P Static Port 4                       | 14.951                | 0.9567     |
| 13                | P Static Port 5                       | 14.8355               | 0.9493     |
| 14                | P Static Port 6                       | 14.857                | 0.9507     |
| 15                | P Static Port 7                       | 14.8619               | 0.9510     |
| 16                | P Static Port 8 (@ leading edge)      | 15.6258               | 0.9999     |
| 17                | P Static Port 9                       | 15.6073               | 0.9987     |
| 18                | P Static Port 10                      | 15.4658               | 0.9896     |
| 19                | P Static Port 11                      | 15.3467               | 0.9820     |

Table B9. Surface pressures at 0.9445 pressure ratio

| Prat of .9392     | Date: 04/05/96                        | Baro=30.06 in Hg      | Tstag=90 F |
|-------------------|---------------------------------------|-----------------------|------------|
| Scanivalve Port # | Scanivalve Port Value                 | Static Pressure (psi) | P/Po       |
| 1                 | P ambient                             | 14.7641               |            |
| 2                 | P calibration                         | 15.7517               |            |
| 4                 | Po (Ref. Upstream Stagnation)         | 15.7097               | 1.0000     |
| 5                 | P hub exit (Static @ 0.5c downstream) | 14.8411               |            |
| 6                 | P up static (Ref. Upstream Static)    | 15.7266               |            |
| 9                 | P Static Port 1 (@ leading edge)      | 15.731                | 1.0014     |
| 10                | P Static Port 2                       | 15.5861               | 0.9921     |
| 11                | P Static Port 3                       | 15.307                | 0.9744     |
| 12                | P Static Port 4                       | 14.9793               | 0.9535     |
| 13                | P Static Port 5                       | 14.8469               | 0.9451     |
| 14                | P Static Port 6                       | 14.8718               | 0.9467     |
| 15                | P Static Port 7                       | 14.8752               | 0.9469     |
| 16                | P Static Port 8 (@ leading edge)      | 15.7156               | 1.0004     |
| 17                | P Static Port 9                       | 15.6932               | 0.9989     |
| 18                | P Static Port 10                      | 15.5362               | 0.9890     |
| 19                | P Static Port 11                      | 15.4039               | 0.9805     |

Table B10. Surface pressures at 0.9392 pressure ratio

| Prat of .9359     | Date: 04/05/96                        | Baro=30.06 in Hg      | Tstag=91 F |
|-------------------|---------------------------------------|-----------------------|------------|
| Scanivalve Port # | Scanivalve Port Value                 | Static Pressure (psi) | P/Po       |
| 1                 | P ambient                             | 14.7641               |            |
| 2                 | P calibration                         | 15.7495               |            |
| 4                 | Po (Ref. Upstream Stagnation)         | 15.7679               | 1.0000     |
| 5                 | P hub exit (Static @ 0.5c downstream) | 14.8419               |            |
| 6                 | P up static (Ref. Upstream Static)    | 15.7873               |            |
| 9                 | P Static Port 1 (@ leading edge)      | 15.7941               | 1.0017     |
| 10                | P Static Port 2                       | 15.6366               | 0.9917     |
| 11                | P Static Port 3                       | 15.3413               | 0.9729     |
| 12                | P Static Port 4                       | 14.9785               | 0.9499     |
| 13                | P Static Port 5                       | 14.8416               | 0.9413     |
| 14                | P Static Port 6                       | 14.8748               | 0.9434     |
| 15                | P Static Port 7                       | 14.8762               | 0.9434     |
| 16                | P Static Port 8 (@ leading edge)      | 15.79                 | 1.0014     |
| 17                | P Static Port 9                       | 15.7491               | 0.9988     |
| 18                | P Static Port 10                      | 15.5812               | 0.9882     |
| 19                | P Static Port 11                      | 15.4452               | 0.9795     |

Table B11. Surface pressures at 0.9359 pressure ratio

| Prat of .9312     | Date: 04/05/96                        | Baro=30.06 in Hg      | Tstag=92 F |
|-------------------|---------------------------------------|-----------------------|------------|
| Scanivalve Port # | Scanivalve Port Value                 | Static Pressure (psi) | P/Po       |
| 1                 | P ambient                             | 14.7641               |            |
| 2                 | P calibration                         | 15.7478               |            |
| 4                 | Po (Ref. Upstream Stagnation)         | 15.8447               | 1.0000     |
| 5                 | P hub exit (Static @ 0.5c downstream) | 14.8544               |            |
| 6                 | P up static (Ref. Upstream Static)    | 15.8694               |            |
| 9                 | P Static Port 1 (@ leading edge)      | 15.8735               | 1.0018     |
| 10                | P Static Port 2                       | 15.7070               | 0.9913     |
| 11                | P Static Port 3                       | 15.3889               | 0.9712     |
| 12                | P Static Port 4                       | 15.0051               | 0.9470     |
| 13                | P Static Port 5                       | 14.8559               | 0.9376     |
| 14                | P Static Port 6                       | 14.8856               | 0.9395     |
| 15                | P Static Port 7                       | 14.89                 | 0.9397     |
| 16                | P Static Port 8 (@ leading edge)      | 15.8606               | 1.0010     |
| 17                | P Static Port 9                       | 15.8372               | 0.9995     |
| 18                | P Static Port 10                      | 15.6559               | 0.9881     |
| 19                | P Static Port 11                      | 15.5034               | 0.9785     |

Table B12. Surface pressures at 0.9312 pressure ratio



# APPENDIX C. LDV DATA

| Date    | Prat   | Run # | Depth  | U-Velocity | U-Non           | V-<br>Velocity | V-Non           | U-<br>Turbulence | V-<br>Turbulence | Flow<br>Angle |
|---------|--------|-------|--------|------------|-----------------|----------------|-----------------|------------------|------------------|---------------|
|         |        |       | (mm)   | (m/s)      | Dimensionalized | (m/s)          | Dimensionalized | (%)              | (%)              | degrees       |
| 4/16/96 | 0.9054 | 1     | 0.0090 | 7.7263     | 0.0098          | 70.6980        | 0.0896          | 9.2920           | 10.8338          | 83.9859       |
|         |        |       | 0.0590 | 7.6138     | 0.0096          | 70.8067        | 0.0897          | 8.8283           | 10.7080          | 84.0281       |
|         |        |       | 0.1790 | 6.3443     | 0.0080          | 72.6799        | 0.0921          | 9.1375           | 10.3136          | 84.6274       |
|         |        |       | 0.4200 | 6.6946     | 0.0085          | 74.0324        | 0.0938          | 8.8455           | 9.6086           | 84.6887       |
|         |        |       | 0.8890 | 7.0147     | 0.0089          | 76.1521        | 0.0965          | 8.8078           | 8.0782           | 84.2938       |
|         |        |       | 1.7790 | 7.6428     | 0.0097          | 79.3038        | 0.1005          | 8.5545           | 6.5872           | 83.8449       |
|         |        |       |        |            |                 |                |                 |                  |                  |               |
|         |        | 2     | 0.0090 | 7.3401     | 0.0093          | 75.1028        | 0.0951          | 8.8467           | 8.1487           |               |
|         |        |       | 0.0590 | 7.3422     | 0.0093          | 74.7188        | 0.0946          | 8.8773           | 8.3646           |               |
|         |        |       | 0.1790 | 6.9598     | 0.0088          | 75.0067        | 0.0950          | 8.6105           | 8.4808           |               |
|         |        |       | 0.4200 | 6.5290     | 0.0083          | 76.0889        | 0.0964          | 8.7808           | 7.8535           |               |
|         |        |       | 0.8890 | 7.5725     | 0.0096          | 77.8091        | 0.0986          | 8.8516           | 7.4860           |               |
|         |        |       | 1.7790 | 8.9538     | 0.0113          | 80.0626        | 0.1014          | 8.9554           | 7.1723           |               |
|         |        |       |        |            |                 |                |                 |                  |                  |               |
|         |        | 3     | 0.0090 | 7.7023     | 0.0098          | 70.3165        | 0.0891          | 8.6246           | 11.2738          |               |
|         |        |       | 0.0590 | 7.7153     | 0.0098          | 71.1984        | 0.0902          | 8.7844           | 10.9511          |               |
|         |        |       | 0.1790 | 7.4003     | 0.0094          | 72.4658        | 0.0918          | 8.6960           | 10.2123          |               |
|         |        |       | 0.4200 | 7.6315     | 0.0097          | 74.2093        | 0.0940          | 9.2821           | 9.4072           |               |
|         |        |       | 0.8890 | 8.4376     | 0.0107          | 76.4671        | 0.0969          | 9.5977           | 7.9965           |               |
|         |        |       | 1.7790 | 9.1613     | 0.0116          | 79.4832        | 0.1007          | 9.3782           | 6.4372           |               |

Table C1. 04/16/96 Laser blank radial survey at 0.9054 pressure ratio

| Date    | Prat   | Wake<br>Position   | Depth  | U-<br>Velocity | U-Non           | V-<br>Velocity | V-Non           | U-<br>Turbulence | V-<br>Turbulenc<br>e | Flow<br>Angle |
|---------|--------|--------------------|--------|----------------|-----------------|----------------|-----------------|------------------|----------------------|---------------|
|         |        | (degrees)          | (mm)   | (m/s)          | Dimensionalized | (m/s)          | Dimensionalized | (%)              | (%)                  | degrees       |
| 4/26/96 | 0.9054 | 0                  | 0.0090 | 7.5867         | 0.0096          | 67.3459        | 0.0850          | 8.2461           | 13.3413              | 83.5726       |
|         |        |                    | 0.0590 | 7.5842         | 0.0096          | 66.5375        | 0.0840          | 8.4709           | 12.4993              | 83.4973       |
|         |        |                    | 0.1790 | 8.0933         | 0.0102          | 65.5193        | 0.0827          | 7.9839           | 12.1199              | 82.9582       |
|         |        |                    | 0.4200 | 8.1258         | 0.0103          | 65.0528        | 0.0821          | 8.3899           | 10.9839              | 82.8800       |
|         |        |                    | 0.8890 | 7.7965         | 0.0098          | 65.1411        | 0.0822          | 8.8630           | 9.8928               | 83.1749       |
|         |        |                    | 1.7790 | 9.4393         | 0.0119          | 75.2531        | 0.0950          | 8.4856           | 9.9922               | 82.8505       |
|         |        |                    |        |                |                 |                |                 |                  |                      |               |
|         |        | Pinned<br>(-2 deg) | 0.0090 | 7.9418         | 0.0100          | 67.4893        | 0.0852          | 8.5371           | 12.4886              | 83.2886       |
|         |        |                    | 0.0590 | 7.9699         | 0.0101          | 67.1699        | 0.0848          | 8.6211           | 11.9539              | 83.2333       |
|         |        |                    | 0.1790 | 8.5587         | 0.0108          | 66.3405        | 0.0837          | 8.3250           | 11.4469              | 82.6488       |
|         |        |                    | 0.4200 | 8.1064         | 0.0102          | 65.8481        | 0.0831          | 8.2266           | 10.3691              | 82.9818       |
|         |        |                    | 0.8890 | 7.7319         | 0.0098          | 65.4274        | 0.0826          | 8.7679           | 9.6328               | 83.2603       |
|         |        |                    | 1.7790 | 10.4489        | 0.0132          | 74.7139        | 0.0943          | 8.9899           | 9.8799               | 82.0387       |

Table C2. 04/26/96 Laser blank radial survey at 0.9054 pressure ratio

| Date    | Prat   | Depth | Wake<br>Position | U-<br>Velocity | U-Non<br>Dimensionalized | V-<br>Velocity | V-Non<br>Dimensionalized | U-<br>Turbulence | V-<br>Turbulence | Flow<br>Angle |
|---------|--------|-------|------------------|----------------|--------------------------|----------------|--------------------------|------------------|------------------|---------------|
|         |        | (mm)  | (degrees)        | (m/s)          |                          | (m/s)          |                          | (%)              | (%)              | degrees       |
| 4/26/96 | 0.9054 | 0.01  | 8.0000           | 8.7570         | 0.0111                   | 61.0770        | 0.0776                   | 6.5409           | 11.9974          | 81.9703       |
|         |        |       | 7.0000           | 8.9116         | 0.0113                   | 61.7911        | 0.0785                   | 6.7514           | 12.6270          | 81.9236       |
|         |        |       | 6.0000           | 8.7271         | 0.0110                   | 61.8813        | 0.0787                   | 6.6094           | 12.4939          | 82.1000       |
|         |        |       | 5.0000           | 8.7370         | 0.0110                   | 61.7979        | 0.0786                   | 6.4054           | 12.3947          | 82.0806       |
|         |        |       | 4.0000           | 9.0774         | 0.0115                   | 62.0636        | 0.0789                   | 5.8996           | 12.6903          | 81.8110       |
|         |        |       | 3.0000           | 8.8678         | 0.0112                   | 62.3786        | 0.0793                   | 5.7717           | 12.1044          | 82.0375       |
|         |        |       | 2.0000           | 8.9612         | 0.0113                   | 62.4936        | 0.0794                   | 5.8697           | 12.6623          | 81.9693       |
|         |        |       | 1.0000           | 8.9421         | 0.0113                   | 62.4349        | 0.0794                   | 6.3205           | 12.8076          | 81.9788       |
|         |        |       | 0.0000           | 8.9111         | 0.0113                   | 61.4553        | 0.0781                   | 6.7566           | 12.5069          | 81.8805       |
|         |        |       | -1.0000          | 8.9763         | 0.0113                   | 62.5559        | 0.0795                   | 6.5990           | 13.1067          | 81.9639       |
|         |        |       | -2.0000          | 8.7992         | 0.0111                   | 62.9436        | 0.0800                   | 6.6703           | 12.7317          | 82.1683       |
|         |        |       | -3.0000          | 8.8903         | 0.0112                   | 60.7911        | 0.0773                   | 6.5965           | 11.9403          | 81.8119       |
|         |        |       | -4.0000          | 8.7644         | 0.0111                   | 61.6588        | 0.0784                   | 6.9645           | 12.3777          | 82.0384       |
|         |        |       | -5.0000          | 8.9914         | 0.0114                   | 61.1861        | 0.0778                   | 6.7237           | 11.5065          | 81.7728       |
|         |        |       | -6.0000          | 9.2114         | 0.0116                   | 61.4081        | 0.0781                   | 6.4447           | 13.3419          | 81.6043       |
|         |        |       | -7.0000          | 9.0160         | 0.0114                   | 61.7278        | 0.0785                   | 6.3016           | 13.9456          | 81.8220       |
|         |        |       | -8.0000          | 9.1600         | 0.0116                   | 63.1058        | 0.0802                   | 6.1572           | 14.4980          | 81.8721       |
|         |        |       |                  |                |                          |                |                          |                  |                  |               |
|         |        | 0.06  | 8.0000           | 9.2007         | 0.0116                   | 61.8903        | 0.0787                   | 6.7256           | 12.9828          | 81.6110       |
|         |        |       | 7.0000           | 9.1781         | 0.0116                   | 61.4019        | 0.0781                   | 6.5109           | 13.0005          | 81.5657       |
|         |        |       | 6.0000           | 9.1200         | 0.0115                   | 62.0508        | 0.0789                   | 6.8248           | 13.3862          | 81.7048       |
|         |        |       | 5.0000           | 9.1354         | 0.0115                   | 61.5695        | 0.0783                   | 6.1339           | 12.9443          | 81.6269       |
|         |        |       | 4.0000           | 8.8697         | 0.0112                   | 61.2918        | 0.0779                   | 6.0526           | 12.5114          | 81.8308       |
|         |        |       | 3.0000           | 9.1518         | 0.0116                   | 61.4036        | 0.0781                   | 5.9164           | 12.5012          | 81.5898       |
|         |        |       | 2.0000           | 8.9826         | 0.0113                   | 61.2838        | 0.0779                   | 5.8574           | 12.4938          | 81.7272       |
|         |        |       | 1.0000           | 9.1263         | 0.0115                   | 61.2486        | 0.0779                   | 6.1394           | 12.9263          | 81.5920       |
|         |        |       | 0.0000           | 8.9294         | 0.0113                   | 61.2309        | 0.0778                   | 6.3844           | 12.9888          | 81.7685       |
|         |        |       | -1.0000          | 9.3722         | 0.0118                   | 61.2948        | 0.0779                   | 6.8244           | 12.7725          | 81.3752       |
|         |        |       | -2.0000          | 9.0669         | 0.0115                   | 60.6321        | 0.0771                   | 6.8014           | 12.1949          | 81.5622       |
|         |        |       | -3.0000          | 9.1668         | 0.0116                   | 61.4783        | 0.0782                   | 6.6025           | 13.0070          | 81.5863       |
|         |        |       | -4.0000          | 9.0649         | 0.0115                   | 61.1101        | 0.0777                   | 6.5926           | 12.9230          | 81.6291       |

| Date | Prat | Depth | Wake<br>Position | U-<br>Velocity | U-Non<br>Dimensionalized | V-<br>Velocity | V-Non<br>Dimensionalized | U-<br>Turbulence | V-<br>Turbulence | Flow<br>Angle |
|------|------|-------|------------------|----------------|--------------------------|----------------|--------------------------|------------------|------------------|---------------|
|      |      | (mm)  | (degrees)        | (m/s)          |                          | (m/s)          |                          | (%)              | (%)              | degrees       |
|      |      |       | -5.0000          | 9.2264         | 0.0117                   | 59.3996        | 0.0755                   | 6.9049           | 13.2696          | 81.2406       |
|      |      |       | -6.0000          | 9.1726         | 0.0116                   | 60.3660        | 0.0767                   | 6.5442           | 12.5975          | 81.4282       |
|      |      |       | -7.0000          | 9.4620         | 0.0120                   | 60.3353        | 0.0767                   | 6.5880           | 13.7378          | 81.1575       |
|      |      |       | -8.0000          | 9.4617         | 0.0120                   | 60.3312        | 0.0767                   | 5.7620           | 12.5894          | 81.1572       |
|      |      |       |                  |                |                          |                |                          |                  |                  |               |
|      |      | 0.18  | 8.0000           | 9.1225         | 0.0115                   | 58.3371        | 0.0742                   | 6.6463           | 10.8126          | 81.1590       |
|      |      |       | 7.0000           | 9.6565         | 0.0122                   | 58.9808        | 0.0750                   | 6.6811           | 10.5627          | 80.7506       |
|      |      |       | 6.0000           | 9.0252         | 0.0114                   | 58.6529        | 0.0746                   | 6.3091           | 10.8814          | 81.2982       |
|      |      |       | 5.0000           | 9.2633         | 0.0117                   | 58.7839        | 0.0747                   | 6.4421           | 10.7820          | 81.0918       |
|      |      |       | 4.0000           | 9.3896         | 0.0119                   | 59.4559        | 0.0756                   | 5.9659           | 10.4109          | 81.0727       |
|      |      |       | 3.0000           | 9.3258         | 0.0118                   | 59.3763        | 0.0755                   | 5.6890           | 9.8853           | 81.1207       |
|      |      |       | 2.0000           | 9.3122         | 0.0118                   | 59.3969        | 0.0755                   | 5.8731           | 10.6835          | 81.1365       |
|      |      |       | 1.0000           | 9.3414         | 0.0118                   | 60.3910        | 0.0768                   | 6.2334           | 10.2768          | 81.2532       |
|      |      |       | 0.0000           | 9.4195         | 0.0119                   | 59.8481        | 0.0761                   | 6.5733           | 9.7079           | 81.1025       |
|      |      |       | -1.0000          | 9.3607         | 0.0118                   | 59.6495        | 0.0758                   | 6.7631           | 10.0447          | 81.1282       |
|      |      |       | -2.0000          | 9.2666         | 0.0117                   | 59.6625        | 0.0758                   | 6.8001           | 10.1740          | 81.2179       |
|      |      |       | -3.0000          | 9.5436         | 0.0121                   | 59.9614        | 0.0762                   | 6.7823           | 10.7888          | 81.0040       |
|      |      |       | -4.0000          | 9.4871         | 0.0120                   | 59.8467        | 0.0761                   | 6.8254           | 10.8933          | 81.0395       |
|      |      |       | -5.0000          | 9.2245         | 0.0117                   | 59.6104        | 0.0758                   | 6.9121           | 11.4045          | 81.2496       |
|      |      |       | -6.0000          | 9.6519         | 0.0122                   | 59.3545        | 0.0755                   | 6.5618           | 10.9097          | 80.8121       |
|      |      |       | -7.0000          | 9.6546         | 0.0122                   | 59.7283        | 0.0759                   | 6.2292           | 11.0594          | 80.8662       |
|      |      |       | -8.0000          | 9.6308         | 0.0122                   | 59.6301        | 0.0758                   | 5.9114           | 10.0893          | 80.8735       |
|      |      |       |                  |                |                          |                |                          |                  |                  |               |
|      |      | 0.42  | 8.0000           | 9.6093         | 0.0121                   | 58.6440        | 0.0745                   | 6.9475           | 8.5302           | 80.7268       |
|      |      |       | 7.0000           | 9.6198         | 0.0122                   | 58.8849        | 0.0749                   | 6.4806           | 8.3530           | 80.7542       |
|      |      |       | 6.0000           | 9.7546         | 0.0123                   | 59.0213        | 0.0750                   | 6.5286           | 9.0157           | 80.6482       |
|      |      |       | 5.0000           | 9.8126         | 0.0124                   | 59.3508        | 0.0754                   | 6.3175           | 8.7052           | 80.6448       |
|      |      |       | 4.0000           | 9.6658         | 0.0122                   | 59.6109        | 0.0758                   | 5.8641           | 8.3807           | 80.8219       |
|      |      |       | 3.0000           | 9.8621         | 0.0125                   | 60.2217        | 0.0766                   | 6.2545           | 9.2189           | 80.7321       |
|      |      |       | 2.0000           | 10.0930        | 0.0128                   | 59.7916        | 0.0760                   | 6.2871           | 8.4031           | 80.4520       |
|      |      |       | 1.0000           | 9.7961         | 0.0124                   | 59.6883        | 0.0759                   | 7.1465           | 8.6011           | 80.7122       |
|      |      |       | 0.0000           | 9.5456         | 0.0121                   | 59.6467        | 0.0758                   | 7.0418           | 8.2379           | 80.9395       |
|      |      |       | -1.0000          | 9.4079         | 0.0119                   | 59.4290        | 0.0755                   | 7.0671           | 8.0504           | 81.0359       |

| Date | Prat | Depth  | Wake<br>Position | U-<br>Velocity | U-Non<br>Dimensionalized | V-<br>Velocity | V-Non<br>Dimensionalized | U-<br>Turbulence | V-<br>Turbulence | Flow<br>Angle |
|------|------|--------|------------------|----------------|--------------------------|----------------|--------------------------|------------------|------------------|---------------|
|      |      | (mm)   | (degrees)        | (m/s)          |                          | (m/s)          |                          | (%)              | (%)              | degrees       |
|      |      |        | -2.0000          | 9.8236         | 0.0124                   | 58.6927        | 0.0746                   | 7.3689           | 8.2178           | 80.5314       |
|      |      |        | -3.0000          | 9.6044         | 0.0121                   | 58.4125        | 0.0743                   | 6.8753           | 8.4234           | 80.6954       |
|      |      |        | -4.0000          | 9.8322         | 0.0124                   | 58.3281        | 0.0741                   | 6.6871           | 8.3061           | 80.4651       |
|      |      |        | -5.0000          | 9.8835         | 0.0125                   | 58.5983        | 0.0745                   | 6.5970           | 8.6453           | 80.4597       |
|      |      |        | -6.0000          | 9.8131         | 0.0124                   | 58.8232        | 0.0748                   | 6.5794           | 8.5165           | 80.5620       |
|      |      |        | -7.0000          | 10.0289        | 0.0127                   | 58.4140        | 0.0743                   | 6.3373           | 8.6078           | 80.2920       |
|      |      |        | -8.0000          | 9.9161         | 0.0125                   | 59.0151        | 0.0750                   | 6.4582           | 8.2266           | 80.4952       |
|      |      |        |                  |                |                          |                |                          |                  |                  |               |
|      |      | 0.8900 | 8.0000           | 9.9965         | 0.0126                   | 60.0407        | 0.0763                   | 6.5887           | 7.6467           | 80.5802       |
|      |      |        | 7.0000           | 10.5149        | 0.0133                   | 59.4985        | 0.0756                   | 6.5281           | 7.6588           | 80.0127       |
|      |      |        | 6.0000           | 10.5122        | 0.0133                   | 59.8526        | 0.0761                   | 6.4432           | 8.4151           | 80.0731       |
|      |      |        | 5.0000           | 10.8461        | 0.0137                   | 60.2165        | 0.0765                   | 6.4400           | 8.2750           | 79.8250       |
|      |      |        | 4.0000           | 10.6144        | 0.0134                   | 60.4791        | 0.0769                   | 5.9827           | 8.4440           | 80.0803       |
|      |      |        | 3.0000           | 10.7056        | 0.0135                   | 61.0712        | 0.0776                   | 6.1018           | 8.2774           | 80.0919       |
|      |      |        | 2.0000           | 10.3515        | 0.0131                   | 61.1472        | 0.0777                   | 6.3947           | 8.0605           | 80.4251       |
|      |      |        | 1.0000           | 10.4739        | 0.0132                   | 60.7170        | 0.0772                   | 6.3898           | 8.1937           | 80.2467       |
|      |      |        | 0.0000           | 10.3550        | 0.0131                   | 60.1497        | 0.0765                   | 7.0236           | 7.1155           | 80.2661       |
|      |      |        | -1.0000          | 10.0215        | 0.0127                   | 60.0845        | 0.0764                   | 6.8388           | 7.0750           | 80.5638       |
|      |      |        | -2.0000          | 9.9767         | 0.0126                   | 60.1453        | 0.0765                   | 7.1133           | 7.0830           | 80.6146       |
|      |      |        | -3.0000          | 10.2565        | 0.0130                   | 60.0480        | 0.0763                   | 6.9256           | 7.2871           | 80.3409       |
|      |      |        | -4.0000          | 10.2692        | 0.0130                   | 59.8772        | 0.0761                   | 6.9702           | 7.4479           | 80.3021       |
|      |      |        | -5.0000          | 10.3514        | 0.0131                   | 59.7628        | 0.0760                   | 6.6431           | 7.5250           | 80.2076       |
|      |      |        | -6.0000          | 10.6230        | 0.0134                   | 59.7802        | 0.0760                   | 6.6676           | 8.1968           | 79.9587       |
|      |      |        | -7.0000          | 10.3550        | 0.0131                   | 60.1413        | 0.0765                   | 6.7896           | 8.2124           | 80.2648       |
|      |      |        | -8.0000          | 10.2497        | 0.0129                   | 59.9124        | 0.0762                   | 6.7121           | 7.7260           | 80.3258       |
|      |      |        |                  |                |                          |                |                          |                  |                  |               |
|      |      | 1.7800 | 8.0000           | 10.5075        | 0.0133                   | 61.5419        | 0.0782                   | 3.7752           | 6.5907           | 80.3447       |
|      |      |        | 7.0000           | 10.7380        | 0.0136                   | 61.3728        | 0.0780                   | 3.6736           | 6.9605           | 80.1103       |
|      |      |        | 6.0000           | 11.0958        | 0.0140                   | 61.3041        | 0.0779                   | 3.4421           | 6.9224           | 79.7764       |
|      |      |        | 5.0000           | 10.9327        | 0.0138                   | 62.2611        | 0.0791                   | 3.6119           | 7.2509           | 80.0754       |
|      |      |        | 4.0000           | 10.8737        | 0.0137                   | 61.8806        | 0.0787                   | 3.5696           | 7.5447           | 80.0684       |
|      |      |        | 3.0000           | 11.1308        | 0.0141                   | 62.5371        | 0.0795                   | 3.5140           | 7.5943           | 79.9429       |
|      |      |        | 2.0000           | 11.1401        | 0.0141                   | 62.4859        | 0.0794                   | 3.6464           | 7.2865           | 79.9266       |

| Date | Prat | Depth | Wake<br>Position | U-<br>Velocity | U-Non<br>Dimensionalized | V-<br>Velocity | V-Non<br>Dimensionalized | U-<br>Turbulence | V-<br>Turbulence | Flow<br>Angle |
|------|------|-------|------------------|----------------|--------------------------|----------------|--------------------------|------------------|------------------|---------------|
|      |      | (mm)  | (degrees)        | (m/s)          |                          | (m/s)          |                          | (%)              | (%)              | degrees       |
|      |      |       | 1.0000           | 11.0462        | 0.0140                   | 62.4443        | 0.0794                   | 3.7845           | 7.2656           | 80.0033       |
|      |      |       | 0.0000           | 11.0897        | 0.0140                   | 62.3987        | 0.0793                   | 3.7912           | 6.3280           | 79.9575       |
|      |      |       | -1.0000          | 10.4026        | 0.0131                   | 62.2212        | 0.0791                   | 3.8873           | 6.3911           | 80.5418       |
|      |      |       | -2.0000          | 10.7487        | 0.0136                   | 62.1578        | 0.0790                   | 3.6834           | 6.2852           | 80.2233       |
|      |      |       | -3.0000          | 10.8329        | 0.0137                   | 62.1273        | 0.0790                   | 3.6855           | 6.4667           | 80.1434       |
|      |      |       | -4.0000          | 11.0899        | 0.0140                   | 61.4829        | 0.0782                   | 3.6068           | 6.6467           | 79.8108       |
|      |      |       | -5.0000          | 10.6160        | 0.0134                   | 61.9295        | 0.0787                   | 3.6791           | 7.4993           | 80.3068       |
|      |      |       | -6.0000          | 10.8497        | 0.0137                   | 61.4407        | 0.0781                   | 3.4613           | 7.0579           | 80.0203       |
|      |      |       | -7.0000          | 10.6387        | 0.0134                   | 61.8889        | 0.0787                   | 3.6087           | 7.5119           | 80.2802       |
|      |      |       | -8.0000          | 10.4167        | 0.0132                   | 61.7202        | 0.0785                   | 3.8202           | 7.5143           | 80.4537       |

Table C3. 04/26/96 Laser blank circumferential survey at 0.9054 pressure ratio

| Date    | Prat   | Wake<br>Position | Depth  | U-<br>Velocity | U-Non           | V-<br>Velocity | V-Non           | U-<br>Turbulence | V-<br>Turbulence | Flow<br>Angle |
|---------|--------|------------------|--------|----------------|-----------------|----------------|-----------------|------------------|------------------|---------------|
|         |        | (degrees)        | (mm)   | (m/s)          | Dimensionalized | (m/s)          | Dimensionalized | (%)              | (%)              | degrees       |
| 4/19/92 | 0.9620 | -8               | 0.0090 | 5.7456         | 0.0073          | 61.1444        | 0.0781          | 9.5115           | 12.2320          | 84.6701       |
|         |        |                  | 0.0590 | 5.2821         | 0.0067          | 60.9264        | 0.0778          | 9.2503           | 11.1208          | 85.0804       |
|         |        |                  | 0.1790 | 4.4444         | 0.0056          | 59.8129        | 0.0764          | 9.9199           | 9.5370           | 85.7808       |
|         |        |                  | 0.4200 | 0.8329         | 0.0011          | 59.9625        | 0.0766          | 10.1712          | 8.0492           | 89.2099       |
|         |        |                  | 0.8890 | 3.2516         | 0.0041          | 60.8124        | 0.0777          | 14.3875          | 8.4654           | 86.9612       |
|         |        |                  | 1.7790 | 12.7285        | 0.0161          | 61.3428        | 0.0783          | 7.0233           | 7.6633           | 78.3593       |
|         |        |                  |        |                |                 |                |                 |                  |                  |               |
|         |        | 0                | 0.0090 | 3.7604         | 0.0048          | 60.2522        | 0.0769          | 8.0066           | 11.3192          | 86.4543       |
|         |        |                  | 0.0590 | 3.7736         | 0.0048          | 59.9021        | 0.0765          | 7.6785           | 10.3852          | 86.4211       |
|         |        |                  | 0.1790 | 3.2045         | 0.0041          | 59.3887        | 0.0758          | 7.3043           | 8.6216           | 86.9335       |
|         |        |                  | 0.4200 | 1.7476         | 0.0022          | 59.4696        | 0.0759          | 6.2254           | 7.8045           | 88.3288       |
|         |        |                  | 0.8890 | 5.2735         | 0.0067          | 60.7388        | 0.0776          | 12.1140          | 7.2078           | 85.0733       |
|         |        |                  | 1.7790 | 11.8807        | 0.0151          | 61.7119        | 0.0788          | 7.2294           | 6.7558           | 79.1791       |
|         |        |                  |        |                |                 |                |                 |                  |                  |               |
|         |        | 7                | 0.0090 | 5.6170         | 0.0071          | 59.7457        | 0.0761          | 8.7389           | 11.1699          | 84.6530       |
|         |        |                  | 0.0590 | 5.3221         | 0.0067          | 59.8740        | 0.0762          | 8.9340           | 10.6864          | 84.9430       |
|         |        |                  | 0.1790 | 4.4359         | 0.0056          | 59.3469        | 0.0756          | 9.4625           | 9.8103           | 85.7444       |
|         |        |                  | 0.4200 | 1.7372         | 0.0022          | 59.3350        | 0.0756          | 9.3038           | 7.9928           | 88.3305       |
|         |        |                  | 0.8890 | 1.9976         | 0.0025          | 60.1984        | 0.0767          | 13.0173          | 7.8159           | 88.1079       |
|         |        |                  | 1.7790 | 12.4215        | 0.0157          | 61.1662        | 0.0779          | 7.3607           | 6.7633           | 78.5706       |

Table C4. 04/19/96 Laser blank radial survey at 0.9620 pressure ratio

| Date    | Prat   | LDV Window                     | Depth | U-<br>Velocity | U-Non<br>Dimensionalized | V-<br>Velocity | V-Non<br>Dimensionalized | U-<br>Turbulence (%) | V-<br>Turbulence (%) | Flow Angle<br>degrees |
|---------|--------|--------------------------------|-------|----------------|--------------------------|----------------|--------------------------|----------------------|----------------------|-----------------------|
|         |        |                                | (mm)  | (m/s)          |                          | (m/s)          |                          |                      |                      |                       |
| 4/30/96 | 0.0962 | Laser Blank                    |       |                |                          |                |                          |                      |                      |                       |
|         |        |                                | 1.78  | 2.9374         | 0.0037                   | 59.2896        | 0.0753                   | 8.0094               | 7.2784               | 87.1837               |
|         |        | Pressurized Window             |       |                |                          |                |                          |                      |                      |                       |
|         |        | Chamber Pressure<br>(mm water) |       |                |                          |                |                          |                      |                      |                       |
|         |        | 0                              | 1.78  | 10.5493        | 0.0134                   | 61.4338        | 0.0780                   | 5.9229               | 5.9988               | 80.2563               |
|         |        |                                | 1.78  | 10.7358        | 0.0136                   | 61.7900        | 0.0785                   | 6.2899               | 6.3154               | 80.1435               |
|         |        |                                | 1.78  | 10.5558        | 0.0134                   | 61.7046        | 0.0784                   | 5.8820               | 6.0196               | 80.2924               |
|         |        |                                |       |                |                          |                |                          |                      |                      |                       |
|         |        | 76.2                           | 1.78  | 10.9306        | 0.0139                   | 61.4216        | 0.0780                   | 6.1382               | 6.0059               | 79.9093               |
|         |        |                                | 1.78  | 11.1289        | 0.0141                   | 61.3917        | 0.0780                   | 6.1905               |                      | 79.7252               |
|         |        |                                |       |                |                          |                |                          |                      |                      |                       |
|         |        | 152.4                          | 1.78  | 11.0337        | 0.0140                   | 61.0734        | 0.0776                   | 6.3454               | 6.4562               | 79.7592               |
|         |        |                                | 1.78  | 10.6817        | 0.0136                   | 61.0624        | 0.0776                   | 6.2015               | 6.5576               | 80.0776               |
|         |        |                                | 1.78  | 10.8223        | 0.0137                   | 61.0932        | 0.0776                   | 6.2952               | 6.4242               | 79.9546               |

Table C5. 04/30/96 Laser blank and pressurized window comparison at 0.9620 pressure ratio



| Date    | Prat   | Chamber Pressure | Depth | U-Velocity | U-Non Dimensionalized | V-Velocity | V-Non Dimensionalized | U-Turbulence | V-Turbulence | Flow Angle |
|---------|--------|------------------|-------|------------|-----------------------|------------|-----------------------|--------------|--------------|------------|
|         |        | (mm water)       | (mm)  | (m/s)      |                       | (m/s)      |                       | (%)          | (%)          | degrees    |
| 5/14/96 | 0.9620 | 0.0              | 0.01  | 11.3153    | 0.0144                | 61.4396    | 0.0782                | 5.7016       | 6.1415       | 79.5648    |
|         |        |                  | 0.06  | 11.1038    | 0.0141                | 61.5593    | 0.0784                | 5.3944       | 6.0199       | 79.7752    |
|         |        |                  | 0.18  | 11.2528    | 0.0143                | 61.5071    | 0.0783                | 5.5404       | 6.2028       | 79.6323    |
|         |        |                  | 0.42  | 11.4629    | 0.0146                | 61.8782    | 0.0788                | 5.1256       | 6.0154       | 79.5050    |
|         |        |                  | 0.89  | 11.6201    | 0.0148                | 62.6365    | 0.0798                | 5.2979       | 5.5779       | 79.4902    |
|         |        |                  |       |            |                       |            |                       |              |              |            |
|         |        | 76.2             | 0.01  | 11.2395    | 0.0143                | 60.9537    | 0.0776                | 5.5153       | 6.1021       | 79.5524    |
|         |        |                  | 0.06  | 11.2783    | 0.0144                | 61.0378    | 0.0777                | 5.4226       | 6.2064       | 79.5312    |
|         |        |                  | 0.18  | 11.1969    | 0.0143                | 61.2629    | 0.0780                | 5.4023       | 6.0874       | 79.6425    |
|         |        |                  | 0.42  | 11.3190    | 0.0144                | 61.4613    | 0.0783                | 5.8823       | 5.8672       | 79.5651    |
|         |        |                  | 0.89  | 11.4433    | 0.0146                | 62.0443    | 0.0790                | 5.3822       | 5.4518       | 79.5499    |
|         |        |                  |       |            |                       |            |                       |              |              |            |
|         |        | 152.4            | 0.01  | 11.2041    | 0.0143                | 60.6618    | 0.0773                | 5.7209       | 6.1861       | 79.5355    |
|         |        |                  | 0.06  | 11.1788    | 0.0142                | 60.8026    | 0.0774                | 5.7005       | 5.9003       | 79.5823    |
|         |        |                  | 0.18  | 11.1890    | 0.0142                | 60.7868    | 0.0774                | 5.6005       | 6.0612       | 79.5703    |
|         |        |                  | 0.42  | 11.2060    | 0.0143                | 60.8454    | 0.0775                | 5.4155       | 5.8966       | 79.5647    |
|         |        |                  | 0.89  | 11.5008    | 0.0146                | 61.9084    | 0.0788                | 5.3217       | 5.7021       | 79.4761    |

Table C6. 05/14/96 Pressurized window radial survey at 0.9620 pressure ratio

| Date    | Prat   | Depth | Wake<br>Position | U-<br>Velocity | U-Non           | V-<br>Velocity | V-Non           | U-<br>Turbulence | V-<br>Turbulence | Flow<br>Angle |
|---------|--------|-------|------------------|----------------|-----------------|----------------|-----------------|------------------|------------------|---------------|
|         |        | (mm)  | (degrees)        | (m/s)          | Dimensionalized | (m/s)          | Dimensionalized | (%)              | (%)              | degrees       |
| 5/10/96 | 0.9620 | 0.01  | 8.0000           | 11.0861        | 0.0142          | 60.5957        | 0.0781          | 6.7788           | 6.3624           | 79.6756       |
|         |        |       | 7.0000           | 11.0617        | 0.0142          | 60.2982        | 0.0781          | 6.2881           | 6.4858           | 79.6951       |
|         |        |       | 6.0000           | 10.8376        | 0.0139          | 60.3806        | 0.0778          | 6.3130           | 6.7593           | 79.8574       |
|         |        |       | 5.0000           | 11.1738        | 0.0143          | 60.8723        | 0.0779          | 6.0381           | 6.8219           | 79.5699       |
|         |        |       | 4.0000           | 11.1802        | 0.0144          | 61.0850        | 0.0776          | 5.9255           | 7.2357           | 79.5155       |
|         |        |       | 3.0000           | 11.6389        | 0.0149          | 61.5732        | 0.0778          | 6.0512           | 7.4339           | 79.1231       |
|         |        |       | 2.0000           | 11.1058        | 0.0143          | 61.3176        | 0.0776          | 6.4217           | 7.3818           | 79.5825       |
|         |        |       | 1.0000           | 10.8577        | 0.0139          | 61.5985        | 0.0781          | 6.7730           | 6.9236           | 79.8743       |
|         |        |       | 0.0000           | 10.5965        | 0.0136          | 61.3842        | 0.0785          | 7.0034           | 6.5053           | 80.1707       |
|         |        |       | -1.0000          | 10.7282        | 0.0138          | 61.0189        | 0.0788          | 6.9105           | 6.2937           | 80.0849       |
|         |        |       | -2.0000          | 10.8710        | 0.0140          | 60.6274        | 0.0784          | 6.4827           | 6.1376           | 79.9105       |
|         |        |       | -3.0000          | 10.9138        | 0.0140          | 60.7931        | 0.0788          | 6.8093           | 6.4816           | 79.9128       |
|         |        |       | -4.0000          | 10.7318        | 0.0138          | 60.6350        | 0.0781          | 6.2998           | 6.4638           | 79.9999       |
|         |        |       | -5.0000          | 11.1605        | 0.0143          | 60.9237        | 0.0779          | 6.6291           | 6.9364           | 79.5735       |
|         |        |       | -6.0000          | 11.3366        | 0.0146          | 60.8027        | 0.0772          | 6.6302           | 7.1385           | 79.3284       |
|         |        |       | -7.0000          | 10.9661        | 0.0141          | 61.0615        | 0.0771          | 6.1756           | 7.7685           | 79.6557       |
|         |        |       | -8.0000          | 11.0737        | 0.0142          | 61.0783        | 0.0775          | 6.0276           | 7.8965           | 79.6066       |
|         |        |       |                  |                |                 |                |                 |                  |                  |               |
|         |        | 0.06  | 8.0000           | 10.6049        | 0.0136          | 60.6716        | 0.0780          | 6.7477           | 6.2782           | 80.0954       |
|         |        |       | 7.0000           | 10.8258        | 0.0139          | 61.0110        | 0.0777          | 6.5411           | 6.0737           | 79.8620       |
|         |        |       | 6.0000           | 11.0348        | 0.0142          | 60.5802        | 0.0777          | 6.2427           | 6.7982           | 79.6688       |
|         |        |       | 5.0000           | 11.2538        | 0.0144          | 60.4480        | 0.0776          | 6.2123           | 6.9744           | 79.4498       |
|         |        |       | 4.0000           | 11.3640        | 0.0146          | 60.9431        | 0.0775          | 6.1308           | 7.3983           | 79.3402       |
|         |        |       | 3.0000           | 11.4905        | 0.0148          | 61.4391        | 0.0779          | 6.2727           | 7.0536           | 79.2714       |
|         |        |       | 2.0000           | 11.2120        | 0.0144          | 61.2874        | 0.0781          | 6.2841           | 7.3942           | 79.5552       |
|         |        |       | 1.0000           | 10.8348        | 0.0139          | 61.3993        | 0.0783          | 6.7771           | 6.4902           | 79.9281       |
|         |        |       | 0.0000           | 10.7220        | 0.0138          | 61.3756        | 0.0785          | 6.8299           | 6.3781           | 80.0552       |
|         |        |       | -1.0000          | 10.8578        | 0.0139          | 61.2227        | 0.0785          | 6.6362           | 6.2870           | 79.9356       |
|         |        |       | -2.0000          | 10.4609        | 0.0134          | 61.0440        | 0.0784          | 7.3379           | 6.7577           | 80.2790       |
|         |        |       | -3.0000          | 10.8944        | 0.0140          | 60.8677        | 0.0786          | 6.7118           | 6.3131           | 79.9088       |
|         |        |       | -4.0000          | 10.2737        | 0.0132          | 60.5953        | 0.0780          | 7.8991           | 6.3998           | 80.3968       |

| Date | Prat | Depth | Wake<br>Position | U-<br>Velocity | U-Non<br>Dimensionalized | V-<br>Velocity | V-Non<br>Dimensionalized | U-<br>Turbulence | V-<br>Turbulence | Flow<br>Angle |
|------|------|-------|------------------|----------------|--------------------------|----------------|--------------------------|------------------|------------------|---------------|
|      |      | (mm)  | (degrees)        | (m/s)          |                          | (m/s)          |                          | (%)              | (%)              | degrees       |
|      |      |       | -5.0000          | 10.1044        | 0.0130                   | 60.6457        | 0.0773                   | 7.6505           | 6.7548           | 80.4762       |
|      |      |       | -6.0000          | 10.8841        | 0.0140                   | 60.7547        | 0.0775                   | 6.8597           | 7.3858           | 79.7782       |
|      |      |       | -7.0000          | 10.8120        | 0.0139                   | 60.7642        | 0.0780                   | 6.5578           | 7.6616           | 79.9147       |
|      |      |       | -8.0000          | 11.1036        | 0.0143                   | 60.9563        | 0.0776                   | 6.4700           | 7.6099           | 79.5919       |
|      |      |       |                  |                |                          |                |                          |                  |                  |               |
|      |      | 0.18  | 8.0000           | 11.1550        | 0.0143                   | 60.9096        | 0.0783                   | 6.6639           | 6.2432           | 79.6373       |
|      |      |       | 7.0000           | 10.4836        | 0.0135                   | 60.8135        | 0.0782                   | 7.4879           | 6.0941           | 80.2337       |
|      |      |       | 6.0000           | 10.7189        | 0.0138                   | 60.6506        | 0.0782                   | 7.3565           | 6.2274           | 80.0229       |
|      |      |       | 5.0000           | 11.4711        | 0.0147                   | 60.8506        | 0.0784                   | 6.2985           | 6.7699           | 79.3577       |
|      |      |       | 4.0000           | 11.4936        | 0.0148                   | 60.6999        | 0.0782                   | 6.0864           | 6.8460           | 79.3072       |
|      |      |       | 3.0000           | 11.5860        | 0.0149                   | 61.5427        | 0.0782                   | 6.0431           | 6.8308           | 79.2290       |
|      |      |       | 2.0000           | 11.5742        | 0.0149                   | 61.7487        | 0.0780                   | 6.3205           | 6.7067           | 79.2196       |
|      |      |       | 1.0000           | 11.1058        | 0.0143                   | 61.4916        | 0.0786                   | 6.8451           | 6.7057           | 79.7129       |
|      |      |       | 0.0000           | 11.0723        | 0.0142                   | 61.5494        | 0.0787                   | 6.4086           | 5.9227           | 79.7655       |
|      |      |       | -1.0000          | 10.8194        | 0.0139                   | 61.4134        | 0.0787                   | 6.6536           | 5.9922           | 79.9852       |
|      |      |       | -2.0000          | 11.0569        | 0.0142                   | 61.0091        | 0.0790                   | 6.3994           | 5.9264           | 79.8117       |
|      |      |       | -3.0000          | 10.2833        | 0.0132                   | 61.1258        | 0.0787                   | 7.6460           | 6.1764           | 80.4799       |
|      |      |       | -4.0000          | 10.8825        | 0.0140                   | 61.0929        | 0.0777                   | 6.3354           | 6.3096           | 79.7994       |
|      |      |       | -5.0000          | 10.8749        | 0.0140                   | 61.2694        | 0.0778                   | 6.6958           | 6.8377           | 79.8311       |
|      |      |       | -6.0000          | 10.7556        | 0.0138                   | 61.1553        | 0.0776                   | 6.8500           | 6.9766           | 79.9079       |
|      |      |       | -7.0000          | 10.9347        | 0.0140                   | 61.1300        | 0.0778                   | 6.1544           | 7.3216           | 79.7702       |
|      |      |       | -8.0000          | 10.9434        | 0.0141                   | 61.2254        | 0.0779                   | 6.4989           | 7.5780           | 79.7781       |
|      |      |       |                  |                |                          |                |                          |                  |                  |               |
|      |      | 0.42  | 8.0000           | 10.8198        | 0.0139                   | 60.8680        | 0.0782                   | 6.3564           | 5.9064           | 79.9323       |
|      |      |       | 7.0000           | 11.0187        | 0.0141                   | 60.8881        | 0.0782                   | 6.5599           | 6.1607           | 79.7423       |
|      |      |       | 6.0000           | 11.1054        | 0.0143                   | 60.9793        | 0.0783                   | 6.1107           | 6.2789           | 79.6854       |
|      |      |       | 5.0000           | 11.3813        | 0.0146                   | 61.4073        | 0.0784                   | 6.1293           | 6.5042           | 79.4451       |
|      |      |       | 4.0000           | 11.6059        | 0.0149                   | 61.4833        | 0.0784                   | 6.0045           | 6.6340           | 79.2347       |
|      |      |       | 3.0000           | 11.7501        | 0.0151                   | 61.5629        | 0.0785                   | 5.9691           | 6.8528           | 79.1265       |
|      |      |       | 2.0000           | 11.8026        | 0.0152                   | 61.7421        | 0.0788                   | 5.7982           | 6.7589           | 79.1191       |
|      |      |       | 1.0000           | 11.5990        | 0.0149                   | 62.0785        | 0.0792                   | 6.2782           | 6.2087           | 79.3445       |
|      |      |       | 0.0000           | 11.5013        | 0.0148                   | 62.1005        | 0.0794                   | 6.0864           | 5.8889           | 79.4699       |
|      |      |       | -1.0000          | 11.4812        | 0.0147                   | 61.8740        | 0.0794                   | 6.3339           | 5.8225           | 79.4843       |

| Date | Prat | Depth  | Wake<br>Position | U-<br>Velocity | U-Non<br>Dimensionalized | V-<br>Velocity | V-Non<br>Dimensionalized | U-<br>Turbulence | V-<br>Turbulence | Flow<br>Angle |
|------|------|--------|------------------|----------------|--------------------------|----------------|--------------------------|------------------|------------------|---------------|
|      |      | (mm)   | (degrees)        | (m/s)          |                          | (m/s)          |                          | (%)              | (%)              | degrees       |
|      |      |        | -2.0000          | 11.2359        | 0.0144                   | 61.6250        | 0.0790                   | 6.2023           | 5.9311           | 79.6492       |
|      |      |        | -3.0000          | 11.2614        | 0.0145                   | 61.3933        | 0.0788                   | 6.2638           | 6.0684           | 79.5967       |
|      |      |        | -4.0000          | 10.7825        | 0.0138                   | 61.2641        | 0.0787                   | 6.7192           | 6.2615           | 80.0174       |
|      |      |        | -5.0000          | 11.0639        | 0.0142                   | 61.3047        | 0.0786                   | 6.1684           | 6.6100           | 79.7499       |
|      |      |        | -6.0000          | 10.9187        | 0.0140                   | 61.2438        | 0.0780                   | 6.2538           | 6.6426           | 79.8121       |
|      |      |        | -7.0000          | 10.5358        | 0.0135                   | 61.1104        | 0.0779                   | 6.3814           | 7.2848           | 80.1478       |
|      |      |        | -8.0000          | 10.6614        | 0.0137                   | 61.1637        | 0.0779                   | 6.1093           | 7.0585           | 80.0295       |
|      |      |        |                  |                |                          |                |                          |                  |                  |               |
|      |      | 0.8900 | 8.0000           | 10.0277        | 0.0129                   | 62.0759        | 0.0794                   | 5.7614           | 5.1875           | 80.7935       |
|      |      |        | 7.0000           | 10.6607        | 0.0137                   | 62.0445        | 0.0794                   | 5.7103           | 5.4611           | 80.2189       |
|      |      |        | 6.0000           | 10.6607        | 0.0137                   | 62.0245        | 0.0792                   | 5.3766           | 6.0886           | 80.1896       |
|      |      |        | 5.0000           | 10.8725        | 0.0140                   | 62.0361        | 0.0798                   | 5.2425           | 5.8680           | 80.0732       |
|      |      |        | 4.0000           | 11.2029        | 0.0144                   | 62.2824        | 0.0797                   | 5.5270           | 5.9209           | 79.7747       |
|      |      |        | 3.0000           | 11.4020        | 0.0146                   | 62.6499        | 0.0794                   | 5.4977           | 6.1510           | 79.5471       |
|      |      |        | 2.0000           | 11.3183        | 0.0145                   | 62.6955        | 0.0794                   | 5.4092           | 5.76476          | 79.6292       |
|      |      |        | 1.0000           | 11.2296        | 0.0144                   | 62.7916        | 0.0800                   | 5.3590           | 5.55178          | 79.7830       |
|      |      |        | 0.0000           | 11.1532        | 0.0143                   | 62.7952        | 0.0803                   | 5.4640           | 5.21952          | 79.8925       |
|      |      |        | -1.0000          | 10.9629        | 0.0141                   | 62.5333        | 0.0803                   | 5.3997           | 5.21232          | 80.0610       |
|      |      |        | -2.0000          | 10.9209        | 0.0140                   | 62.0724        | 0.0802                   | 5.2171           | 5.44242          | 80.0834       |
|      |      |        | -3.0000          | 10.8128        | 0.0139                   | 62.0292        | 0.0801                   | 5.9833           | 5.64056          | 80.1726       |
|      |      |        | -4.0000          | 10.7911        | 0.0139                   | 62.3329        | 0.0797                   | 5.8139           | 5.52799          | 80.1352       |
|      |      |        | -5.0000          | 10.5377        | 0.0135                   | 62.3519        | 0.0794                   | 6.0813           | 6.1604           | 80.3249       |
|      |      |        | -6.0000          | 10.2973        | 0.0132                   | 61.8777        | 0.0793                   | 5.9863           | 6.32056          | 80.5399       |
|      |      |        | -7.0000          | 10.4477        | 0.0134                   | 62.0669        | 0.0794                   | 5.4399           | 6.73985          | 80.4073       |
|      |      |        | -8.0000          | 10.8125        | 0.0139                   | 62.0948        | 0.0794                   | 5.4240           | 6.87407          | 80.0838       |

Table C7. 05/10/96 Pressurized window circumferential survey at 76.2 mm water chamber pressure and 0.9620 pressure ratio

## APPENDIX D. 3 HOLE COBRA PROBE DATA

| Date   | Tare   | Cal    | Ptl.1  | Ptl.2  | p1     | p23   | Pt2    | p2     | Patmos | Pt2/p2 | Mach  | X     | Beta  |
|--------|--------|--------|--------|--------|--------|-------|--------|--------|--------|--------|-------|-------|-------|
| 8/7/96 | -0.086 | 67.933 | 3.804  | 3.746  | 3.454  | 0.303 | 3.708  | 0.084  | 29.920 | 1.009  | 0.113 | 0.050 | 0.008 |
|        | -0.067 | 67.603 | 7.640  | 7.600  | 6.897  | 0.335 | 7.643  | -0.007 | 29.920 | 1.019  | 0.163 | 0.073 | 0.016 |
|        | -0.078 | 67.899 | 11.496 | 11.532 | 10.048 | 0.562 | 11.604 | -0.036 | 29.920 | 1.029  | 0.201 | 0.090 | 0.023 |
|        | -0.075 | 67.915 | 15.539 | 15.474 | 13.626 | 0.769 | 15.659 | -0.074 | 29.920 | 1.039  | 0.234 | 0.104 | 0.031 |
|        | -0.085 | 67.915 | 19.541 | 19.522 | 17.195 | 1.170 | 19.499 | -0.072 | 29.920 | 1.048  | 0.260 | 0.116 | 0.038 |
|        | -0.073 | 67.919 | 24.205 | 24.055 | 20.972 | 1.355 | 24.208 | -0.168 | 29.920 | 1.060  | 0.290 | 0.129 | 0.046 |
|        | -0.097 | 67.901 | 27.631 | 27.559 | 24.177 | 1.539 | 27.914 | -0.240 | 29.920 | 1.069  | 0.311 | 0.138 | 0.053 |
|        | -0.112 | 67.639 | 28.200 | 28.160 | 24.648 | 1.343 | 27.655 | -0.310 | 29.920 | 1.069  | 0.310 | 0.137 | 0.054 |
|        | -0.080 | 67.895 | 27.720 | 27.618 | 24.136 | 1.254 | 27.007 | -0.386 | 29.920 | 1.067  | 0.307 | 0.136 | 0.053 |
|        | -0.113 | 67.924 | 23.534 | 23.476 | 20.440 | 1.071 | 23.893 | -0.266 | 29.920 | 1.059  | 0.289 | 0.128 | 0.045 |
|        | -0.100 | 67.903 | 19.473 | 19.394 | 17.050 | 0.924 | 19.138 | -0.181 | 29.920 | 1.048  | 0.259 | 0.115 | 0.038 |
|        | -0.084 | 67.885 | 15.712 | 15.568 | 13.623 | 0.709 | 15.383 | -0.122 | 29.910 | 1.038  | 0.232 | 0.103 | 0.031 |
|        | -0.034 | 67.827 | 11.540 | 11.480 | 10.387 | 0.563 | 11.856 | -0.094 | 29.910 | 1.029  | 0.204 | 0.091 | 0.024 |
|        | 0.035  | 67.809 | 7.852  | 7.781  | 6.934  | 0.321 | 7.889  | -0.056 | 29.910 | 1.020  | 0.167 | 0.074 | 0.016 |
|        | 0.157  | 67.661 | 3.723  | 3.737  | 3.281  | 0.015 | 3.815  | -0.032 | 29.910 | 1.009  | 0.116 | 0.052 | 0.008 |

Table D1. 3-Hole cobra probe calibration data

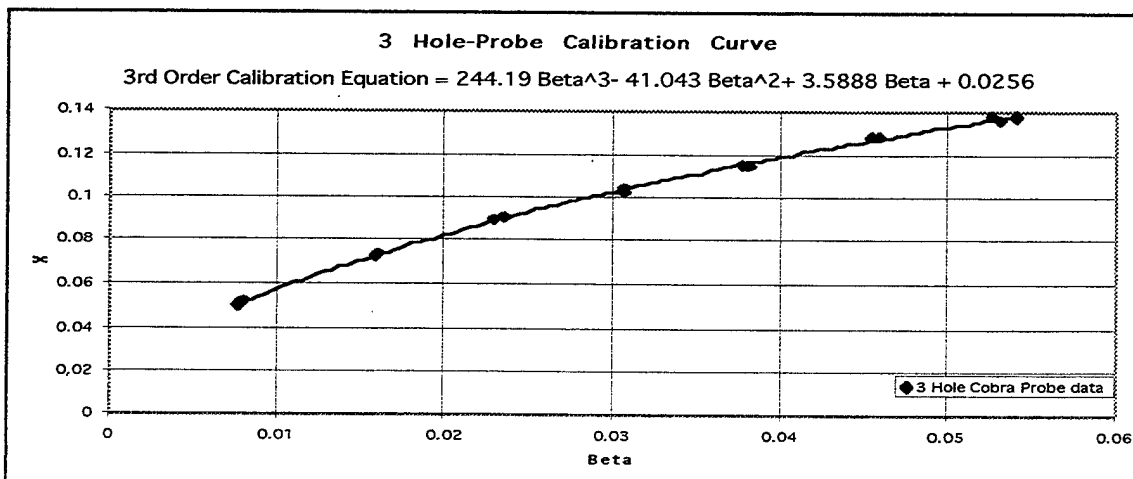


Figure D1. 3-Hole cobra probe calibration curve

| Date    | Tare   | Cal    | Ptl,1  | Ptl,2  | p1     | p23   | Pt2    | p2    | Flow Angle | Patmos | Pt2/p2 | Beta  | Y (mm) | X     |
|---------|--------|--------|--------|--------|--------|-------|--------|-------|------------|--------|--------|-------|--------|-------|
| 8/12/96 | 0.047  | 67.483 | 15.839 | 15.781 | 9.622  | 2.583 | -0.006 | 0.058 | 92.000     | 29.830 | 1.000  | 0.017 | 0.420  | 0.076 |
|         | 0.046  | 67.434 | 15.709 | 15.244 | 12.154 | 3.119 | -0.007 | 0.061 | 90.000     | 29.830 | 1.000  | 0.022 | 0.890  | 0.087 |
|         | 0.047  | 67.398 | 15.632 | 15.281 | 12.827 | 3.312 | -0.119 | 0.055 | 90.000     | 29.830 | 1.000  | 0.023 | 1.780  | 0.089 |
|         | 0.023  | 67.469 | 15.712 | 15.556 | 12.847 | 3.297 | -0.212 | 0.049 | 91.000     | 29.830 | 0.999  | 0.023 | 1.780  | 0.089 |
|         | -0.007 | 67.493 | 15.713 | 15.352 | 12.499 | 3.142 | -0.213 | 0.043 | 91.000     | 29.830 | 0.999  | 0.022 | 0.890  | 0.088 |
|         | -0.019 | 67.531 | 15.638 | 15.252 | 9.904  | 2.547 | -0.007 | 0.062 | 94.600     | 29.830 | 1.000  | 0.018 | 0.420  | 0.078 |
|         | -0.030 | 67.450 | 15.505 | 15.249 | 10.106 | 2.601 | -0.137 | 0.056 | 92.000     | 29.825 | 1.000  | 0.018 | 0.420  | 0.079 |
|         | -0.062 | 67.532 | 15.671 | 15.315 | 12.534 | 3.168 | -0.052 | 0.053 | 90.000     | 29.825 | 1.000  | 0.022 | 0.890  | 0.088 |
|         | -0.074 | 67.535 | 15.732 | 15.435 | 13.195 | 3.343 | -0.208 | 0.047 | 90.000     | 29.820 | 0.999  | 0.024 | 1.780  | 0.091 |

Table D2. A radial survey utilizing the 3-hole cobra probe at a Prati of 0.9620

# APPENDIX E. PRESSURIZED WINDOW DRAWINGS

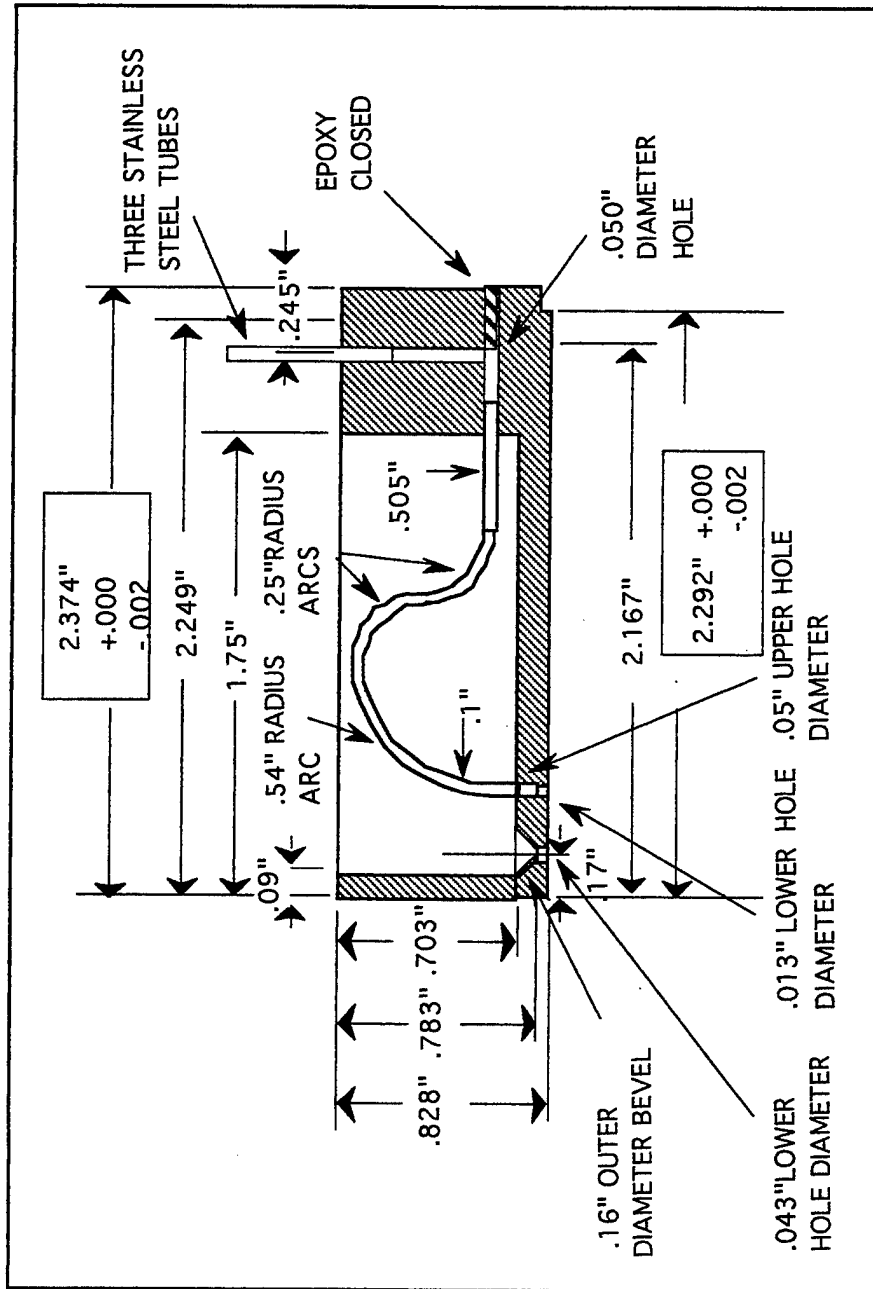


Figure E1. Side view of pressurized window





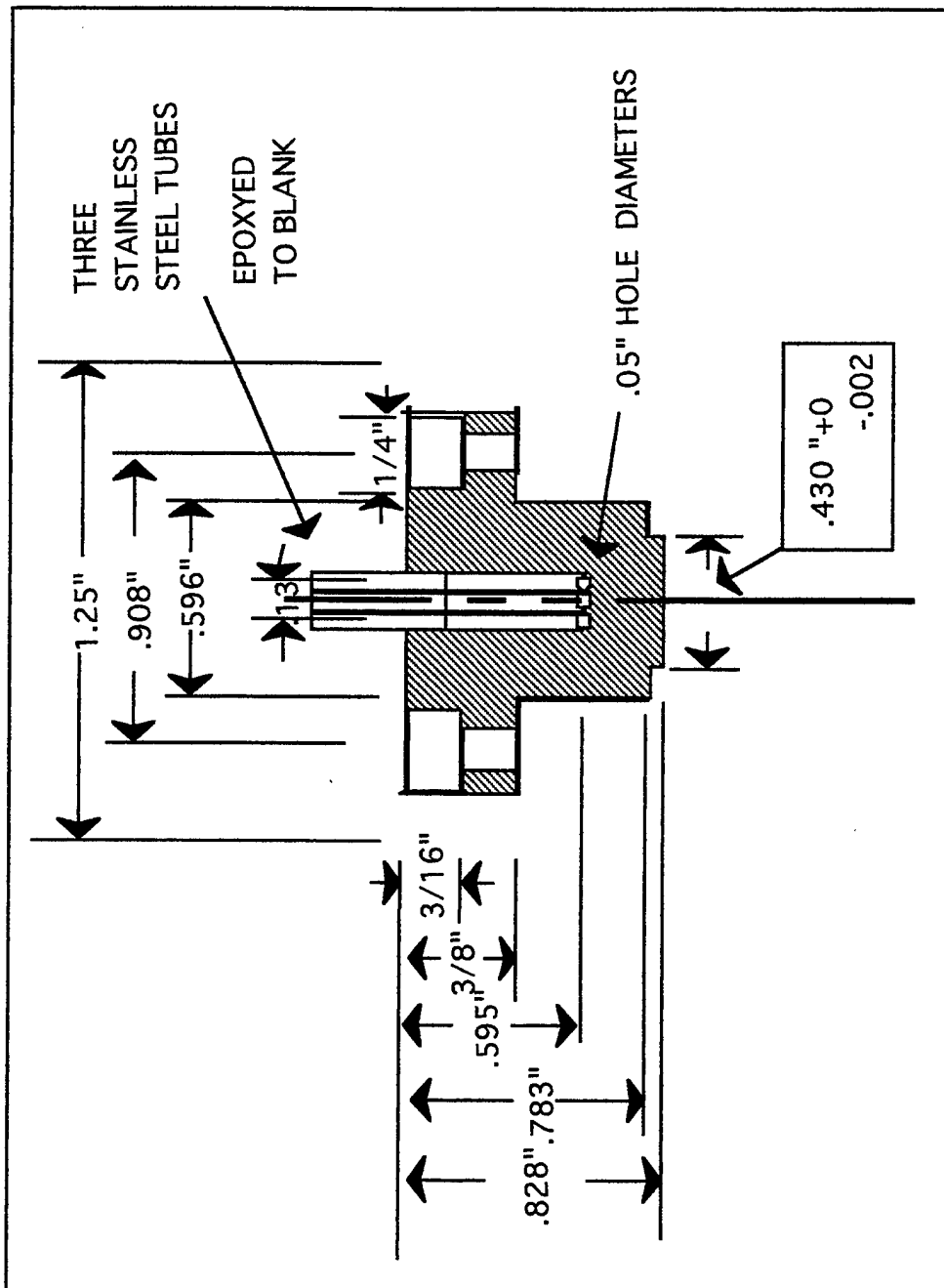


Figure E3. Front view of pressurized window

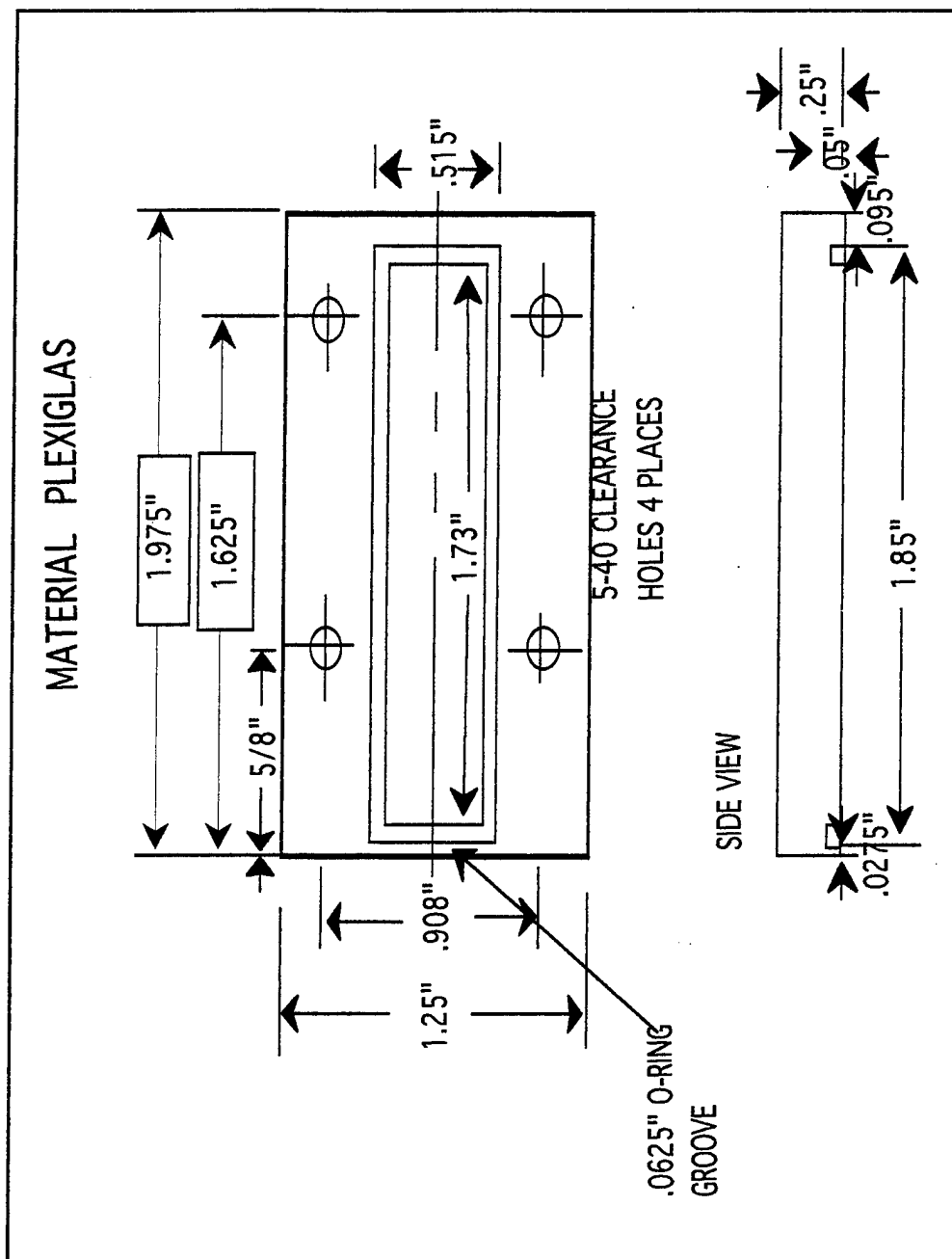


Figure E4. Plexiglas window cover

# APPENDIX F. FREEJET

| Date    | Prat   | Temp (F) | X      | Height | U-Velocity | V-Velocity | UV-Mag.<br>Mean | U-<br>Turb.Intensity | V-<br>Turb.Intensity | Flow Angle |
|---------|--------|----------|--------|--------|------------|------------|-----------------|----------------------|----------------------|------------|
|         |        |          | (mm)   | (mm)   | (m/s)      | (m/s)      | (m/s)           | (%)                  | (%)                  | (degrees)  |
| 3/8/96  | 0.9900 | 110      | -20.00 | -50.00 | 25.878     | 26.256     | 36.865          | 3.026                | 3.237                | 36.865     |
|         |        |          | -20.00 | -40.00 | 25.903     | 25.994     | 36.697          | 2.469                | 2.671                | 36.697     |
|         |        |          | -20.00 | -30.00 | 25.908     | 25.713     | 36.502          | 2.365                | 2.457                | 36.502     |
|         |        |          | -20.00 | -20.00 | 26.054     | 25.847     | 36.700          | 2.615                | 3.070                | 36.700     |
|         |        |          | -20.00 | -10.00 | 26.041     | 26.156     | 36.909          | 2.534                | 2.900                | 36.909     |
|         |        |          | -20.00 | 0.00   | 26.016     | 26.036     | 36.806          | 2.439                | 2.794                | 36.806     |
|         |        |          | -20.00 | 10.00  | 26.010     | 26.113     | 36.857          | 2.696                | 2.877                | 36.857     |
|         |        |          | -20.00 | 20.00  | 26.079     | 26.142     | 36.925          | 2.377                | 2.485                | 36.925     |
|         |        |          | -20.00 | 30.00  | 26.080     | 26.252     | 37.004          | 2.515                | 2.812                | 37.004     |
|         |        |          | -20.00 | 40.00  | 26.116     | 26.173     | 36.974          | 2.285                | 2.527                | 36.974     |
|         |        |          | -20.00 | 50.00  | 26.038     | 26.224     | 36.954          | 2.442                | 2.468                | 36.954     |
|         |        |          |        |        |            |            |                 |                      |                      |            |
|         | 0.9615 | 112      | -20.00 | -50.00 | 56.127     | 57.501     | 80.353          | 1.771                | 3.367                | 45.693     |
|         |        |          | -20.00 | -40.00 | 56.426     | 57.120     | 80.290          | 1.753                | 3.666                | 45.350     |
|         |        |          | -20.00 | -30.00 | 56.925     | 56.971     | 80.536          | 2.016                | 3.433                | 45.023     |
|         |        |          | -20.00 | -20.00 | 57.266     | 56.839     | 80.685          | 1.984                | 4.788                | 44.786     |
|         |        |          | -20.00 | -10.00 | 57.291     | 57.064     | 80.862          | 2.114                | 6.188                | 44.886     |
|         |        |          | -20.00 | 0.00   | 56.547     | 58.077     | 81.059          | 1.780                | 2.501                | 45.765     |
|         |        |          |        |        |            |            |                 |                      |                      |            |
| 3/14/96 | 0.9900 | 105      | -20.00 | -50.00 | 27.523     | 28.189     | 39.397          | 2.232                | 2.474                | 45.416     |
|         |        |          | -20.00 | -40.00 | 27.716     | 28.187     | 39.530          | 2.106                | 2.363                | 45.100     |
|         |        |          | -20.00 | -30.00 | 27.822     | 28.403     | 39.759          | 2.293                | 2.249                | 44.784     |
|         |        |          | -20.00 | -20.00 | 27.874     | 28.136     | 39.605          | 2.816                | 2.900                | 44.771     |
|         |        |          | -20.00 | -10.00 | 27.866     | 28.039     | 39.531          | 2.218                | 2.694                | 45.126     |
|         |        |          | -20.00 | 0.00   | 27.886     | 28.095     | 39.585          | 2.572                | 2.794                | 45.022     |
|         |        |          | -20.00 | 10.00  | 27.855     | 28.277     | 39.692          | 2.625                | 2.768                | 45.113     |
|         |        |          | -20.00 | 20.00  | 27.926     | 28.157     | 39.657          | 2.403                | 2.742                | 45.069     |

| Date | Prat   | Temp (F) | X      | Height | U-Velocity | V-Velocity | UV-Mag.<br>Mean | U-<br>Turb.Intensity | V-<br>Turb.Intensity | Flow Angle |
|------|--------|----------|--------|--------|------------|------------|-----------------|----------------------|----------------------|------------|
|      |        |          | (mm)   | (mm)   | (m/s)      | (m/s)      | (m/s)           | (%)                  | (%)                  | (degrees)  |
|      |        |          | -20.00 | 30.00  | 28.038     | 28.103     | 39.698          | 2.560                | 2.836                | 45.188     |
|      |        |          | -20.00 | 40.00  | 27.957     | 27.863     | 39.471          | 3.568                | 3.894                | 45.063     |
|      |        |          | -20.00 | 50.00  | 27.394     | 27.091     | 38.528          | 4.739                | 5.366                | 45.204     |
|      |        |          |        |        |            |            |                 |                      |                      |            |
|      | 0.9615 | 112      | -20.00 | -30.00 | 60.079     | 61.490     | 85.968          | 2.058                | 1.994                | 45.665     |
|      |        |          | -20.00 | -20.00 | 60.445     | 61.340     | 86.118          | 1.879                | 2.116                | 45.421     |
|      |        |          | -20.00 | -10.00 | 60.878     | 61.377     | 86.448          | 1.648                | 1.859                | 45.234     |
|      |        |          | -20.00 | 0.00   | 61.056     | 61.222     | 86.463          | 1.628                | 1.628                | 45.078     |
|      |        |          | -20.00 | 10.00  | 61.543     | 61.222     | 86.808          | 1.456                | 1.740                | 44.850     |
|      |        |          | -20.00 | 20.00  | 61.295     | 61.610     | 86.907          | 1.561                | 1.937                | 45.147     |

Table F1. Freejet data

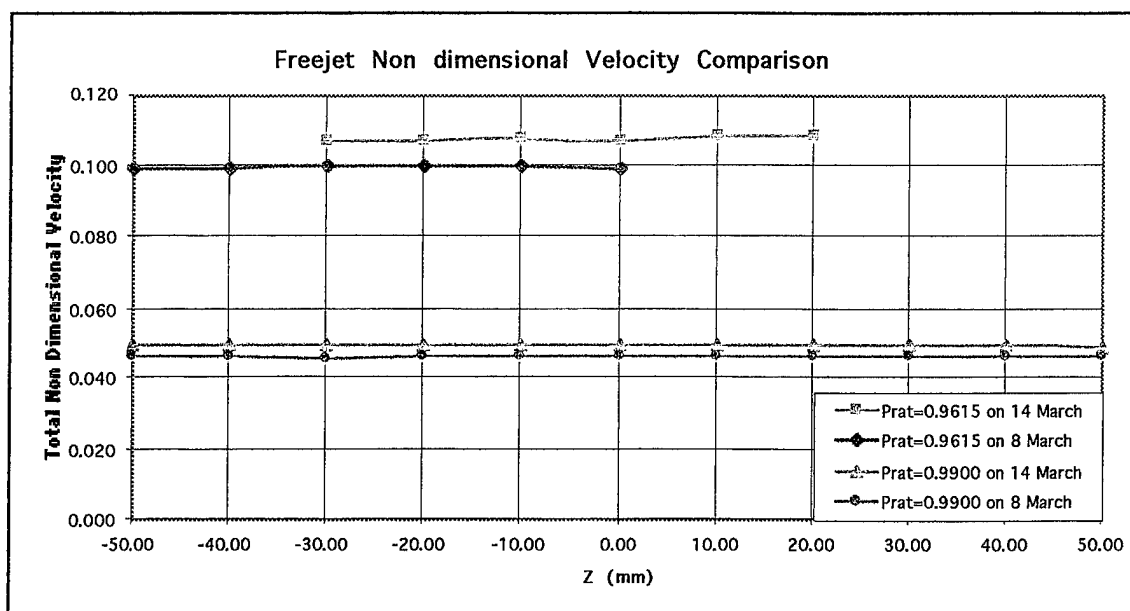


Figure F1. Freejet Survey

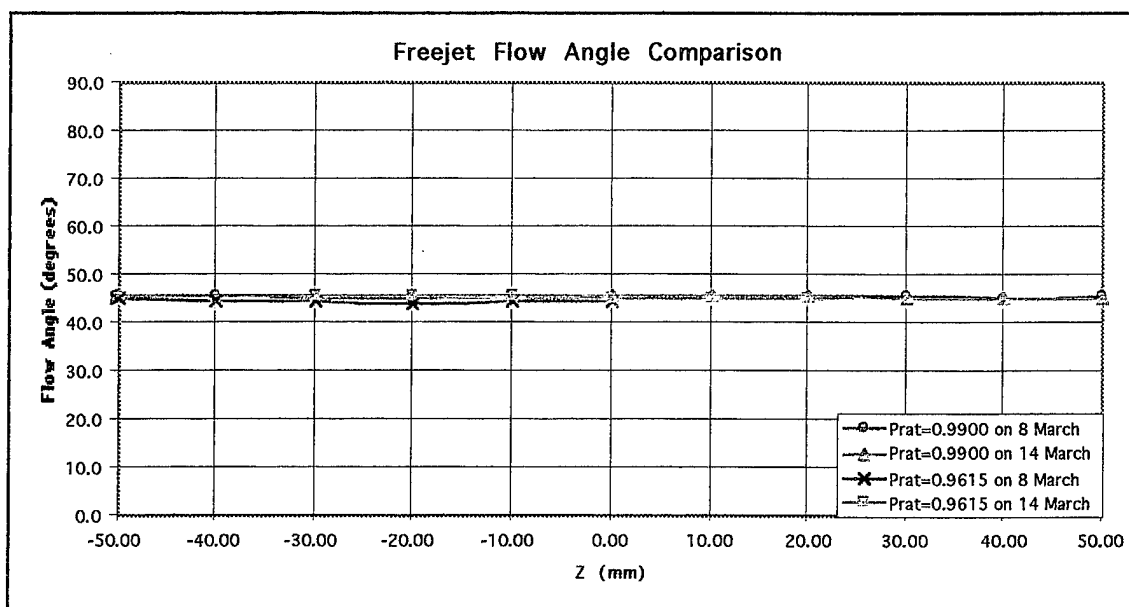


Figure F2. Freejet Survey

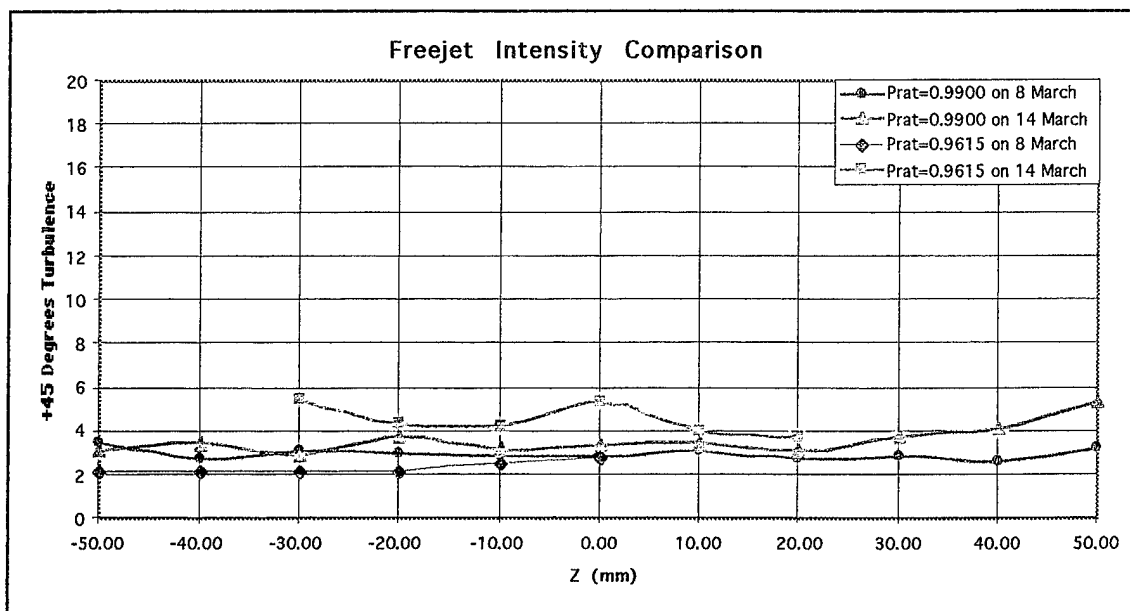


Figure F3a. Freejet Survey

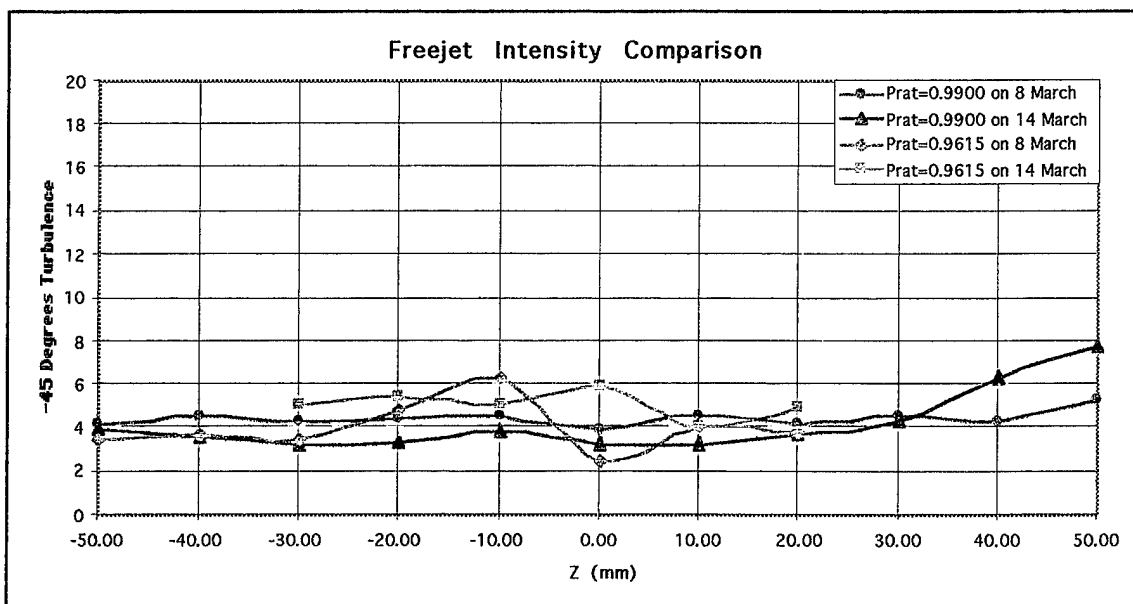


Figure F3b. Freejet Survey

# APPENDIX G. PRESSURIZED WINDOW AT PRAT OF 0.9054

| Date   | Prat  | Chamber<br>Pressure | Run<br># | Depth<br>(mm) | U-<br>Velocity<br>(m/s) | U-Non<br>dim.<br>Velocity | V-<br>Velocity<br>(m/s) | V-Non<br>dim.<br>Velocity | U-Turbulence<br>Intensity<br>(%) | V-Turbulence<br>Intensity<br>(%) | Flow<br>Angle<br>(degrees) |
|--------|-------|---------------------|----------|---------------|-------------------------|---------------------------|-------------------------|---------------------------|----------------------------------|----------------------------------|----------------------------|
| 5/7/96 | .9054 | 3                   | 1        | 0.01          | 3.398                   | .0043                     | 67.975                  | .0866                     | 8.022                            | 11.862                           | 87.14                      |
|        |       |                     |          | 0.06          | 3.001                   | .0038                     | 68.373                  | .0872                     | 7.692                            | 12.266                           | 87.49                      |
|        |       |                     |          | 0.18          | 5.117                   | .0065                     | 69.404                  | .0885                     | 8.898                            | 12.292                           | 85.78                      |
|        |       |                     |          | 0.42          | 3.407                   | .0043                     | 71.727                  | .0914                     | 8.270                            | 11.362                           | 87.28                      |
|        |       |                     |          | 0.89          | 11.631                  | .0148                     | 69.201                  | .0882                     | 9.309                            | 9.388                            | 80.46                      |
|        |       |                     |          |               |                         |                           |                         |                           |                                  |                                  |                            |
|        |       |                     | 2        | 0.01          | 2.081                   | .0026                     | 67.502                  | .0860                     | 6.561                            | 12.056                           | 88.23                      |
|        |       |                     |          | 0.06          | 1.818                   | .0023                     | 67.970                  | .0866                     | 6.389                            | 12.073                           | 88.47                      |
|        |       |                     |          | 0.18          | 2.674                   | .0034                     | 68.722                  | .0876                     | 7.628                            | 12.274                           | 87.77                      |
|        |       |                     |          | 0.42          | 1.296                   | .0016                     | 71.341                  | .0909                     | 5.686                            | 10.785                           | 88.96                      |
|        |       |                     |          | 0.89          | 11.644                  | .0148                     | 72.996                  | .0930                     | 8.657                            | 9.788                            | 80.94                      |
|        |       |                     |          |               |                         |                           |                         |                           |                                  |                                  |                            |
|        |       | 6                   | 1        | 0.01          | .521                    | .0007                     | 67.324                  | .0858                     | 3.696                            | 12.163                           | 89.56                      |
|        |       |                     |          | 0.06          | .256                    | .0003                     | 67.376                  | .0859                     | 2.848                            | 12.338                           | 89.78                      |
|        |       |                     |          | 0.18          | .347                    | .0004                     | 68.554                  | .0874                     | 3.293                            | 11.846                           | 89.71                      |
|        |       |                     |          | 0.42          | .738                    | .0009                     | 70.991                  | .0905                     | 4.489                            | 11.210                           | 89.40                      |
|        |       |                     |          | 0.89          | 11.505                  | .0147                     | 74.124                  | .0945                     | 9.041                            | 9.520                            | 81.18                      |
|        |       |                     |          |               |                         |                           |                         |                           |                                  |                                  |                            |
|        |       |                     | 2        | 0.01          | .529                    | .0007                     | 67.633                  | .0862                     | 3.854                            | 12.645                           | 89.55                      |
|        |       |                     |          | 0.06          | .396                    | .0005                     | 68.027                  | .0867                     | 3.478                            | 12.197                           | 89.67                      |
|        |       |                     |          | 0.18          | 0.4929                  | .0006                     | 68.055                  | .0867                     | 3.740                            | 11.884                           | 89.59                      |
|        |       |                     |          | 0.42          | 3.5915                  | .0046                     | 70.609                  | .0900                     | 8.548                            | 11.835                           | 87.09                      |
|        |       |                     |          | 0.89          | 11.69                   | .0149                     | 71.031                  | .0905                     | 8.772                            | 11.681                           | 80.65                      |

Table G1. Pressurized window data at a Prat of 0.9054

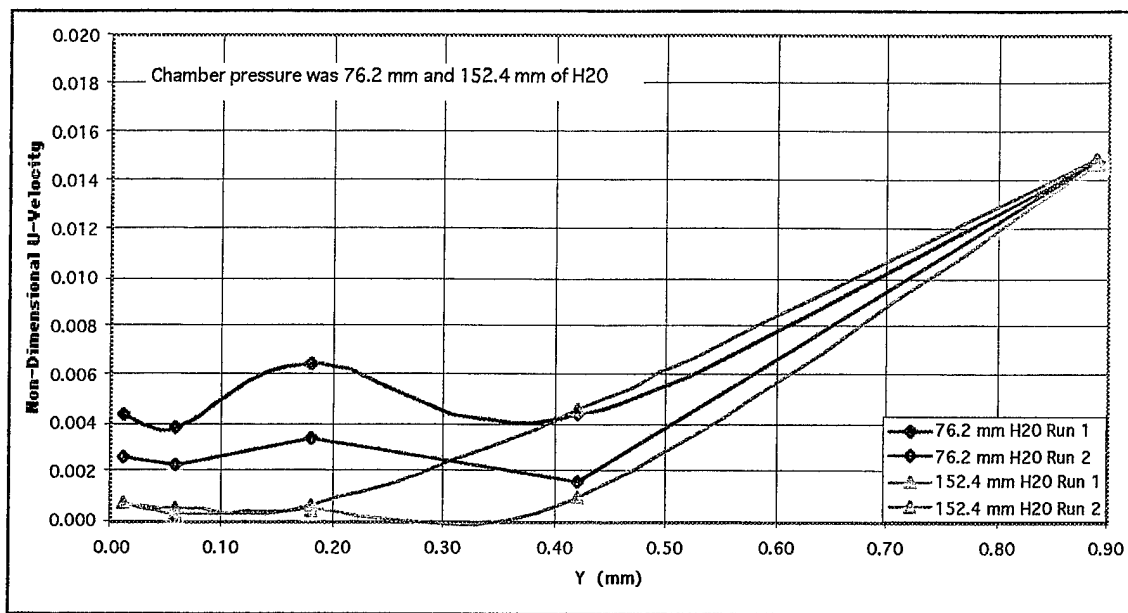


Figure G1a. A radial survey through the pressurized window at a Prandtl of 0.9054

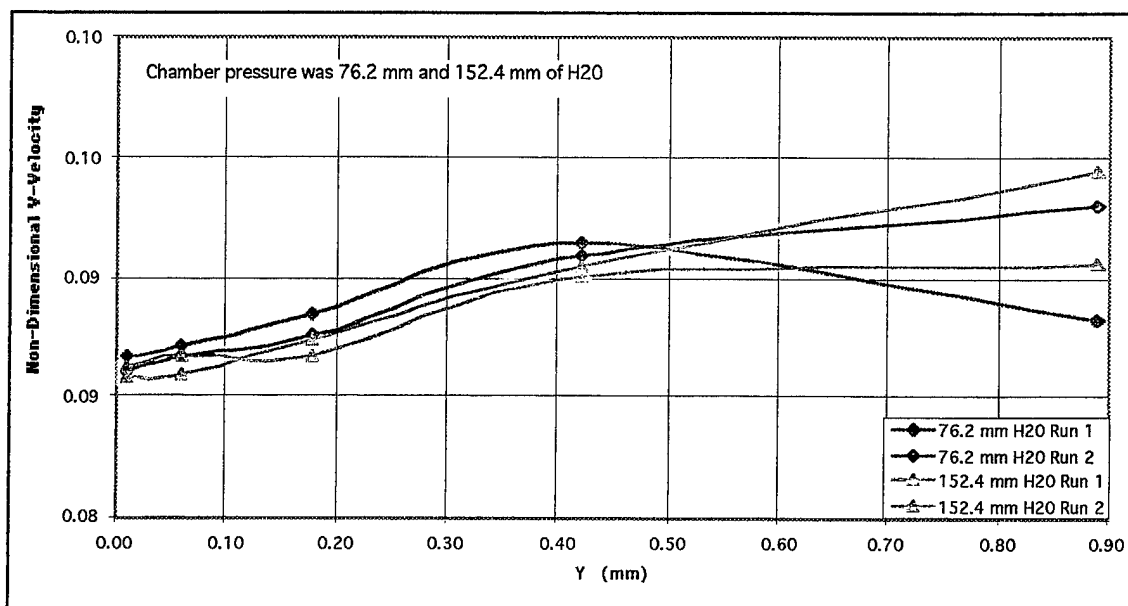


Figure G1b. A radial survey through the pressurized window at a Prandtl of 0.9054



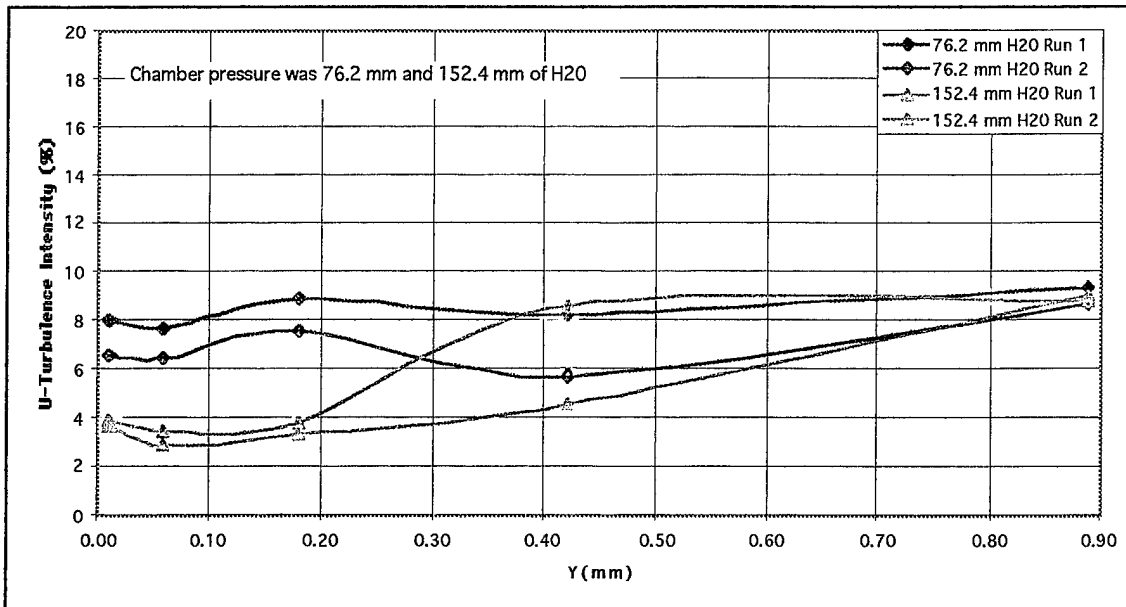


Figure G2a. A radial survey through the pressurized window at a Pr at of 0.9054

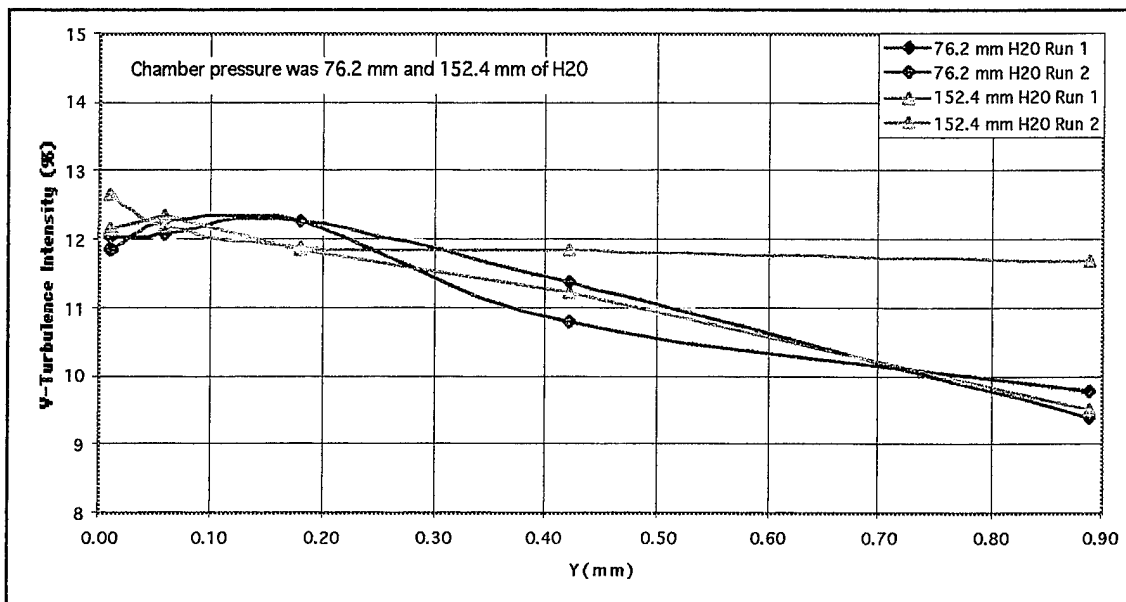


Figure G2b. A radial survey through the pressurized window at a Pr at of 0.9054

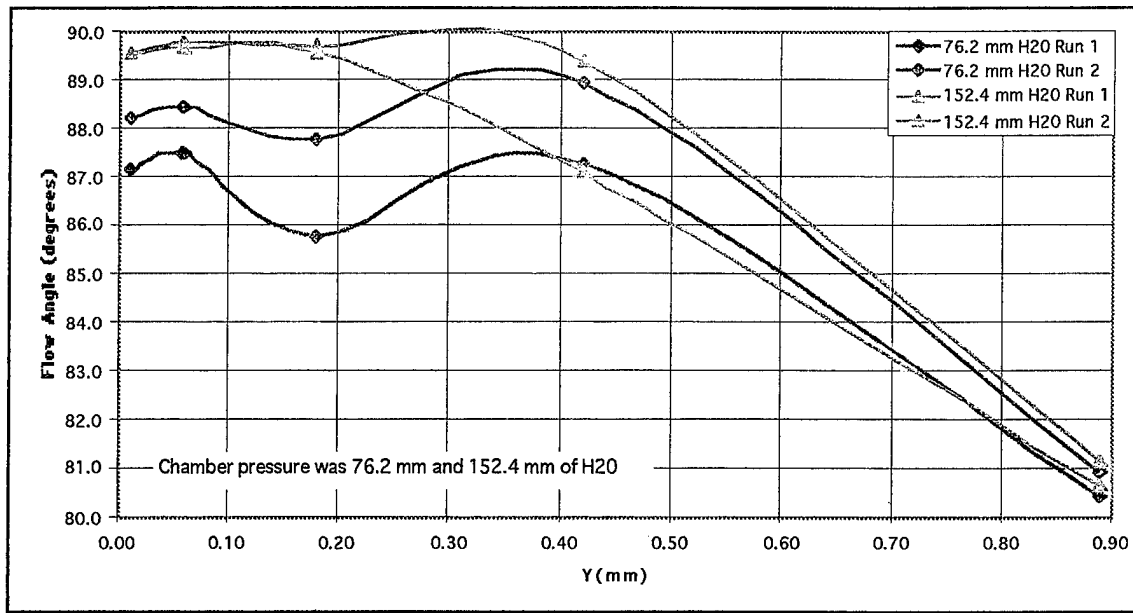


Figure G3. A radial survey through the pressurized window at a Pr<sub>at</sub> of 0.9054

## LIST OF REFERENCES

1. Chima, R. V. and Yokota, J. W., "Numerical Analysis of Three-Dimensional Viscous Flows in Turbomachinery," AIAA Journal, Vol. 28, No. 5, May 1990, pp. 798-806.
2. Donovan, B.H., "Experimental and Computational Investigation of the Flow Through an Annular Turbine Cascade," Master's Thesis, Naval Postgraduate School, Monterey, CA, June 1995.
3. Spitz, J.D., "Laser Anemometry and Viscous Computation of the Flow Through an Annular Turbine Cascade," Master's Thesis, Naval Postgraduate School, Monterey, CA, March 1994.
4. Thomas, G. D., "Measurement and Prediction of the Flow Through an Annular Turbine Cascade," Master's Thesis, Naval Postgraduate School, Monterey, CA, June 1993.



## INITIAL DISTRIBUTION LIST

|    |  | No. Copies |
|----|--|------------|
| 1. | Defense Technical Information Center<br>8725 John J. Kingman Road., Ste 0944<br>Ft. Belvoir, VA 22060-6218   | 2          |
| 2. | Dudley Knox Library<br>Naval Postgraduate School<br>411 Dyer Rd.<br>Monterey, CA 93943-5101  | 2          |
| 3. | Professor Daniel J. Collins<br>Department of Aeronautics and Astronautics<br>Code AA/CO<br>Naval Postgraduate School<br>699 Dyer Road-Room 137<br>Monterey, CA 93943-5106  | 1          |
| 4. | Professor Garth V. Hobson<br>Department of Aeronautics and Astronautics<br>Code AA/HG<br>Naval Postgraduate School<br>699 Dyer Road-Room 137<br>Monterey, CA 93943-5106    | 10         |
| 5. | Professor Raymond P. Shreeve<br>Department of Aeronautics and Astronautics<br>Code AA/SF<br>Naval Postgraduate School<br>699 Dyer Road-Room 137<br>Monterey, CA 93943-5106 | 1          |
| 6. | Naval Air Systems Command<br>AIR-4.4.T (Attn: Mr. C. Gordon)<br>Washington, DC 20361-5360  | 1          |
| 7. | Naval Air Warfare Center Aircraft Division<br>AIR-4.4.3.1(Attn: D. Parish)<br>Propulsion and Power Engineering, Building 106<br>Patuxent River, MD 20670-5304              | 1          |
| 8. | Michael H. Guerrero<br>94-419 Noholoa Loop<br>Mililani Town, HI, 96789   | 3          |